

**SOURCES, CYCLING, AND FATE OF ORGANIC MATTER IN LARGE
LAKES: INSIGHTS FROM STABLE ISOTOPE AND RADIOCARBON
ANALYSIS IN LAKES MALAWI AND SUPERIOR**

A DISSERTATION

SUBMITTED TO THE FACULTY OF THE UNIVERSITY OF MINNESOTA

BY

BRITTANY RUTH KRUGER

IN PARTIAL FULFILLMENT OF THE REQUIREMENTS FOR THE DEGREE OF
DOCTOR OF PHILOSOPHY

ADVISORS: ELIZABETH C. MINOR AND JOSEF P. WERNE

August 2014

ACKNOWLEDGMENTS

I extend my most sincere gratitude to my co-advisors; without their encouragement, guidance, and support I am certain this would not have been possible. Liz, thank you for sharing your passion for science with me and encouraging me to be the best scientist possible at all times. Joe, thank you for your constant optimism and unwavering excitement for science. You are both brilliant scientists and I have been inspired by you both from the very beginning of my higher education. Thank you for affording me the opportunity to learn from you both for so many years. I am forever grateful to each of you for your steadfast support during both scientific and personal trials.

I would also like to acknowledge the support and encouragement from my committee members, Dr. Tom Johnson, Dr. Donn Branstrator, Dr. Jim Cotner, and Dr. Steph Guildford. Each of you are truly excellent scientists and excellent people, and I feel very lucky to have had the support and guidance that I did from each of you, personally and professionally. Further acknowledgment is due to the open and supportive community of scientists at the Large Lakes Observatory. It is a rare opportunity to have so many excellent scientists in such a collaborative and encouraging environment, and I feel blessed to have completed my education there. Finally, thank you a thousand times over to all the peers I was lucky enough to have along the way for the good times and support, the late nights in the lab and the great memories. To Melissa Berke and Prosper Zigah- ‘thank you’ doesn’t come close to expressing my gratitude for your mentorship and your friendship.

Heartfelt acknowledgment is also due to the world class research institutions of the National Ocean Sciences Accelerator Mass Spectrometry (NOSAMS) facility at Woods Hole Oceanographic Institute (WHOI), and the Japan Agency for Marine-Earth Science and Technology (JAMSTEC). Without the ability to travel to these incredible institutes much of the data in this dissertation would not have been possible. Particular thank you to Dr. Ann McNichol at the NOSAMS facility and to Dr. Naohiko Ohkouchi at JAMSTEC for welcoming me to visit your lab groups and perform sample analyses that

would otherwise not have been possible, and to Dr. Yoshito Chikaraishi for the extensive guidance and teaching.

Finally, thank you to my parents, Rita and Jim Rowland, for their constant support and encouragement throughout my education. Thank you to my sister, Michelle Larson, and all my family, friends, and loved ones who also provided constant love and support. This wouldn't have been possible without knowing you were standing behind me throughout.

Major funding for this research came from the Petroleum Research Fund and SeaGrant. Additional funding and research-travel opportunities were provided by the NOSAMS graduate student internship program, the Elsevier/Organic Geochemistry Research Scholarship, the EAOG Travel Scholarship, the Butler and Jessen award, the Kerry Kelts Award, and the WRS Travel Grant.

SOURCES, CYCLING, AND FATE OF ORGANIC MATTER IN LARGE LAKES:
INSIGHTS FROM STABLE ISOTOPE AND RADIOCARBON ANALYSIS IN
LAKES MALAWI AND SUPERIOR

Brittany Ruth Kruger

Abstract

Organic matter (OM) in lake systems is sourced from *in situ* aquatic primary production (autochthonous), land based plant primary production or detrital material that ultimately originated from photosynthesis (allochthonous), or resuspension of organic rich sedimentary material that was ultimately sourced from a combination of all such sources. Studying the stable and radioisotopic signature of multiple chemical components of lacustrine OM can help elucidate which of the above is the dominant OM source to the lake, as well as how OM is incorporated into and cycles through lake systems. The high organic content and biodiversity in large lakes of the world make them excellent sites to investigate such questions, and this dissertation focuses on such questions in Lake Malawi (SE Africa), and Lake Superior (North America). In Lake Malawi, the organic carbon (OC) recently deposited (within the last 50 years) is largely dominated by aquatic input, and the influence of terrestrial riverine inputs dissipates as distance from shore and water depth increase. This confirms that parameters typically used to investigate historic lake levels (and thereby to infer past climates) can in fact function as robust indicators of distance from shore, and thereby lake level. This is supported by bulk and compound specific stable carbon isotopic and radiocarbon analysis of multiple sediment fractions. Most fractions exhibited isotopic signatures nearshore that were distinct from more offshore, open-lake locations. In Lake Superior, compound specific nitrogen isotope analysis (CSNIA) of specific amino acids from species occupying all levels of the food chain showed that *Limnocalanus macrurus*, a copepod, occupies a trophic level much higher than expected from known feeding habits, which may indicate the consumption of additional or unique food sources. Bulk radiocarbon

analysis of the same suit of species from that lake showed *Diporeia*, a benthic amphipod, consumes an aged carbon source that does not appear to be significantly incorporated by other (more pelagic) organisms in this study, which rely primarily upon recently synthesized autochthonous organic carbon.

Table of Contents

List of Tables.....	viii
List of Figures.....	ix
Chapter 1: Introduction.....	1
1.1 Organic Matter in Lake Systems	1
1.2 Radiocarbon- genesis and application as a biochemical tracer.....	3
1.3 Focusing Research on Large Lakes.....	4
1.4 Lake Malawi.....	5
1.4.1 Modern Physical, Chemical, and Hydrologic Characteristics	5
1.4.2 Geologic Setting and Historic Lake Levels.....	8
1.4.3 Primary Production and Biota.....	9
1.5 Lake Superior.....	11
1.5.1 Physical, Chemical, and Hydrologic Characteristics.....	11
1.5.2 Geologic Setting and Historic Lake Levels	13
1.5.3 Primary Production and Biota.....	13
1.6 Dissertation outline.....	15
Chapter 2: Characterizing sediment compositional change with water depth and distance from shore in a tropical rift lake.....	17
2.1 Introduction.....	17
2.2 Methods.....	18
2.2.1 Sediment Collection.....	18
2.2.2 Sediment Analyses.....	19
2.3 Results and Discussion.....	21
2.3.1 Si:Ti	21
2.3.2 Elemental and Isotopic Analysis.....	23
2.3.3 Water Content, Grain Size, and Sedimentation.....	26
2.3.4 Diatom Relative Abundance.....	28
2.4 Conclusion.....	29

Chapter 3: Sources and cycling of Lake Malawi organic carbon: insights from multi-fraction stable isotope and radiocarbon analyses of sediments.....	38
3.1 Introduction.....	38
3.2 Methods.....	41
3.2.1 Sediment collection.....	41
3.2.2 Lipid extraction.....	42
3.2.3 Compound isolation and radiocarbon analysis.....	43
3.2.4 Additional Fraction Analyses.....	45
3.2.5 Water column	45
3.3 Results	46
3.3.1 Bulk elemental analysis and biomarker relative abundance.....	46
3.3.2 Multi-fraction stable carbon isotope.....	47
3.3.3 Multi-fraction radiocarbon	47
3.4 Discussion.....	48
3.4.1 Bulk elemental analysis and biomarker relative abundance.....	48
3.4.2 $\delta^{13}\text{C}$ of multiple sediment fractions.....	51
3.4.3 Radiocarbon signatures of multiple sediment fractions.....	54
3.5 Conclusion.....	62
Chapter 4: Organic Matter Transfer in Lake Superior's Food Web: Insights from Bulk and Molecular Stable Isotope and Radiocarbon Analyses.....	72
4.1 Introduction.....	72
4.2 Methods.....	74
4.2.1 Sample Collection.....	74
4.2.2 Sample Processing.....	76
4.2.3 Radiocarbon Analysis.....	77
4.2.4 CSNIA.....	77
4.2.5 Trophic Level Calculations.....	78
4.3 Results	79
4.3.1 Bulk Isotope Signatures.....	79

4.3.2 Calculated Trophic Positions.....	81
4.3.3 Radiocarbon Signatures.....	82
4.4 Discussion.....	83
4.4.1 Food Web Structure from Bulk Stable Isotopes.....	83
4.4.2 Unique Stable Isotopic Signatures of <i>Limnocalanus macrurus</i>	85
4.4.3 A Comparison of Trophic Level Calculation Methods and Implications for Food Web Structure.....	89
4.4.4 Carbon Pool Interactions as Indicated by Radiocarbon Signatures.....	92
4.5 Conclusion.....	96
Chapter 5: System Comparison.....	106
References.....	108

List of Tables

Table 2.1. Core names of short cores collected from Lake Malawi's northern basin in 2009, and their associated water depth at coring location and distance from the nearest lake shoreline. **Page 30.**

Table 3.1. Cores collected from the northern basin of Lake Malawi in 2009 for this study, the associated water depth at the coring location (m) for each, and the distance from each coring location to the nearest lake shoreline (km). **Page 64.**

Table 4.1. Scientific and common name of species studied in Lake Superior, and predominant diet items for each. **Page 98.**

Table 4.2. Calculated trophic levels for each species at each location, and of each size for those divided into size classes. N/a represents no animals recovered from that sampling location. **Page 99.**

List of Figures

Figure 2.1. Coring locations in Lake Malawi's northern basin, core 2MC is the most nearshore core in the sampling line (82 m water depth), and core names increase numerically until core 11MC (demarcated) at 386 m water depth. **Page 31.**

Figure 2.2 Bulk surface sediment (0-1 cm) parameters (a) %TOC, (b) %TON, (c) C/N, (d) Si:Ti where the increase in Si:Ti from 5MC to 9MC is described by $y = 0.00082x - 0.0947$, $R^2 = 0.96$, (e) $\delta^{13}\text{C}$ in ‰, and (f) $\delta^{15}\text{N}$ in ‰, for cores 2MC – 11MC. Error bars (where present) represent average error between duplicate analyses. **Page 32.**

Figure 2.3. 10 mm averaged Si:Ti values with depth in core for cores 2MC through 9MC as obtained by XRF scanning. **Page 33.**

Figure 2.4. %TOC (a), %TON (b), C/N (c), Si:Ti (d), $\delta^{13}\text{C}$ (e), and $\delta^{15}\text{N}$ (f) with depth in Pb-210 age-modeled cores. The five parameter values nearest the core top represent average values of analyses 0.5 cm above and below the level of age determination. **Page 34.**

Figure 2.5. Surface sediment (0-1 cm) percent water content by weight (filled circles) for cores 2MC – 9MC, and mean (filled triangles) and modal grain size (open triangles) for cores 4MC – 10MC, in μm . **Page 35.**

Figure 2.6. (a) Age vs. Depth of Pb210 dated cores 2MC, 5MC, 8MC, and 9MC (b) Calculated linear sedimentation rate; (c) calculated mass accumulation rate; and (d) calculated total organic carbon mass accumulation rate for age modeled cores 2MC, 5MC, 8MC, and 9MC. **Page 36.**

Figure 2.7. Diatom relative percent abundance as enumerated from surface sediment (1 cm) smear slides of cores 2MC – 9MC, divided into planktonic, tychoplanktonic, and benthic life strategy groups. **Page 37.**

Figure 3.1. Coring locations in Lake Malawi's northern basin, core 2MC is the most nearshore core in the sampling line (82 m water depth), and core names increase numerically until core 11MC (demarked) at 386 m water depth. **Page 65.**

Figure 3.2. Bulk sediment parameters as measured for the 0-4 cm homogenized horizons used for subsequent fraction isolation. $\delta^{15}\text{N}$ is reported in units of per mil (‰) as described in the text. **Page 66.**

Figure 3.3. Percent relative abundance of aquatic (C20, 22, and 24) and terrestrial (C28 and 30) *n*-alcohols analyzed after polar lipid isolation from TLE (a), and the concentration of each alcohol normalized to g OC of the analyzed sediment. **Page 67.**

Figure 3.4. Stable carbon isotopic ratio in units of per mil (‰) for bulk sediment (0-4 cm) and fractions isolated from that sediment including protokerogen, total lipid extract (TLE), and aquatic *n*-alcohols (C20, 22, and 24). The approximate boundary of permanent anoxia and the potential extent of the chemocline zone are noted, although these boundaries are highly mobile and affected by numerous parameters (see text). **Page 68.**

Figure 3.5. Radiocarbon signatures presented as $\Delta^{14}\text{C}$ (units of per mil, ‰) for bulk sediment (0-4 cm) and fractions isolated from that sediment including protokerogen, total lipid extract (TLE), aquatic *n*-alcohols (C20, 22, and 24), and terrestrial *n*-alcohols (C28 and 30). The approximate boundary of permanent anoxia and the potential extent of the chemocline zone are noted, although these boundaries are highly mobile and affected by numerous parameters (see text). **Page 69.**

Figure 3.6. Stable carbon isotopic ratio in units of per mil (‰) of water column organic carbon fractions DIC and POC from 30 and 350 m water depth where successful. The approximate boundary of permanent anoxia and the potential extent of the chemocline zone are noted, although these boundaries are highly mobile and affected by numerous parameters (see text). **Page 70.**

Figure 3.7. Radiocarbon signatures presented as $\Delta^{14}\text{C}$ (units of per mil, ‰) of water column organic carbon fractions DIC, DOC and POC from 30 and 350 m water depth where successful. The approximate boundary of permanent anoxia and the potential extent of the chemocline zone are noted, although these boundaries are highly mobile and affected by numerous parameters (see text). **Page 71.**

Figure 4.1. Sampling map reflecting the three sampling locations in the western arm of Lake Superior. **Page 100.**

Figure 4.2. Stable isotope signatures (all in units of per mil (‰)) of all organisms at all sites a) as measured without sample pre-treatment, and b) with post-analysis lipid correction applied to zooplankton species using $\delta^{13}\text{C}_{\text{ex}} = \delta^{13}\text{C}_{\text{bulk}} + 6.3((\text{C:N}_{\text{bulk}} - 4.2)/\text{C:N}_{\text{bulk}})$ as refined by Smyntek et al. (2007) and described in text. Horizontal error bars represent average error in $\delta^{13}\text{C}$ between bulk analyses with no pre-treatment and analyses with acid pre-treatment to remove inorganics as a preparative step for radiocarbon analysis and may also represent error associated with separate instrumentation. **Page 101.**

Figure 4.3. $\delta^{13}\text{C}$ versus $\Delta^{14}\text{C}$ of surface and deep water column DOC, POC, and DIC at all sampling locations, both in units of per mil (‰). **Page 103.**

Figure 4.4. Organism trophic levels from all sampling locations (a) and of multiple size classes for *Mysis* and *Diporeia* (b) as calculated by: $\text{TL}_{(\text{Glu/Phe})} = (\delta^{15}\text{N}_{\text{Glu}} - \delta^{15}\text{N}_{\text{Phe}} - 3.4)/7.6 + 1$ from Chikaraishi et al. 2009. **Page 104.**

Figure 4.5. Radiocarbon signature of organisms sampled at all locations including only large size classes of *Mysis* and *Diporeia*, in units of per mil (‰). **Page 105.**

Chapter 1: Introduction

1.1 Organic Matter in Lake Systems

Biogeochemical cycling of earth's most biologically important elements (carbon, nitrogen, oxygen, sulfur, and trace metals) is linked by the presence, transport, and transformations of organic matter. Organic matter (OM) is the material produced by living organisms and composed largely of organic compounds rich in carbon, but can also include considerable amounts of the elements listed above. Studying the chemical composition of organic matter can provide insight to the origin of the material, the age of the material, and how that material is transported and assimilated in different environments. In doing so, light is also shed on the functioning of major biogeochemical processes that affect all life on earth, such as the carbon and nitrogen cycles. Almost all OM on earth originates through biologically mediated autotrophic synthesis of organic compounds from abiotic chemical sources. In lakes, organic matter produced *in situ* by aquatic organisms is referred to as 'autochthonous'. This OM is synthesized from dissolved CO₂ photosynthetically or chemosynthetically by algae and other microbial species. Organic matter produced by organisms outside the lake, such as photosynthesized by land plants, is referred to as 'allochthonous'. Organic matter can partition into different phases, including dissolved organic matter (DOM) or particulate organic matter (POM), depending on its chemical structure and the conditions of the system. DOM is operationally defined as the material passing through a 0.1 – 1.0 µm filter, while POC refers to the material retained by the filter. This research utilized 0.7 µm filters for separation of water column OM fractions.

Once OM is fixed by primary producers in any system, it is either incorporated into the food chain through heterotrophic consumption or becomes part of the standing organic pool of detrital biomass of the system, where further microbial consumption often occurs. In lakes, the POM not immediately incorporated into the food web sinks out of the water column and accumulates as sediment on the lake floor. Any material not further consumed by microbial reworking after sedimentation is buried and preserved

long term. In this way, OM sources to lake systems can include the autochthonous material synthesized *in situ*, allochthonous material composed of recently fixed plant material, allochthonous material composed of aged plant and/or animal detrital material, or re-suspension of organic rich sediments which may have ultimately originated from a combination of all the above sources.

Using organic matter as a tool for learning about lake systems is typically accomplished through study of its various chemical components. Since most organic matter is composed predominately of carbon, the amount of OC is often measured to indicate the amount of organic material in a system. In lakes, the amount of OC in water column or sediment fractions is dependent on the productivity of the system and on the amount of loading from allochthonous sources. Beyond quantification of OM, natural abundance isotopic analysis of different organic matter components (such as C, N, O, S, and others) has become a powerful tool to study its origin, transport, and transformation. The C and N isotopic signatures of various OM components were used heavily in this research to learn about such processes in large lake systems.

While ^{12}C is the vastly predominant carbon isotope in the environment (98.9%), the stable isotope ^{13}C constitutes roughly 1.1% of naturally occurring carbon. Stable carbon isotope ^{13}C can be oxidized into $^{13}\text{CO}_2$ and incorporated into organic matter through photo or chemosynthesis. Biogenic substances typically contain greater amounts of lighter ^{12}C than the substrate it was sequestered from, due to kinetic isotopic fractionation of the isotopes; assimilation of the heavier ^{13}C is slower and therefore selected against (Killops and Killops, 2005; Mackenzie and Lerman, 2006). This fractionation can occur with each biological transfer of carbon, giving organic matter with distinct assimilation pathways an identifiable stable carbon signature (^{13}C relative to ^{12}C content, Mackenzie and Lerman, 2006). Similar kinetic fractionations occur with respect to biochemical processes involving nitrogen. The naturally occurring nitrogen isotope ^{15}N , which accounts for roughly 0.4% of nitrogen atoms, is heavier than the most abundant isotope ^{14}N (99.6%), and its slower reaction can result in products depleted in ^{15}N . The stable isotopic ratios of any given sample in this research are represented in conventional delta

(δ) notation as per mil (‰) deviations from a standard according to the following equation:

$$\delta x (\text{‰}) = ((R_{\text{sample}} - R_{\text{standard}})/R_{\text{standard}}) * 1000$$

where R is the ratio of the heavier to lighter isotope in question and x is the element whose isotopic ratio is being measured (e.g., C or N in this research).

1.2 Radiocarbon- genesis and application as a biochemical tracer

Radiocarbon (^{14}C) forms naturally in the upper stratosphere and lower troposphere by neutron bombardment of ^{14}N , which prompts the addition of a neutron and the formation of the ^{14}C isotope (Libby, 1946; Libby et al., 1949). This unstable isotope constitutes just <0.0001% of all carbon atoms. Advances in analytical technology, such as the ability to isolate and analyze very small samples (Pearson et al., 1998) as well as individual chemical compounds (Eglinton et al., 1996) for radiocarbon content are opening doors to understanding the carbon cycle in ways that were previously impossible. The ability to obtain a radiocarbon age for a substance is based on abundance of the two less common naturally occurring carbon isotopes; stable isotope ^{13}C , and radioactive ^{14}C relative to ^{12}C (Libby, 1946; Libby et al., 1949; Killops and Killops, 2005). Once formed, ^{14}C is rapidly oxidized to $^{14}\text{CO}_2$, allowing for incorporation into organic matter through photosynthesis by autotrophic organisms. Upon organism death $^{14}\text{CO}_2$ accumulation ceases, at which point the amount of ^{14}C in an organism begins to decline, as the unstable nature of the ^{14}C isotope prompts its decay back into ^{14}N (Ingalls and Pearson, 2005; Killops and Killops, 2005). Since the half life of ^{14}C is known (5730 yr), the content of ^{14}C in organic matter can be compared the corresponding carbon stable isotope content to determine an ‘age’ of the material relative to modern (Killops and Killops, 2005). To isolate the age component in this measurement, the ratio of ^{14}C relative to ^{12}C is corrected for biogeochemical fractionation by measuring the ^{13}C to ^{12}C ratio in the same sample and assuming that ^{14}C fractionation is twice that of ^{13}C . This is most typically accomplished through accelerator mass spectrometry analysis (McNichol and Aluwihare, 2007). An additional, but often useful, complication to radiocarbon measurements is the fact that above-ground

nuclear testing added considerable anthropogenic ^{14}C to the global atmosphere. Therefore ‘modern’ in radiocarbon terms corresponds to the 1950s, just prior to the spike in radiocarbon from nuclear weapons testing, and it is possible for a substance to have a radiocarbon age ‘younger than modern’, expressed as ‘Fraction Modern’ values greater than 1, given the equation:

$$\text{Fraction Modern (Fm)} = (\text{sample} - \text{blank}) / (\text{modern reference} - \text{blank})$$

(McNichol and Aluwihare, 2007). Thus, organic matter with different cycling characteristics or differently aged source material can have a radiocarbon signature distinct from other material. The Fm value described above can then be used to calculate $\Delta^{14}\text{C}$, defined as:

$$\Delta^{14}\text{C} = (\text{Fm} * e^{\lambda * (1950 - \text{yc})} - 1) * 1000$$

where Fm = the fraction modern value, $\lambda = 1/8267$, and yc = year collected, following the convention of Stuiver and Polach (1977). This transformation into $\Delta^{14}\text{C}$ values serves to normalize radiocarbon measurements to $\delta^{13}\text{C} = -25\text{‰}$ (to account for kinetic fractionation from biological transfers), and also to correct the value to account for decay time between year of collection and year of analysis (necessary because of the declining atmospheric radiocarbon level post-1950s weapons testing).

1.3 Focusing Research on Large Lakes

Large lakes around the world are particularly useful systems from which to gain vital understanding of carbon cycling processes; however, many characteristics of the carbon cycle within these systems remain unresolved. Globally, the area covered by large lakes (those with areas greater than 500 km^2) is just 0.4% of that occupied by marine waters, however these lakes accumulate $\sim 1/10^{\text{th}}$ the amount of organic carbon sequestered in oceanic sediments (Alin and Johnson, 2007). Despite this, the nature of carbon that accumulates in lake sediments is often unclear; for example, in Lake Malawi, one of the great African rift lakes, there are conflicting results regarding the proportion of aquatic versus terrestrial organic carbon contained in surface sediments (Filippi and Talbot, 2005; Castaneda et al., 2007). In another system, that of Lake Superior in the

USA (the world's largest lake by surface area (Herndendorf, 1990)), the degree to which allochthonous carbon inputs support the aquatic food web is unclear. In this system, annual carbon balance estimates indicate that carbon export from the lake is far greater than carbon input (Cotner et al., 2004; Urban et al. 2005). Since Lake Superior has been found to be net heterotrophic in nature (Urban et al., 2005), this carbon budget imbalance suggests carbon in the lake is supplemented by an uncharacterized source, which may be allochthonous in nature, but could also be derived from old autochthonous (aquatically produced) material. These two lake systems are the focus of my research.

1.4 Lake Malawi

1.4.1 Modern Physical, Chemical, and Hydrologic Characteristics

For all their similarities, the large lakes of the world are remarkably distinct from one another in a myriad of ways, including their hydrologic regime and physical and chemical limnology. Lake Malawi, the southernmost of the Great African Rift Lakes, is no exception, exhibiting characteristics that are unique even to its northern African rift lake neighbors.

Lake Malawi is the fourth largest lake in the world by volume (7,775 km³), the eighth largest by surface area (29,600 km²), and the third deepest non sub-glacial lake (706 m max depth). Although it exists in an area of tropical climate, it is far enough south of the equator to experience seasonal cycling of wind, temperature, and precipitation. A rainy season occurs from November through March, at which time the Intertropical Convergence Zone (ITCZ) lies just south of the lake. Winds during this time are predominately northerly. Around April/May the region enters a dry season when the ITCZ shifts northward, which induces a concurrent shift in wind direction to predominately southerly (Eccles, 1974). Although the average monthly rainfall levels for Lake Malawi are actually comparable to those of the North American Great Lake Ontario, evaporation levels on the African continent are much higher, given the more continuous warm air temperatures (Spiegel and Coulter, 1996), meaning the water budget of the lake relies heavily on evaporation to balance inputs (Eccles, 1974; Spiegel and

Coulter, 1996). Adding to this dependence on evaporation is the nearly-closed basin morphometry; the Shire River is the lone output for Lake Malawi and is typically only a few meters in depth (Eccles, 1974). When this river was 3.5 m deep in 1974, it was estimated to account for only 20% of the water loss from Lake Malawi, with evaporation accounting for the other 80% (Eccles, 1974). A more detailed water budget calculated from compiled data by Spigel and Coulter (1996) had similar results, estimating 50 of the 52.7 km³ water/yr lost from the lake to result from evaporation (95%), with river drainage making up the 5% difference. Lake inputs were found to be dominated by precipitation (67%), while 33% was due to river inflow and storm runoff (Spigel and Coulter, 1996). Clearly, there is a delicate hydrologic balance in Lake Malawi, in which the relative amounts of precipitation and evaporation are critically important to the character of the system.

Along with warm air temperatures, the orientation of the lake basin helps produce the extremely high evaporation rates (more than double those of Lake Ontario; Spigel and Coulter 1996) estimated in the Lake Malawi water budget. As is common in rift-formed lakes, Lake Malawi has a long, narrow shape. Although it is roughly 560km long at its longest point, it has a maximum width of merely 75km (Eccles, 1974). The north-south orientation of the lake allows the prevailing winds of the region to blow along the long axis of the lake most of the year. Relatively strong wind events with multiple day durations also occur, further facilitating high evaporation (Eccles, 1974).

These continuous and occasionally intense wind events are, however, insufficient to induce complete vertical mixing of the lake's water column. The lake's great depth (~700 m) and lack of significant temperature induced density fluctuations (as found in temperate great lakes; Bootsma and Hecky, 2003) prevent such mixing. The water below about 250 m therefore remains anoxic and unmixed with the oxygenated water above (Eccles, 1974; Bootsma and Hecky, 2003). This results in a meromictic mixing regime, in which the bottom ~450m of water remains isothermal (slightly less than 23°C) for the entire year and circulates internally, while the upper 250m undergoes a seasonal stratification cycle within itself (Eccles, 1974; Bootsma and Hecky 2003). This surface

water stratification is most pronounced during the wet season, and weakens during the dry season due to evaporative cooling and mixing induced by the dry southerly winds (Spigel and Coulter, 1996). However, the range of water temperatures between the surface and bottom waters is minimal despite the stable density gradient; water is roughly 22.5°C in the hypolimnion while a maximum temperature of roughly 29°C is reached in the epilimnion during the peak of austral summer stratification (Wuest et al., 1996). During austral winter when the surface water stratification decomposes, surface water temperatures can be as low as 23°C: a mere 0.5°C (or less) warmer than the permanently anoxic water below (Wuest et al., 1996). Complete water column mixing is prevented during these times by additional density stability formed due to chemical gradients of dissolved solids and non-ionic compounds (Wuest et al., 1996).

Although wind driven mixing is incomplete in Lake Malawi, the long lake fetch and consistent wind events allow for various water transport mechanisms to establish. Surface seiches with an amplitude of 12 cm have been observed, lasting anywhere from 6 to 24 hours (Eccles, 1974), and internal seiches are likely (Eccles 1974; Johnson, 1996). Winds traveling parallel to the long fetch of Lake Malawi can also generate longshore currents, allowing for lateral transport of sediment and nutrients along the shoreline (Johnson, 1996). Such alongshore winds can also facilitate the offshore movement of water through Eckman transport, thereby allowing for upwelling of the deeper waters (Bakun, 1990). An additional and critical water circulation process driven in part by wind is the formation of profile driven density currents. The southern basin of the lake is relatively shallow and undergoes complete mixing (Spigel and Coulter, 1996), allowing for high rates of evaporative cooling. This cooled water is more dense and subsequently sinks, where it travels along the lake's floor following the downward sloping basin profile until it reaches the deep basin north of Nkhata Bay (Eccles, 1974). It is hypothesized that this influx of cooled water to the anoxic bottom waters is essential in maintaining the permanent thermocline at 250m; the bottom waters must be mixing internally since they remain isothermal, therefore without an influx of cooled water sources one would expect the 250m thermocline to gradually migrate deeper as the result

of oscillation driven mixing with the slightly warmer water at the temperature boundary (Eccles, 1974; Johnson 1996). Wind, therefore not only affects surface water movement, but contributes to the cooling necessary to replenish the isothermal anoxic hypolimnion.

Chemically, the surface waters of Lake Malawi are relatively low in salinity and dissolved ion content (Hecky and Bootsma, 2003); while the anoxic bottom waters contain more concentrated nutrient pools. An analysis of estimated annual nitrogen, phosphorus and silicon inputs to the surface mixed layer of the lake indicate that approximately 89% of phosphorus and 88% of silicon delivered to the mixed waters are sourced from the anoxic waters below, with atmospheric deposition and river inflow accounting for the remaining inputs (Hecky et al., 1996). Conversely, vertical transport, river influx, and atmospheric deposition combined accounted for only about 21% of nitrogen inputs to the surface waters. This deficit is balanced by very high rates of biological nitrogen fixation, particularly by cyanobacteria species (Hecky et al, 1996 and sources therein). Additionally, free hydrogen sulfide is contained in the deep anoxic bottom waters (Eccles, 1974).

1.4.2 Geologic Setting and Historic Lake Levels

Lake Malawi, along with great lakes such as Tanganyika (Africa) and Baikal (Russia), is one of only a few deep and very old lakes still in existence. Formed by an active continental rift system, it has existed for millions of years, although exact age estimates differ. It is generally believed that the Malawi Rift Basin began formation in the late Miocene, roughly ~8.6 million years ago (although earlier rifting events are also believed to have occurred), and deep water lake conditions may have existed for the past ~4.5 million years (Cohen et al., 1993; Ebinger et al., 1993; Delvaux 1995; Contreras et al., 2000). The subsequent period of nearly continuous sedimentation has resulted in over 4km of organic rich sediment accumulation in some parts of the African rift lakes (Cohen et al., 1993; Rosendahl, 1987).

This vast sediment record has been used extensively by paleoclimatologists in an effort to understand how climates, both locally and globally, have changed through time.

Both the world climate and Lake Malawi water levels have fluctuated historically (Johnson, 1996; Beadle, 1981). Work by Castaneda et al. (2007) (using carbon isotopes measured from plant leaf waxes within Lake Malawi sediment cores) showed that whether or not previous wet and arid phases of southeast Africa corresponded to those of the world's tropical regions may relate directly to the position of the ITCZ as it shifted due to glacial influence. That Lake Malawi has shown low water levels during both wet and arid phases of the continent, and that its fluctuations are typically out of phase with the Great African Lakes to the north, is likely a signal of its dependence on the position of the ITCZ (Johnson, 1996; Finney et al., 1996). By examining calcite, ^{14}C , and diatom records from additional sediment cores recovered from Lake Malawi, it seems the most recent major lake lowstand occurred between 6,000-10,000 years ago, when the lake was approximately 100-150m below its current level (Johnson, 1996; Ricketts and Johnson, 1996; Finney et al., 1996). Another more drastic lowstand occurred from approximately 28,000-40,000 years ago, when water levels were thought to be 200-300m below present levels (Finney et al., 1996; Johnson, 1996).

1.4.3 Primary Production and Biota

Lake Malawi is characterized by its oligotrophic nature. In a comparative study, both surface water total phosphorus (0.1 – 0.5 $\mu\text{mol/L}$) and total nitrogen (4.7 – 14.8 $\mu\text{mol/L}$) in the lake were the lowest of all measured systems, which included Lake Superior, large and small Canadian lakes, Lake Victoria, and a number of marine locations (Guildford and Hecky, 2000). These low values were attributed to a combination of Lake Malawi's very long mean annual flushing time of 700 years (Spigel and Coulter, 1996) and its unique deep water chemistry. Specifically, for nitrogen, a relatively high rate of denitrification occurs at the oxic/anoxic boundary of the permanently anoxic bottom water, such that vertical diffusion of N to the surface mixed layer accounts for little to no contribution to the overall available mixed layer N (Hecky et al., 1996). Enhanced regeneration of phosphorus from metal oxides also occurs in the deep water and creates a low N:P ratio in those bottom waters. Mixing of those deep

waters with the water above can create N-limitation, which is likely balanced by N-fixation (Hecky 2000). Phytoplankton responsible for primary productivity consume nutrients in a fairly fixed proportion, and their growth is often constrained by the unique nutrient limitations of the system in question (Hecky and Kilham, 1988). Of the major required nutrients for algal growth, namely C, N, and P, both C and N are readily available from atmospheric sources and subsequent diffusion or fixation, while P does not exist in a gaseous form (Hecky and Kilham, 1988; Hecky et al., 1996). A positive correlation is often found between algal biomass, as indicated by chlorophyll *a* (chl *a*) concentration, and total P concentration in freshwater systems. This relationship is also observed in Lake Malawi and could indicate a degree of P limitation, although some correlation also exists between chl *a* and total N (Guildford and Hecky, 2000). As a result of nutrient dependence, primary production in Lake Malawi also seems to be highly dependent on hydrologic conditions which affect the amount of mixing that occurs between the more nutrient rich bottom waters and the surface water (Patterson et al, 2000). Some of the earliest studies of primary production rates in Lake Malawi observed that maximum production and plankton biomass occurred during the surface water mixing period of May to September (Degnbol and Mapila, 1982). This trend was generally supported by a two year investigation of light attenuation and production in Lake Malawi's central basin, which found average annual primary production to be 329.4 g C m⁻²y⁻¹ for 1992, and 518.3 g C m⁻²yr⁻¹ for 1993, and concluded that the greater production in 1993 was a result of increased seiche activity in that year and increased mixing (Patterson et al., 2000). Other estimates of primary production in Lake Malawi are nearer to 240 g C m⁻² yr⁻¹ (Guildford and Hecky, 2000).

Phytoplankton of Lake Malawi are dominated by Cyanophyta (cyanobacteria), Chlorophyta (green algae), and Bacillariophyta (diatom) species (Lehman, 1996). The open-water zooplankton community is relatively species poor, and is dominated by just four crustacean species; a calanoid copepod (*Tropodiatomus cunningtoni*), two cyclopoid copepods (*Mesocyclops aequatorialis aequatorialis* and *Thermocyclops neglecus*), and a cladoceran (*Diaphanasoma excisum*) (Lehman, 1996; Irvine and Waya,

1999). Most pelagic zooplankton are preyed upon by the lakefly *Chaoborus edulis* and larvae of the cyprinid fish *Engaulicypris sardella*, though numerous other pelagic fish species exist that also feed to a lesser extent on the open water zooplankton population (Lehman, 1996; Irvine and Waya, 1999). In general, the fish community of the lake is dominated by the remarkably diverse community of cichlid species. This group of fishes is thought to have existed in Lake Malawi for roughly 700,000 years, and over 400 species of cichlids are endemic to Lake Malawi alone (Moran et al., 1994). This remarkable speciation has been a point of extensive study for evolutionary and molecular biologists, and it is believed that species radiation occurred quite rapidly in the lake via three bursts of cladogenesis, and may actually be monophyletic in origin (Moran et al., 1994; Albertson et al., 1999; Danley and Kocher, 2001). This rapid species radiation has resulted in extremely specified feeding strategies that include piscivores, planktivores, lepidophages (scale eaters), fin biters, ectoparasite cleaners, molluscivores, crevice feeders, periphyton feeders, aufwuchs feeders (algae growing on surfaces other than plants), and paedophages (those that steal eggs or larvae from mouth-brooding cichlid species) (Albertson et al., 2003).

1.5 Lake Superior

1.5.1 Physical, Chemical, and Hydrologic Characteristics

Lake Superior differs substantially from Lake Malawi in a number of ways, but not in its large size. Lake Superior is the largest lake in the world by surface area (82,100 km²) and the third largest by water volume (12,200 km³), though, with a maximum depth of ~400m, it is much shallower than Lake Malawi. It is located in an area of temperate climate in North America, and experiences four distinct seasons that each differ in temperature and precipitation patterns. The combination of this climatic seasonality and the relatively shallow depth of Lake Superior creates a dimictic mixing cycle within the lake, whereby the entire water column mixes completely twice a year, in spring and fall, and reaches stratification in both summer and winter between mixings (Bennet, 1978). The lake experiences at least partial ice cover each winter, and the freezing or near 0°C

surface water allows for the formation of a relatively weak inverse winter stratification, since the temperature of maximum water density is 4°. The relatively brief period of warming combined with the lakes large volume results in the coldest average surface water temperatures of all the Laurentian Great Lakes, with average summer and winter temperatures only 12 - 16°C and 0 - 2°C, respectively (Bennet, 1978). Recent evidence from Austin and Colman (2007) indicates that the surface water of Lake Superior is warming more rapidly than the associated increase in atmospheric temperature, and average summer surface water seems to have warmed by ~2.5°C over the traditional averages in the last three decades. This exaggerated warming was attributed to an approximately 11% reduction in winter ice over the last century, and has likely influenced the mixing dynamics of the lake, apparently extending the average length of the summer stratification by ~25 days (Austin and Colman, 2008). Additionally, the strength and persistence of wind events over the lake may be increasing as a result of the reduced water-air temperature gradients (Desai et al., 2009). This has implications for change to major circulation and vertical mixing events, as most are predominantly wind driven (Desai et al., 2009 and sources therein).

Lake Superior's water budget is much more hydrologically balanced than that of Lake Malawi. River output counts for 59.7% of major water losses and evaporation makes up the remaining loss (40.3%), while river input (with runoff included) and precipitation account for 43.5% and 56.5% of water contribution, respectively (Spigel and Coulter, 1996; Bootsma and Hecky, 2003). This illustrates a system much less reliant on evaporative loss and more equally influenced by major water inputs and outputs.

In Bootsma and Hecky's comparative study of African and North American great lakes (2003), Lake Superior had the lowest conductivity and dissolved ion concentration of the eight lakes in question. Though Lake Superior's flushing time of roughly 170 yrs is much longer than other Laurentian great lakes, it is much shorter than that of Lake Malawi (~700 yrs). The extremely low ion concentrations and conductivity despite its relatively long flushing time illustrates the unreactive nature of the granitic bedrock in

which the lake sits, which contributes little in the way of dissolved nutrients to the lake (Bootsma and Hecky, 2003). The dissolved silica content within Lake Superior is 38 times greater than that of Lake Ontario, and 4 times greater than that of Lake Michigan, though less than 0.001% of oceanic concentrations (Schelske, 1985). Concentrations of major metal ions are generally considered uniform across most of the lake, with slightly more variation seen in the far western arm adjacent to the city of Duluth, MN, though seasonality of nitrates and silica are observed in the surface layer as a result of annual production cycles (Weiler, 1978).

1.5.2 Geologic Setting and Historic Lake Levels

The Lake Superior basin exists almost entirely in the Canadian Shield, a large area of exposed Precambrian metamorphic and igneous rock which is highly resistant to weathering (Matheson and Munawar, 1978). Basin shaping was the result of multiple glacial erosion events, and lake formation began ~11,000 years ago as a result of both isostatic rebounding and ice shelf retreat, reaching deep water levels around 10,000 years ago. The major Sault Ste. Marie outlet formed roughly 2000 years ago, establishing the lake in its present form. Sediment underlying Lake Superior is 20-40m deep, and consists of a 10-30 m base of glacial till overlain by roughly 10 m or less of recently deposited material. Linear sedimentation within the lake is low, 0.1 – 2.0 mm/yr, and consists of relatively low organic content material rich in iron oxides (Matheson and Munawar, 1978). Since the initial fluctuations caused by isostatic rebound and melting ice shelves as the lake formed, lake levels have remained relatively constant since the occurrence of deep-water conditions.

1.5.3 Primary Production and Biota

Lake Superior is also classified as an oligotrophic lake. Nutrient structure of lake water is unique due to its relatively high surface water total nitrogen (20.4 – 31.9 $\mu\text{mol/L}$) and low total phosphorus (0.1 – 0.3 $\mu\text{mol/L}$) (Guildford and Hecky, 2000). This extreme stoichiometric imbalance has been a focus area of study, and it seems the discrepancy is

becoming further exacerbated as nitrate (NO_3^- , which accounts for ~80% of total water N) seems to have been increasing in concentration since the 1980's (Sterner et al., 2007). Early explanations for this NO_3^- buildup included the conclusion that much of the NO_3^- was sourced from atmospheric deposition to the lake (Ostrom et al., 1998). In contrast, by examining whole lake NO_3^- and total N budgets in conjunction with stable oxygen isotope analysis of NO_3^- and potential nitrate sources, Sterner et al. (2007) concluded that substantial amounts of the NO_3^- within the lake must originate from in-lake oxidation of reduced N forms. They suggested a number of mechanisms in support of their conclusion: a greater contribution from ammonia oxidizing microbes than previously recognized, recognizing that the biotic consumption of NO_3^- is generally constrained by the lack of phosphate availability, and inferring that denitrification may be limited since organic C within Lake Superior is not sufficient to induce the anoxic conditions (which can result from oxygen consumption during organic carbon decay) appropriate for high levels of denitrification (Sterner et al., 2007). Primary production in this unique nutrient system is extremely low in comparison to other great lakes of the world, just $65 \text{ g C m}^{-2} \text{ yr}^{-1}$, compared to $100 - 170 \text{ g C m}^{-2} \text{ yr}^{-1}$ in other Laurentian Great Lakes and 240, 290, and $1500 \text{ g C m}^{-2} \text{ yr}^{-1}$ in African lakes Malawi, Tanganyika, and Victoria (Hecky, 2000). In an extensive study of primary production in Lake Superior, lowest rates typically occurred at open lake sites, while the highest rates were measured at select nearshore locations (Munawar et al. 2009).

Unsurprisingly, the increase in water temperature of this temperate lake associated with the warming season between May and September also corresponds to an increase in phytoplankton biomass from about 70 to 150 mg/m^3 for that same time period (Munawar and Munawar, 1978). More recent research has reported much higher phytoplankton biomass, though a smaller relative increase from 948 to 1069 mg/m^3 between spring and late summer seasons (Munawar et al., 2009). Generally, phytoplankton in Lake Superior are dominated by phytoflagellates (53%) and diatoms (38%), with cyanobacteria and green algae making up the difference (Munawar and Munawar, 1978). Munawar et al. (2009) observed that diatom biomass increased by

~70% in the lake between spring and summer, while biomass of Cyanophyta decreased by 60%. This also resulted in an increase in average plankton cell size between the seasons, though spatial variability was high (Munawar et al., 2009). Lake Superior also supports a large and diverse community of picoplankton, organisms <0.3 μm , which are responsible for up to 50% of total primary production (Fahnenstiel et al., 1986). This group consists of eukaryotic flagellates, non-motile eukaryotic cells, and chroococcoid cyanobacteria including new species of *Synechococcus spp.* not described elsewhere (Fahnenstiel et al., 1986; Ivanikova et al., 2007). The zooplankton community is dominated by crustacean species, and biomass is often predominantly composed of copepods such as *Limnocalanus macrurus*, *Diaptomus sicilis*, and *Diacyclops thompsoni*, the three of which have been shown to make up 99% of the crustacean zooplankton biomass in May (Brown and Branstrator, 2004). Other important zooplankton species include cladocerans such as *Daphnia mendote*, *Bosmina longirostris*, and *Holopedium gibberum*, as well as the predators *Mysis relicta* and invasive *Bythotrephes longimanus*, and the benthic amphipods *Diporeia spp.* Fish species in the lake's offshore zone are characterized by deepwater scuplin (*Myoxocephalus thompsonii*), siscowet lake trout (*Salvelinus namaycush siscowet*), and the Coregonids kiyi (*Coregonus Kiyi*) and lake herring (*Coregonus artedi*). Nearshore fish communities are similar though include many more species in lower abundance, most notably rainbow smelt, wild lake trout, lake whitefish, longnose suckers, and sticklebacks (Gamble et al., 2011b). Despite the greater species diversity nearshore than offshore, both communities were found to have similar food web structures that are primarily supported by *Mysis* and *Diporeia* (Gamble et al. 2011b).

1.6 Objectives of this dissertation

The goal of this research was to carry out a comprehensive and systematic study of how organic matter cycles between, and within, different parts of large lake systems, and the results of that work are described in this dissertation. Research was approached in two parts; first, by focusing on organic matter that is deposited as lake sediments in

Lake Malawi, Africa. First, parameters traditionally used to characterize sediment organic matter and mineral composition were examined across a nearshore to offshore transect, to determine if proximity to shore was reflected by these values. Characteristics of sediment such as %TOC, %TON, $\delta^{13}\text{C}$, $\delta^{15}\text{N}$, Si:Ti, and diatom microfossil abundances were examined, and this work is described in chapter 2. Then, focus was placed on the organic carbon component of the same sediment transect in Lake Malawi, by using compound class specific radiocarbon dating in combination with stable isotope signatures to tease apart the sources and ages of this sediment-sequestered carbon. That work is presented in chapter 3. Research focus then shifted to the food web of Lake Superior, USA, to investigate how organic matter is transferred between trophic levels and major organisms. Compound specific stable nitrogen isotope (CSNIA) of amino acids was applied to characterize trophic position of major food web organisms, and radiocarbon signature of major zooplankton and fish species was applied to shed light on the age of carbon sources to the food chain. This work constitutes chapter 4 of this dissertation. Together, these studies provided a thorough and novel understanding of how carbon inputs are utilized, cycled, and preserved within large lakes.

Chapter 2: Characterizing sediment compositional change with water depth and distance from shore in a tropical rift lake

This chapter examines traditionally applied methods of paleolimnology to determine if sedimentary parameter response can in fact indicate proximity to lakeshore in a modern great lake system. Almost all parameters were found to reflect changing distance from shore and water depth in a manner consistent with their traditional interpretations in sediment records, which are often used to infer previous lake level and regional climate conditions. With increasing water depth and distance from shore, generally, grain size decreased while sediment water content increased, %TOC increased, and both $\delta^{13}\text{C}$ and C/N decreased, although each record records subtleties reflecting terrestrial input nearshore and changing water chemistry as distance from shore increased. Si:Ti also increased concurrently, and chemocline position was clearly reflected in the sedimentary record. Diatom microfossil abundance showed a shift from tychoplankton domination nearshore to planktonic species domination offshore, while benthic species contribution remained consistently low throughout.

2.1 Introduction

Discerning the history of hydroclimate in a lake catchment is a major goal of paleolimnology, and one way this is accomplished is by estimating historic changes in lake level. Environmental changes that influence local hydrology and lake level also induce considerable change in sediment composition, due to the heavy influence hydrologic balance has on lake water chemistry, ecosystem composition, and sedimentation processes (Scholz, 2002). This may lead to changes in sediment composition with water depth and distance from shore, for example in grain size, fossil assemblages, abundance and composition of organic and inorganic constituents (Gasse and Street, 1978; Hofmann, 1998; Winder and Schindler, 2004). These and other parameters preserved in the sediment record, such as C/N ratios in bulk organic matter, may therefore indicate historic proximity to lakeshore and influence from terrestrial

sediment sources, and subsequently past lake level and hydroclimate (Fritz, 1996; Alin and Cohen, 2003; Scholz et al, 2007).

In Lake Malawi, the southernmost of the East African great lakes, sandy horizons in some deep-water sediment cores have been interpreted as nearshore deposits, indicating past times of lower lake level (Finney and Johnson, 1991). Relative abundances of planktonic versus benthic diatom species in fossil assemblages have been used to infer lake level changes in Lake Malawi and other great lakes, and are a viable proxy due to the sensitivity diatom species exhibit to their aquatic environment (Owen and Crossley, 1992; Wolin et al., 2001; Gasse et al. 2002). The C/N ratio, in concert with carbon and nitrogen stable isotope composition of bulk organic matter in Lake Malawi sediment cores, has been interpreted to reflect aquatic versus terrestrial dominance of organic matter, and as an indication of proximity to shore and terrestrial inputs (Fillipi and Talbot, 2005).

While these indicators are widely applied, little examination of these parameters has occurred in the modern sediment of tropical rift lake basins to assess their actual sensitivity to water depth or proximity to lakeshore. The goal of this study was to determine which of these, and other, commonly applied sediment proxies may in fact vary systematically with distance from shore. We analyzed ten short cores from the northern basin of Lake Malawi, recovered along a depth transect from a major river mouth and extending into the lake's deep offshore basin. Developing a relationship between modern water depth (and therefore distance from shore) and sediment chemical signature serves as a test of past interpretations of historic lake levels from long sediment cores that were based on some of the parameters described above.

2.2 Methods

2.2.1 Sediment Collection

Ten short cores (M09-2MC to M09-11MC) were recovered with an Ocean Instruments Multi-Corer from the northern basin of Lake Malawi in 2009 aboard the Malawi Fisheries vessel F/V Ndunduma. The core sites were located on the prodelta

slope of the Songwe River, beginning approximately 7.8 km from the river mouth in 81.7 m depth and extending down into the lake's deep offshore basin to a depth of 386 m (Fig. 2.2.1). The core transect line was surveyed with a swept frequency pulse (CHIRP) seismic reflection profiling system (Fig. 2.2), and care was taken to avoid coring in slumped or disturbed areas. Upon recovery of the multi-corer, the top 3 cm of one of the four cores with a well-preserved sediment-water interface was extruded in 1cm intervals. Extruded horizons were placed in glass jars with Teflon-lined lids, and immediately frozen. The remainder of this core and a second whole core were capped and stored in a refrigerator at ~4° C prior to shipment back to the U.S. Cores and frozen samples were air-freighted back to the Large Lakes Observatory (LLO), for subsequent stratigraphic and sedimentological analyses.

2.2.2 Sediment Analyses

The completely intact core from each site was scanned for magnetic susceptibility and bulk density with a Geotek standard multi-sensor core logger at the LacCore facility at the University of Minnesota Twin Cities Campus. Each core was then split lengthwise into working and archive halves. The archive half was first digitally imaged with a DMT CoreScan Digital line scan camera and subsequently transported to LLO and scanned at 1 mm resolution for elemental analysis on an ITRAX X-ray Fluorescence Core Scanner (Cox Analytical Systems, 60 sec scan times using a Mo x-ray source set to 30 kV and 15 mA). The working core-half was sampled at LRC every 10 cm in core 2MC and every 5 cm in cores 3MC through 9MC for inorganic and organic elemental and isotopic analyses. Approximately 3-4 ml of wet sediment were extracted with a modified syringe and transferred to pre-weighed 5 ml vials for elemental and isotopic analysis. Additionally, smear slides were prepared at 3cm intervals from cores 2MC-9MC for microscopic analyses and 20-30 mg of surface sediment was collected for grain size analysis. Cores 2MC, 5MC, 8MC, and 9MC were subsampled for ²¹⁰Pb dating analysis.

Core subsamples were weighed pre- and post-freeze drying to determine water content. Total carbon and inorganic carbon were determined using a UIC Carbon

Coulometer calibrated to pure calcium carbonate. Duplicates were run every sixth sample and standards every ten samples. Total carbon measurements were obtained by six minutes of combustion at 950°C, inorganic carbon content was determined by exposing a second aliquot of the same sample to 2N HCl for six minutes. A Costech Elemental Analyzer coupled to a Finnigan Delta Plus XP Mass Spectrometer was used to determine total organic carbon, total organic nitrogen, $\delta^{13}\text{C}$ ($\pm 0.42\text{‰}$, accurate within 0.97%), and $\delta^{15}\text{N}$ ($\pm 0.15\text{‰}$, accurate within 5.6%) of bulk sediment after acid fumigation to remove carbonates. Briefly, after sediment was weighed into tin capsules, 10 μL of milli-Q water was added to each, and the samples were left in an enclosed dessication chamber with an open beaker of 12N HCl for 8 hours. Samples were then left on a 40°C hot plate covered lightly in foil for 8 hours to allow acid fumes to dissipate, then dried in a 60°C oven.

Relative abundances of diatom genera were determined by petrographic microscope examination of smear slides at a magnification of 200X. Quantification focused on common genera including *Stephanodiscus*, *Aulacoseira*, *Surirella*, *Navicula* and *Fragilaria* as well as diatom fragments. A minimum of 300 individuals or fragments were enumerated per slide for relative percent abundance calculation.

Grain size analysis of bulk surface sediments was conducted on a Beckman Coulter LS ¹³ 320 Laser Diffraction Particle Size Analyzer after removal of carbonates, organic carbon, and biogenic silica. Inorganic carbon was removed by treating the sample with 6M HCl for 2 hours in a 70°C water bath. Samples were subsequently rinsed in deionized water and centrifuged at 2800 RPM three times for HCl removal. Organic matter was removed by addition of 10% H₂O₂ and immersion in a 70°C water bath for two days, followed by three rinses as described above. Biogenic silica was removed by subjecting the sample to 0.5M NaOH for 45 min at 85°C. These samples were rinsed 4x in de-ionized water (as above) to ensure no residual NaOH remained to interact with inorganic sediment components. The prepared samples were then introduced to the grain size analyzer.

2.3 Results and Discussion

2.3.1 Si:Ti

The ratio of Si to Ti (each determined by XRF scanning) in 0-1 cm surface sediment is relatively stable at 0.05-0.06 in the first three near-shore cores (2MC-4MC), followed by a sharp drop to 0.02 in core 5MC and a steady linear increase ($R^2 = 0.96$) to 0.09 in core 9MC (Fig. 2.2d). The normalization of sedimentary silica content to that of titanium helps remove dilution effects, since titanium exists mainly within detrital mineral matrices and is therefore little affected by diagenesis (Brown et al., 2000). Furthermore, the XRF measured Si:Ti ratio in Lake Malawi has been shown to correlate linearly to the biogenic silica (BSi) content of sediment as: $\%BSi = 142.86(Si:Ti) - 7.14$ (Johnson et al., 2011). Therefore, the observed trend in surface sediment Si:Ti with water depth in Lake Malawi is a reflection of BSi content and preservation in the system.

The discrepancy in Si:Ti values between the first three cores and the following occurs at a depth where influence from the chemocline likely occurs. While the chemocline is typically believed to exist between ~170-200 m, chemocline boundaries are not static and the zone of altered water chemistry (including fluctuations between oxic and anoxic states) could reach 141 m where core 5MC was collected (Halfman, 1993; Vollmer et al., 2002). Water column profiling done in January of 2010 by Woltering et al. (in prep) showed the suboxic zone to extend to roughly 140 m water depth. However, the observed shift in Si:Ti is more likely a result of shifting Si source than an altered chemical condition of the water column. Although other researchers have proposed an increase in BSi preservation in anoxic bottom water due to a saturation of soluble reactive Si which discourages BSi dissolution (Bootsma et al., 2003), the inverse relationship between Si:Ti and sediment grain size across the sampling line (Fig. 2.2d) suggests the relative contribution of inorganic Si is shifting as distance from shore increases. Grain size has been found to correlate positively with quartz content in large lakes (Thomas, 1969), a mineral composed of SiO_2 . Therefore, the sharp drop in Si:Ti ratio at the 145m water depth is likely a reflection of decreasing quartz (and therefore silica) content of the sediments as distance from shore increases and larger grains settle

out of solution. The subsequently increasing Si:Ti ratio as water depth increases likely reflects the greater relative influence of BSi production on sediment silica content at more open lake sites.

Some downcore vertical structure is apparent for Si:Ti, namely in cores 4MC and 6-8MC, which show generally increasing Si:Ti with core depth. Considering downcore Si:Ti values between coring sites, there is a general trend of lower values found in the most nearshore cores, increasing with water depth and distance from shore (Fig. 2.3). Core 5MC is an obvious outlier to this trend, with the depressed values seen in this core's surface sediment propagated downcore. There is no evidence to suggest this core is disturbed or is influenced by turbidites, as indicated by ^{210}Pb data (discussed below). Over much longer geologic timescales than is represented by these cores, periods of increased Si:Ti in Lake Malawi's northern basin sedimentary record are interpreted either as periods of increased riverine transport of dissolved silica to the lake, low lake level (if fossilized periphytic diatom abundance is also high, indicating a shift in habitable benthic surface area), or a period of predominant or strong northerly winds in the region promoting upwelling, production, and subsequent diatom burial in the north basin (Johnson et al, 2011, Brown et al, 2007, Johnson et al., 2002). Given the results presented here from a nearshore to offshore examination of surface sediment Si:Ti, it becomes apparent that consideration for the relative contribution of mineral silica sources versus biogenic sources must be included in paleoclimate interpretation of Si:Ti records. Though, again, a large shift in Si:Ti sedimentary record may be attributed to shifting chemocline position affecting the silica dissolution rate. A shifting chemocline would also affect sedimentary preservation of metal species, as a changing redox state affects dissolution and precipitation of numerous metal species. Brown et al. (2000) used downcore concentrations of multiple metal species to infer past lake conditions and resulting chemocline shifts in a core from Lake Malawi's central basin. Of the cores in this study that exhibit downcore trends in Si:Ti, there were no apparent concurrent downcore trends in Fe, Mn, or Al concentration (as analyzed by XRF, data not shown here), indicating that there was no significant shift in chemocline across the timeframe

represented by these cores. This also supports the previous conclusion that the large variation in Si:Ti seen in nearshore to offshore surface sediment is reflective of shifting contribution from different silica source pools.

2.3.2 Elemental and Isotopic Analysis

Elemental composition and isotopic signatures of sediment in this study are consistent with other reported values for the northern basin of Lake Malawi (Filipi and Talbot, 2005; etc etc). Surface sediment (0-1 cm) percent total organic carbon (TOC) increased from ~2% in nearshore cores to values of 3-4% in the most off-shore cores, while total organic nitrogen (TON) content also increased steadily from ~0.2% in nearshore cores to ~0.4% in the most offshore cores (Fig. 2.2a,b). The decrease in %TOC in the most nearshore cores likely reflects dilution by clastic material from river inflow. TOC content often increases as grain size decreases in aquatic systems as a result of differing sediment density, porosity, and adsorption ability between grain sizes (Thompson and Eglinton, 1978; Burdige, 2007), a trend that is confirmed here with comparison to the surface sediment grain size record of these cores (Fig. 2.5).

Resulting surface sediment C/N ratios (by weight) decreased from roughly 10 in nearshore cores to 8.3 in the deepest offshore core (Fig. 2.2c). C/N ratio is a common parameter used in the interpretation of both modern and paleo sedimentary organic matter source, with fresh phytoplanktonic OM having C/N values of 4-10, while that of vascular plants is often over 20 (Meyers and Teranes, 2002). It has been shown, however, that primary producers in highly N-limited systems can produce OM with significantly higher C/N (Healy and Hendzel, 1980). This is noteworthy, as Lake Malawi has been shown to experience both N and P limitation (Guildford et al., 2003). Subsequently, Hecky (1993) has proposed that in Lake Victoria phytoplankton produce OM with C/N <8.3 without N limitation, 8.3-14.6 under moderate N limitation, and can achieve values >14.6 under severe physiological N-limitation. However, C/N values of sedimentary OM resulting from each N-limitation situation are likely slightly higher, as sedimentation and diagenesis tend to selectively consume N within the first few centimeters of sediment,

beyond which C/N values stabilize. Talbot and Laerdal (2000) suggest that sedimentary C/N increases by roughly 5 units within the first three centimeters of Lake Victoria surface sediment. To account for the likelihood that OM was produced under N-limiting conditions in that lake, they added 5 to the ranges proposed by Hecky (1993) to allow for interpretation of OM source using downcore C/N values that had been altered by diagenesis. The 0-1 cm surface sediment C/N values reported in this study (Fig. 2.2c) are well within the range of predominant photosynthetic production, and in comparison to the N-limitation scenarios proposed for Lake Victoria, fall within the range of no N-limitation assuming some effects of diagenesis, or moderate N-limitation assuming little effects of diagenesis. Recently obtained biomarker abundance values from sinking particulates collected from sediment traps in Lake Malawi show that biomarkers of N-fixing cyanobacteria (heterocystous glycolipids) vary seasonally in abundance. This indicates seasonal variation in nitrogen limitation, as cyanobacteria are most abundant when there is some degree of N-limitation (Werne, J., University of Pittsburgh, personal communication).

Surface sediment $\delta^{13}\text{C}$ decreased from about -22‰ nearshore to -24.9‰ offshore (Fig. 2.2e), while $\delta^{15}\text{N}$ is enriched in nearshore cores, around 2.7‰, decreasing rapidly at 4MC, and continuing to decline to about 0.5‰ in the most offshore cores (Fig. 2.2f). While these $\delta^{13}\text{C}$ values overlap with the range typically associated with C3 land plants (C3 plants: $\delta^{13}\text{C}$ -25 to -35, C4 plants: $\delta^{13}\text{C}$ -10 to -16), the very low corresponding C/N values indicate a prominent lacustrine algae source at all sampling locations (Meyers, 1997). The slightly heavier $\delta^{13}\text{C}$ values nearshore may reflect limited influence of carbon sourced from maize, a C4 agricultural crop that has increased in cultivation within the Lake Malawi watershed in recent decades (Orr, 2000; Heck et al. 2003). While C/N values in this range could also reflect contribution from soil or sediment microbial sources (Peterson and Fry 1987; Fry 1991), the increasing BSi through this transect (as described above) supports the interpretation of diatom predominance, particularly as water depth increases. Therefore, the depletion of $\delta^{13}\text{C}$ and decreasing C/N in combination with the increasing Si:Ti indicates the recently deposited surface sediment

becomes more aquatic in nature as water depth and distance from shore increase. This interpretation is consistent with multiple studies that have used a similar combination of parameters to draw conclusions about the aquatic versus terrigenous nature of lake sediments (Meyers, 1997; Tenzer et al., 1997; Talbot and Laerdal, 2000).

Interpretation of the bulk sediment stable nitrogen isotopic signature is more complex, as these values are affected by both the dissolved inorganic nitrogen (DIN) sources and metabolic pathways of N assimilation. Furthermore, multiple organism groups and metabolic pathways produce organic matter with overlapping $\delta^{15}\text{N}$ ranges (Meyers and Teranes, 2002). The difference in $\delta^{15}\text{N}$ produced by N-fixation versus nitrate utilization is perhaps the most exploited comparison with regard to assessing sediment N source. Dissolved nitrate (NO_3^-), the DIN species most utilized by aquatic algae for primary production, is expected to have a $\delta^{15}\text{N}$ signature between +7 to 10‰, although this range seems to be more variable in lakes than in marine systems. OM produced by algae utilizing NO_3^- typically exists in a slightly larger $\delta^{15}\text{N}$ range, from -3‰ to +18‰, as a result of metabolic differences and kinetic fractionation (Cifuentes et al, 1988; Fogel and Cifuentes, 1991 and sources therein). Direct fixation of atmospheric N, however, involves little fractionation (Fogel and Cifuentes, 1991). Atmospheric nitrogen exists at 0‰, and organisms that rely on N-fixation also produce OM with $\delta^{15}\text{N}$ values from -2 to +2‰ (Minagawa and Wada, 1986; Peterson and Holworth, 1987). Though the decline in surface sediment $\delta^{15}\text{N}$ in this study (Fig. 2.2f) could reflect increased contribution from N-fixing cyanobacteria as water depth and distance from shore increase, Gondwe et al. (2008) found higher rates of N-fixation in Lake Malawi's southern basin surface water occurred at nearshore rather than offshore locations, though the southern basin is very different from the northern in hydrologic and chemical cycling. That finding also contradicts the relative importance of N-fixation to the lake, as it is known to be by far the most important source of N to this and other great African lakes, supplying 78% of total N to Lake Malawi (Bootsma and Hecky, 1993; Hecky et al., 1996). The increased $\delta^{15}\text{N}$ values in nearshore sediment could then indicate increased utilization of more enriched N sources, potentially from higher plant production or

anthropogenic inputs in addition to the baseline N-fixation contribution. This is a feasible result of watershed fertilization and land use changes, which are ongoing in the Lake Malawi watershed, but likely have the most influence in the southern basin of the lake (Orr, 2000; Hecky et al., 2003). The $\delta^{15}\text{N}$ signature of OM from higher plants and that of natural fertilizer or human waste often overlap. Fertilizers made from natural material (waste or compost) usually have $\delta^{15}\text{N}$ values from +3 to 30‰ (Teranes and Bernasconi, 2000; Kendall et al., 2007). However, the production method used in the manufacture of synthetic fertilizers results in a $\delta^{15}\text{N}$ signature closer to 0‰, and usually -4 to +4‰ (Kendall et al., 2007).

In age-modeled cores 2MC, 5MC, 8MC, and 9MC, some vertical structure and differences between core locations are evident. Percent TOC increases as water depth and distance from shore increase at most core horizons (Fig. 2.4a). Core 2MC appears the most distinctly unique of these four cores, having the greatest C/N, and most enriched $\delta^{13}\text{C}$ and $\delta^{15}\text{N}$ at all core horizons. Generally, the magnitude of variation in parameters resulting from different coring locations is greater than variation observed downcore.

2.3.3 Water Content, Grain Size, and Sedimentation

Percent water content of surface sediment increases steadily ($R^2 = 0.92$) from 54% nearshore (core 2MC) to 82% in core 9MC (Fig. 2.5). Modal grain size was consistent around 9.4 μm in cores 2MC-4MC, then decreased as water depth and distance from shore increased, reaching a modal value of 5.4 μm in core 10MC (Fig. 2.5). Average grain size follows a similar trend although values are larger (16 μm nearshore to 8-10 μm at depth) and the decreasing size trend is less consistent. The modal grain size therefore is a more accurate representation of grain size trends in this sample set. The decrease of sediment grain size with water depth is an expected result; winnowing and wave action mobilize small grains more readily (and those contained in river inflow remain mobilized more easily), and their extended suspension time allows for transport to deep offshore locations before sinking out of the water column (Meyers and Terranes, 2002). Increasing sediment water content with increasing water depth is also an expected

result. The well-sorted fine sediments that accumulate in deep offshore basins have higher porosity than nearshore sediment of mixed sizes, allowing for greater water saturation.

Due to the inverse relationship between grain size and TOC concentration described previously, other parameters are often employed to shed light on sedimentation patterns and subsequent carbon accumulation. The slope of sediment age versus depth is very similar in all four age modeled cores in this study (2MC, 5MC, 8MC, 9MC) (Fig. 2.6a), indicating relatively consistent sedimentation patterns throughout this sampling transect without the influence of large sediment disturbances such as turbidity flow events. The resulting linear sedimentation rate (LSR) is also similar between these four age modeled cores (Fig. 2.6b), with values of 0.4 - 0.6 cm/yr near the surface sediment, and decreasing with core depth to 0.1 to 0.3 cm/yr. Mass accumulation rate (MAR) and TOC-MAR (%TOC x MAR) are often calculated as an alternative to %TOC for investigation of sediment delivery and preservation. These terms account for differences in sediment porosity and density, which contribute to the grain size/TOC relationship described above. MAR ($\text{g}\cdot\text{cm}^{-2}\cdot\text{yr}^{-1}$) was calculated by:

$$\text{MAR} = \text{LSR} \cdot (1-p) \cdot d$$

where p = sediment porosity and d = sediment density. Core 2MC shows distinctly higher MAR and TOC-MAR than all other age-modeled cores at all sampled core horizons, often double and sometimes triple the values of the most proximal core at all horizons (Fig. 2.6c,d). While sedimentation is expected to be greatest at nearshore locations in all aquatic systems (Burdige, 2007), these exaggerated sediment and carbon accumulation rates in the most near-shore core 2MC may also reflect changing land use in the Lake Malawi watershed. Deforestation and cultivation of new agricultural land disturbs soil horizons and mobilizes fine particles that are transported to rivers during runoff and erosion events (Hecky et al, 2003) and are subsequently deposited in Lake Malawi sediments. Areas of the Lake Malawi watershed experiencing such land use changes are increasing in both abundance and scale (Orr, 2000). While this speculation of changing land use influence is potentially supported by the stable nitrogen isotope

ratios as discussed above, more specific investigations are necessary before this high accumulation rate can be unambiguously linked to land use changes, such as isotopic ratio quantification of carbon and nitrogen found in runoff and riverine organic matter.

2.3.4 Diatom Relative Abundance

Diatom microfossils enumerated from surface sediment (1 cm) smear slides of cores 2MC-9MC reveal a shift in relative percent abundance of different diatom genera with increasing water depth and distance from shore (Fig. 2.7). A total of 54 diatom species or genera were identified, and classified into one of three groups based on known life strategies: planktonic (*Aulacoseiroid*, *Cyclostephanoid*), tychoplanktonic (*Fragilarioid*, *Nitzschioid*) and benthic diatoms (*Monoraphid*, *Naviculoid*, *Gomphocymbelloid*, *Rhopalodoid*, *Surirelloid*). Tychoplanktonic diatoms were the most abundant group in nearshore surface sediments at 46%, followed by 35% planktonic diatoms and 19% benthic diatoms. As water depth and distance from shore increase, relative abundance of tychoplanktonic and benthic diatom microfossils decrease. Concurrently, planktonic diatoms increase and become the most dominant diatom microfossil from 5MC on, reaching 62% relative abundance in core 9MC while tychoplanktonic and benthic microfossils constitute 29% and 9%, respectively. This switch in diatom community structure has not been described by previous studies of Lake Malawi diatom fossils, which have concluded that the northern basin of Lake Malawi is particularly dominated by planktonic *Aulacoseira* and *Stephanodiscus* (included in the *Cyclostephanoid* group) (Owen and Crossley, 1992; Otu et al., 2011). However, coring locations of those studies did not extend to include near shore locations, focusing instead on deep open lake sites. Our results, showing dominance of planktonic diatoms at the most offshore locations, are therefore consistent with interpretations made by other investigators for deep lake locations. However, our nearshore to deep-lake sampling scheme clearly exposes habitat dependent community structure changes based on proximity to lake shore. This helps to validate numerous paleolimnological studies that have exploited this relationship to help interpret past lake level (and subsequently

hydroclimate) conditions from fossilized diatom remains in long cores (Gasse et al., 2002; Otu et al., 2011)

2.4 Conclusion

Sediment parameters measured in this study showed directional shifts in value as distance from shore and water depth increased. This suggests that, barring substantial post-depositional diagenesis, these parameters likely record changes in proximity to shoreline within the sedimentary record. Extreme shifts in Si:Ti may reflect marked changes to chemocline position in meromictic lakes. When interpreting C/N ratios, care should be taken to assess the concurrent trophic position of the lake at the time in question, as nutrient limitation can affect the ratio of elements in biomass fixed by primary producers such that traditional source interpretations are skewed. Nitrogen isotopic signature and the exaggerated MAR in nearshore sampling areas, while likely due to a combination of influences, may reflect recent land use shifts in the Lake Malawi basin, influences that need to be taken into account when interpreting recently deposited material. We found traditional designations of basin-scale diatom abundance did not apply to the nearshore sampling zones, where a distinct abundance of tychoplanktonic species dominated, transitioning to dominance by planktonic groups with increasing distance from shore and water depth. Though diatom microfossil preservation is affected by the dissolved silica concentrations that occur near the sediment-water interface, ratios of diatom abundance preserved in sediment records may be indicative of shifting proximity to shoreline, if it can be concluded that species specific preservation issues have not occurred. In sum, we conclude that this group of parameters typically applied in paleolimnological sediment assessment can infer proximity to lakeshore, as is traditionally assumed.

Table 2.1. Core names of short cores collected from Lake Malawi's northern basin in 2009, and their associated water depth at coring location and distance from the nearest lake shoreline.

Core	Water Depth at Coring Location (m)	Distance from Nearest Lakeshore (km)
2MC	82	2.16
3MC	98	2.97
4MC	116	4.48
5MC	141	6.42
6MC	157	7.81
7MC	181	9.65
8MC	197	10.8
9MC	220	12.4
10MC	301	20.38
11MC	386	21.25

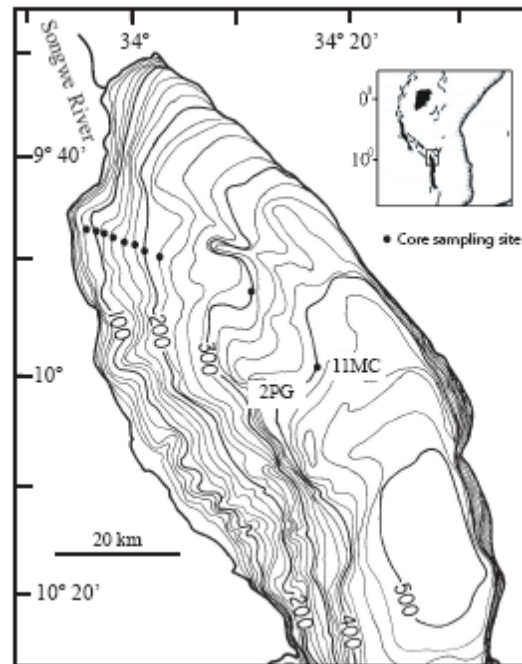


Figure 2.1. Coring locations in Lake Malawi's northern basin, core 2MC is the most nearshore core in the sampling line (82 m water depth), and core names increase numerically until core 11MC (demarked) at 386 m water depth.

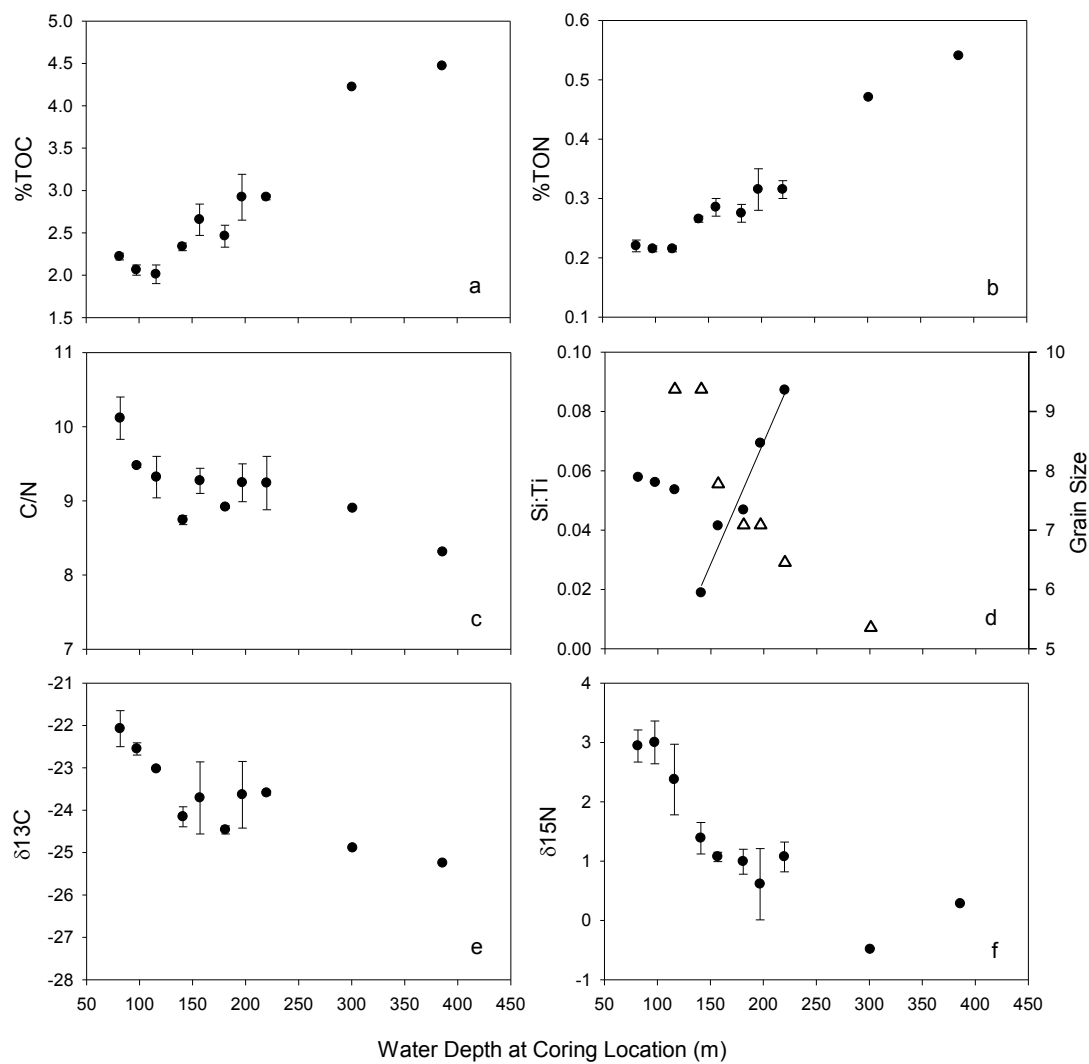


Figure 2.2. Bulk surface sediment (0-1 cm) parameters (a) %TOC, (b) %TON, (c) C/N, (d) Si:Ti (filled circles) where the increase in Si:Ti from 5MC to 9MC is described by $y = 0.00082x - 0.0947$, $R^2 = 0.96$, and modal grain size (open triangles, in μm) (e) $\delta^{13}\text{C}$ in ‰, and (f) $\delta^{15}\text{N}$ in ‰, for cores 2MC – 11MC. Error bars (where present) represent average error between duplicate analyses.

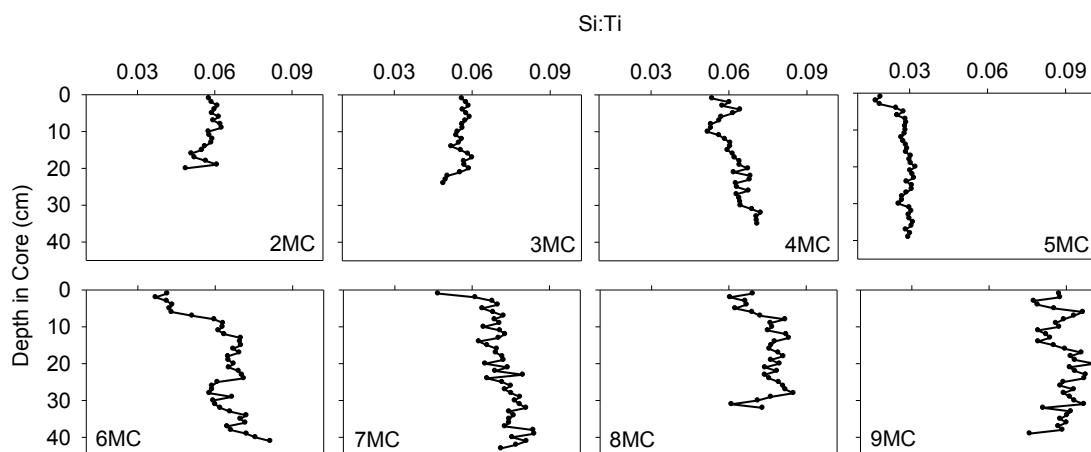


Figure 2.3. 10 mm averaged Si:Ti values with depth in core for cores 2MC through 9MC as obtained by XRF scanning.

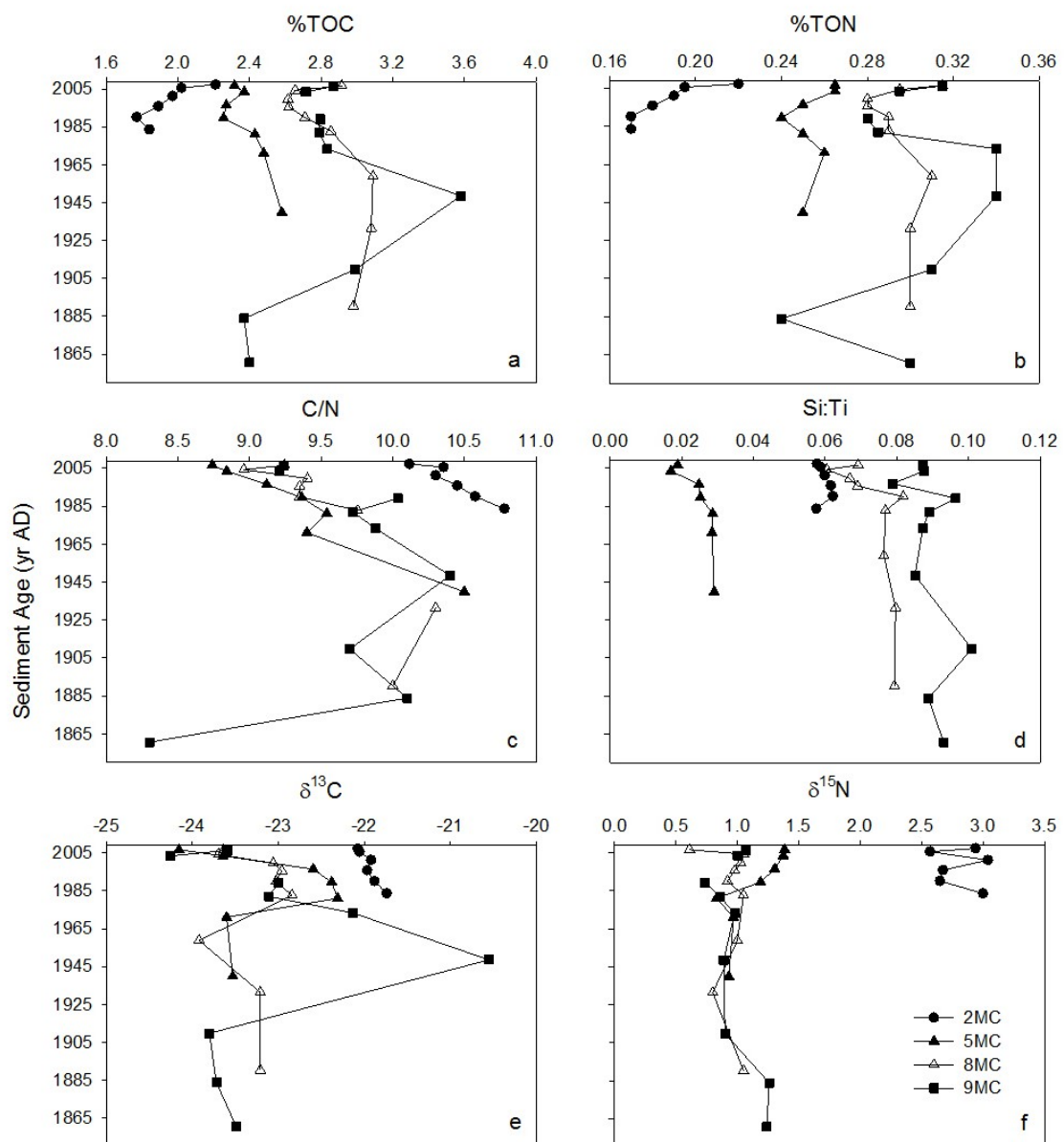


Figure 2.4. %TOC (a), %TON (b), C/N (c), Si:Ti (d), $\delta^{13}\text{C}$ (e), and $\delta^{15}\text{N}$ (f) with depth in Pb-210 age-modeled cores. The five parameter values nearest the core top represent average values of analyses 0.5 cm above and below the level of age determination.

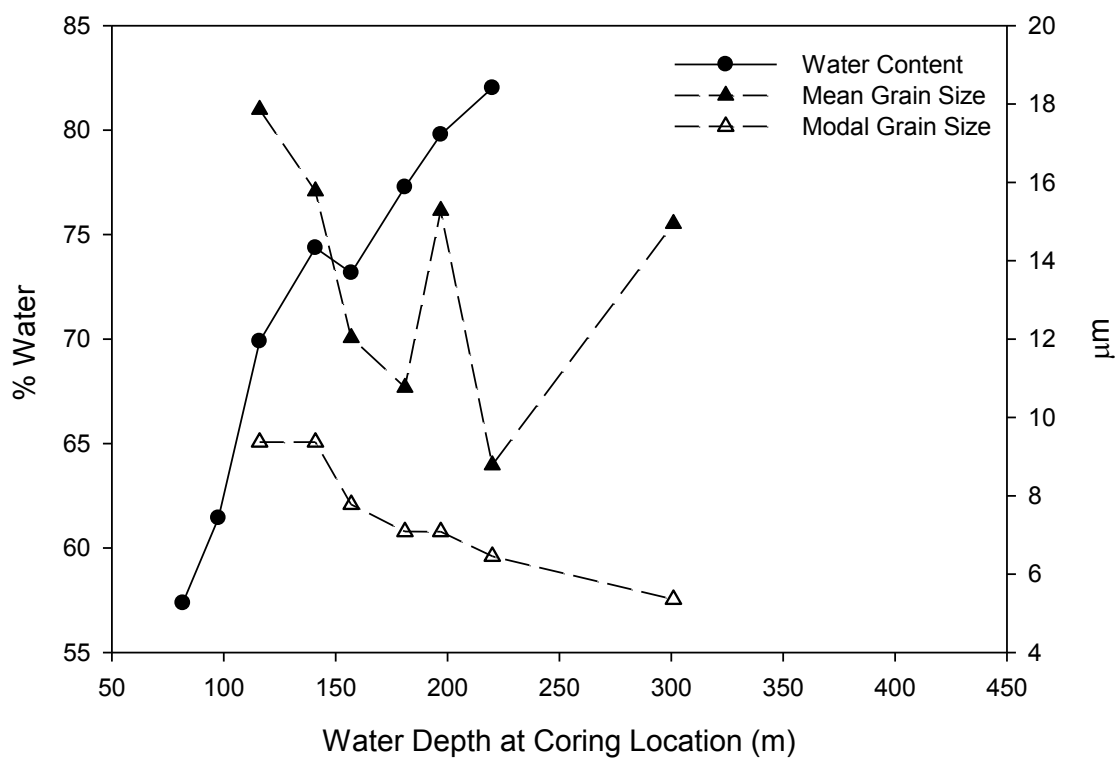


Figure 2.5. Surface sediment (0-1 cm) percent water content by weight (filled circles) for cores 2MC – 9MC, and mean (filled triangles) and modal grain size (open triangles) for cores 4MC – 10MC, in μm .

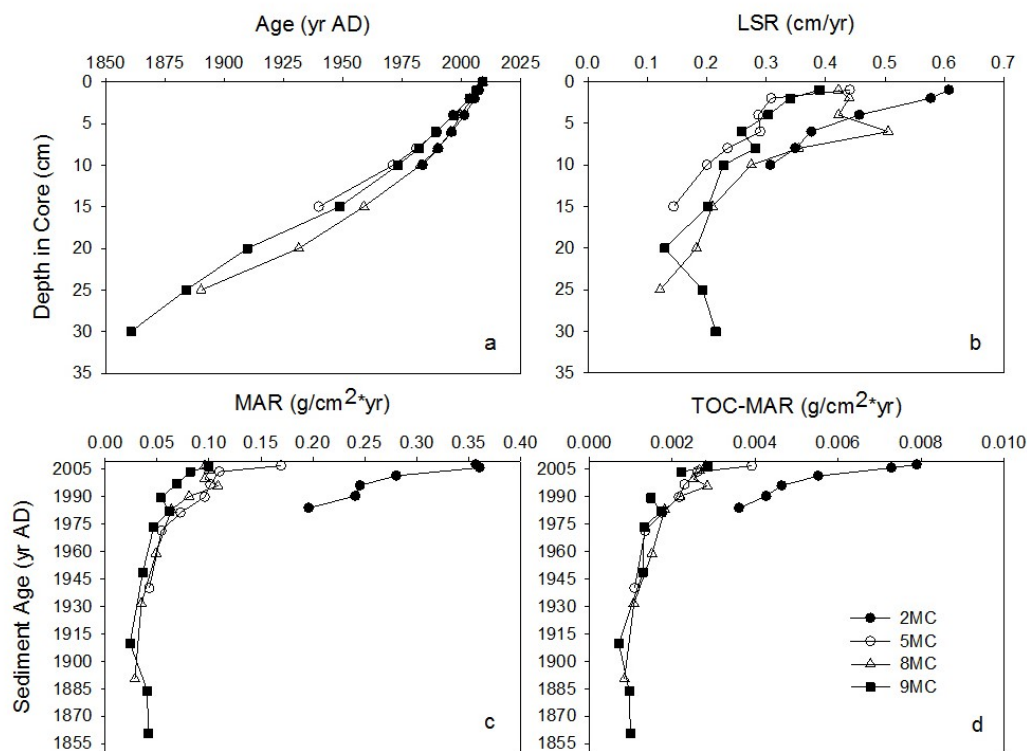


Figure 2.6. (a) Age vs. Depth of Pb210 dated cores 2MC, 5MC, 8MC, and 9MC (b) Calculated linear sedimentation rate; (c) calculated mass accumulation rate; and (d) calculated total organic carbon mass accumulation rate for age modeled cores 2MC, 5MC, 8MC, and 9MC.

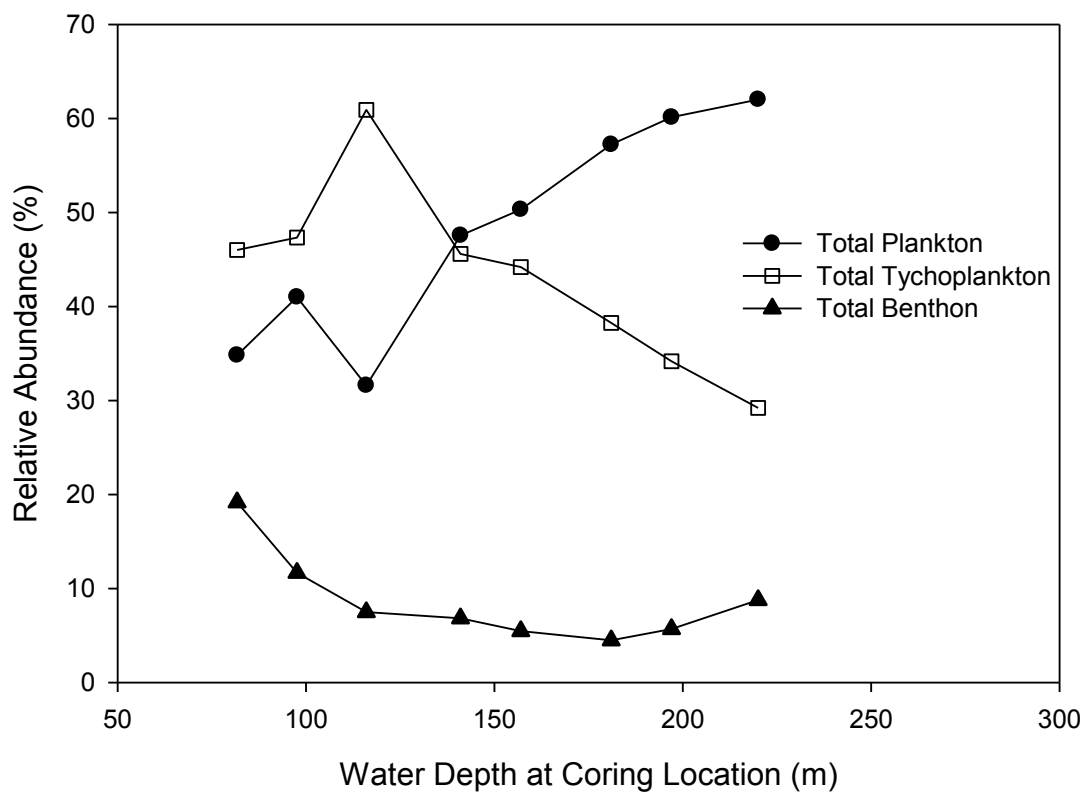


Figure 2.7. Diatom relative percent abundance as enumerated from surface sediment (1 cm) smear slides of cores 2MC – 9MC, divided into planktonic, tycho planktonic, and benthic life strategy groups.

Chapter 3: Sources and cycling of Lake Malawi organic carbon: insights from multi-fraction stable isotope and radiocarbon analyses of sediments

This chapter examines the source of organic carbon that is ultimately deposited as sediment in Lake Malawi, Africa, as water depth and distance from shore increase. A multi-fraction approach was applied, in which bulk sediment, the acid insoluble protokerogen fraction, total lipids, and specific aquatic and terrestrial biomarkers (short and long chain *n*-alcohols) were analyzed for stable carbon and radiocarbon isotopic signature. Surface sediment was modern across the nearshore to offshore transect and dominated by aquatic input throughout, although influence from riverine input is evident in the most nearshore locations. Protokerogen stable isotope signature tracked that of the bulk sediment. Lipids were ^{13}C depleted throughout the sampling transect, but also very ^{14}C -depleted at the most nearshore locations, indicating an aged lipid carbon source that ultimately derives from similar sources as lipids at more offshore locations.

3.1 Introduction

The rift lakes of East Africa are some of the largest and oldest in the world. Sediment accumulation in the deep basins of lakes Malawi and Tanganyika has been ongoing for roughly 10-15 million years (Cohen et al., 1993). The result is over 4 km of underlying sediment in some areas (Rosendahl, 1987), containing the microfossil, structural, and chemical signals that correspond to millennia of lake changes. These continuous records are exploited by paleolimnologists to reconstruct historic hydrologic and climatic conditions of the tropics.

Furthermore, sediments accumulating in large lakes are often rich in organic carbon (Alin and Johnson, 2007), which can lead to concentrated hydrocarbon reserves with fossil fuel development potential (Killops and Killops, 2005). Continental rift systems such as that occupied by Lake Malawi, the southernmost of the great African rift lakes, are known to produce conditions favorable for such fossil fuel production in freshwater systems (Robbins, 1983; Frostick and Reid, 1990). The type of fossil fuels

produced from lacustrine carbon deposits is influenced in part by the proportion of aquatic to terrestrial compounds present in the parent organic matter (Killops and Killops, 2005), a ratio that remains unelucidated in Lake Malawi (29,600 km²).

Lake Malawi is the southernmost of the East African rift lakes and the fifth largest lake in the world by volume. It exists in tropical climate but is far enough south of the equator to experience seasonal cycling of wind, precipitation, and temperature driven by the migrating Intertropical Convergence Zone (ITCZ) (Eccles, 1974). The lake is meromictic and water below ~250 m remains anoxic and does not mix with the independently circulating oxygenated water above it (Eccles, 1974; Bootsma and Hecky, 2003). This permanently anoxic hypolimnion may facilitate high sulfur removal rates and rapid denitrification of lake water, as well as high phosphorus mobilization rates resulting in biological nitrogen limitation (Bootsma and Hecky, 2003).

Some have concluded sedimentary organic carbon in Lake Malawi is derived primarily from in-lake phytoplankton production based on bulk sediment analysis of carbon and nitrogen isotopes, hydrogen index, and coupling with microscopic sediment examination (Filippi and Talbot, 2005). Conversely, the isotopic signature of bulk sediment has been shown to track that of the corresponding long chain *n*-alkane sediment fraction (Castaneda et al., 2007). These compounds are most often derived from terrestrial plant sources (Eglinton and Hamilton, 1967; Pearson and Eglinton, 2000; Volkman, 2006) indicating much sedimentary organic matter could be derived from terrestrial rather than aquatic sources (Castaneda et al., 2007).

Recent analytical advances are facilitating a greater understanding of carbon cycling processes. Stable and radiogenic carbon isotope quantification of bulk soil and sediment has long been employed by geochemists to describe provenance and age of organic matter (Ingalls and Pearson, 2005; Hajdas, 2009). Now, advances in compound separation techniques such as preparative capillary gas chromatography (PCGC) also allow for stable carbon isotope ratio ($\delta^{13}\text{C}$) and natural abundance radiocarbon analysis of individual compounds from complex natural samples (Eglinton et al, 1996; Pearson et al., 1998). Such isolation and analysis of lipid biomarkers affords more precise

interpretations of sedimentary organic matter sources and temporal cycling differences among sediment constituents.

This study sought to clarify the terrigenous versus aquatic origins of recently deposited organic matter in Lake Malawi sediments and to compare the relative age of each fraction as distance from land increased. This was accomplished through isolation of *n*-alcohol biomarkers of both aquatic and terrigenous origin from Lake Malawi sediments. While less commonly applied than other biomarkers to infer organic matter provenance, previous investigation of Lake Malawi sediments revealed *n*-alcohols to be abundant enough to make successful compound-specific radiocarbon analysis likely. The exact sources of these saturated straight chain biomarkers can be ambiguous (Volkman et al., 1998), though they can be sourced from breakdown products of wax ester compounds produced by plants (Meyers and Ishiwatari, 1993) and may serve as important food reserves or buoyancy regulators in copepod and other plankton species (Lee et al., 1971). The length of the associated carbon chain for these compounds is dependent on source: terrestrial plants produce long chain *n*-alcohols (C₂₆+) while aquatically produced *n*-alcohols yield shorter chain lengths (Meyers and Ishiwatari, 1993). *N*-alcohols have been demonstrated to be robust biomarkers resistant to degradation, and the proportion of long to short chain compounds has been shown to accurately record terrigenous versus aquatic organic matter source in multiple systems and in both anoxic and oxic environments (Fukushima and Ishiwatari, 1984; Kawamura and Ishiwatari, 1985; Grossi et al., 2001). Lake Malawi sampling locations transected the prodelta slope from two adjacent perennial river mouths into the deep offshore basin of the lake to capture a zone of transition between high terrestrial influence and deep open-lake conditions. Biomarkers were analyzed for natural abundance radiocarbon content and corresponding $\delta^{13}\text{C}$ signatures. The same analyses were also performed on bulk sediment and total extracted lipids, as well as a highly recalcitrant acid-insoluble organic carbon fraction isolated from all sediment samples. This fraction is referred to as 'protokerogen' and provides insight to the nature of organic carbon preserved long term in sedimentary records (Tegelar et al., 1991; Aycard et al., 2003).

3.2 Methods

3.2.1 Sediment collection

Ten short cores (2MC to 11MC, Table 3.1) were recovered with an Ocean Instruments Multi-Corer from the northern basin of Lake Malawi in 2009 aboard the Malawi Fisheries vessel F/V Ndunduma. The core sites were located on the prodelta slope of both the Songwe River and North Rukuru River, beginning approximately 7.8 km from the river mouths in 81.7 m water depth (between the two river mouths) and extending into the lake's deep offshore North basin to a water depth of 386 m (Fig. 3.1). The core transect line was surveyed with a swept frequency pulse (CHIRP) seismic reflection profiling system, and care was taken to avoid coring in slumped or disturbed areas. Upon recovery of the multi-corer, the top 3 cm of one of the four cores with well-preserved sediment-water interface was extruded in 1-cm intervals. Extruded horizons were placed in glass jars with Teflon-lined lids, and immediately frozen. Remaining core lengths were capped and refrigerated at ~4°C. Cores and sections were air freighted to the Large Lakes Observatory (U.S.A.) for additional sectioning and analysis. Individual 1-cm horizons from each core were freeze-dried and homogenized, and ranged from 1 – 33 g (total dry weight), with lighter values resulting from upper core horizons with higher water content. Bulk sediment elemental and isotopic analysis for each horizon occurred at the Large Lakes Observatory using a Costech ECS 410 elemental analyzer (EA) coupled to a Finnigan DELTA^{Plus} XP isotope ratio mass spectrometer (IRMS). Stable isotope ratios are reported as $\delta^{13}\text{C}$ and $\delta^{15}\text{N}$ and represent the ratio of isotopes in the sample relative to a standard, which was VPD Belemnite carbonate for $\delta^{13}\text{C}$ and atmospheric air for $\delta^{15}\text{N}$. Stable carbon isotope ratios (both from LLO and reported by NOSAMS for sediment fractions obtained during radiocarbon analysis) are expressed in conventional delta (δ) notation in per mil (‰) deviations from a standard, according to the equation:

$$\delta x (\text{‰}) = ((R_{\text{sample}} - R_{\text{standard}})/R_{\text{standard}}) * 1000$$

where R is the ratio of the heavier to lighter isotope in question and x is the element whose isotopic ratio is being measured (e.g., C or N in this research). $\delta^{13}\text{C}$ precision is $\pm 0.42\text{‰}$, and is accurate within 0.97%, $\delta^{15}\text{N}$ precision is $\pm 0.15\text{‰}$, and is accurate within 5.6%.

3.2.2 Lipid extraction

Resulting sediment samples underwent lipid extraction via DIONEX accelerated solvent extraction (ASE) using 9:1 DCM:MeOH (all solvents for lipid preparation were Fisher Optima grade). Total lipid extract (TLE) from horizons comprising the top 4 cm (top 5 cm for core 9MC, and top 3 cm for core 10MC) of each core were combined and homogenized to ensure isolation of sufficient material for compound-specific radiocarbon measurements from each coring location. Based on previous ^{210}Pb age modeling of this same suit of cores, the top 4 cm of sediment represent the last 10 – 14 years of sediment accumulation (Kruger et al., in prep). Elemental sulfur was removed from the TLE by exposure to copper beads activated with HCl rinsing and cleaned with solvent rinsing after Wakeham and Pease (1992), although due to the high elemental sulfur content of the Lake Malawi TLEs activated copper beads were placed directly into lipid extracts, rather than passing the TLE through a column containing activated copper. Copper beads were allowed to sit in TLEs for at least 24 hours, and a black coating was observed to form on the beads as CuS formed.

The TLE was then separated into neutral, free fatty acid, and phospholipid fatty acid fractions on Orchem Tech Inc. aminopropyl-bonded silica powder packed into large volume glass columns to a height of $\sim 1/3$ the column ($\sim 5\text{g}$ silica). Packed columns were then cleaned prior to sample loading with 3 full column volumes of both methanol (MeOH) and 2:1 dichloromethane (DCM):isopropyl alcohol. Neutral, free fatty acid, and phospholipid fatty acid fractions were eluted with 2:1 DCM:isopropyl alcohol, 4% acetic acid in ethyl ether, and MeOH, respectively. Neutral fractions were further separated into apolar and polar fractions using activated alumina column chromatography (using activated alumina hand packed into glass pipettes) with 9:1 hexane:DCM and 1:1

DCM:MeOH, respectively. An internal standard (1-nonadecanol) injected directly onto the bulk sediment before extraction, then quantified from the isolated polar fraction seems to indicate only an 8.6% *n*-alcohol recovery between the bulk sediment and polar fraction. Neutral-polar fractions were filtered by gentle N₂ pressure across ashed GFF filters packed into pipette tubes, then separated into compound-class fractions using long-silica column chromatography as described by Wakeham and Pease (1992). L5 and L6 fractions were combined to ensure complete recovery of alcohols, as preliminary GC/MSD analysis showed *n*-alcohols consistently eluting in both fractions.

Cyclic and straight chain alcohols were separated through urea adduction after Pearson and Eglinton (2000). Briefly, 40 mg/mL urea/MeOH solution was introduced to the L5/L6 fraction dissolved in 2:1 (v/v) hexane:dichloromethane, shaken, and allowed to sit in an ice bath for 5 minutes. This causes precipitation of urea crystals, which entrap straight chain alcohols (*n*-alcohols). Crystals were dried under N₂, washed with three rinses of hexane to remove the non-adducted (cyclic alcohol) fraction, and redissolved by Milli-Q water addition. The adducted fraction (*n*-alcohols), now liberated into solution, was then extracted from the water via three additions of 4:1 (v/v) hexane:DCM, trace amounts of water were removed with Na₂SO₄. The result was highly purified *n*-alcohol fractions, as confirmed by GC/MSD analysis of a small sample split that had been converted to derivatized by exposure to N, O-bis(trimethylsilyl)trifluoroacetamide (BSTFA) and acetonitrile at 65°C for two hours, after Wakeham and Pease (1992).

3.2.3 Compound isolation and radiocarbon analysis

The *n*-alcohol fractions were derivatized via acetylation (derivative carbon $\delta^{13}\text{C} = -22.85$, $F_m = 0.0053$, $\Delta^{14}\text{C} = -994.7$) prior to PCGC separation into two groups representing aquatic and terrigenous sourced alcohols. Shorter carbon chain length *n*-alcohols (C20, 22, and 24) were grouped as aquatic, while C28 and 30 *n*-alcohols were grouped as terrestrial. These groupings are not inclusive of all aquatically or terrigenously sourced *n*-alcohols found in samples, as quantification of total alcohols from each source was not the objective. Rather, each grouping contains a subset of *n*-

alcohols from each source that did not co-elute with other compounds and were therefore highly amenable to PCGC isolation with low likelihood of influence from other compounds, and were representative of their source with low likelihood of being produced universally. While the group designated as aquatic are longer in chain length than are typically associated with autochthonous sources, each system is unique, and the distribution of alcohols in Malawi supported this division based on relative abundance of all alcohols found in this work and others (Castañeda, 2007). PCGC isolated groups were cleaned to remove contaminants from column bleed (via short column silica chromatography and elution with 2 mL 3:97 ethyl acetate:hexane) and analyzed for radiocarbon content via accelerator mass spectrometry (AMS). The isotopic contribution from derivative carbons was removed by mass balance correction. PCGC and AMS analyses were performed at the National Ocean Sciences Accelerator Mass Spectrometry (NOSAMS) facility at Woods Hole Oceanographic Institute (WHOI) as described in Pearson et al. (2001). Radiocarbon results are reported here as $\Delta^{14}\text{C}$, as defined as:

$$\Delta^{14}\text{C} = (f_m * e^{\lambda * (1950 - \text{yc})} - 1) * 1000$$

where f_m = fraction modern value reported by NOSAMS, $\lambda = 1/8267$, and yc = year collected, following the convention of Stuiver and Polach (1977). The $\Delta^{14}\text{C}$ value is $\delta^{13}\text{C}$ corrected, and corrected for decay time between year of collection and year of analysis. Control samples submitted to NOSAMS to test the accuracy and precision of reported $\delta^{13}\text{C}$ and $\Delta^{14}\text{C}$ results included bulk, dried corn leaves grown in 2012, bulk crushed Devonian aged (e.g. radiocarbon dead) shale, and the combined L5/L6 fraction extracted from each following the lipid extraction procedures described above. $\Delta^{14}\text{C}$ of the extracted L5/L6 fraction was 28‰ and 1.2‰ lower than the bulk material for corn and shale, respectively, while $\delta^{13}\text{C}$ of the L5/L6 fraction was 6.4‰ lower and 0.4‰ higher than the bulk material for corn and shale, respectively. The low $\delta^{13}\text{C}$ of the corn L5/L6 fraction can be attributed to the typically ^{13}C depleted lipids contained in the fraction (discussed below), while the lack of offset between fractions for the shale is likely due to the low lipid content of these ancient, thermally mature rocks. To test possible fractionation imparted by PCGC analysis, three alcohol standards (C19, 24, and 28) were

isolated from a standard mixture via PCGC following methods used for all samples, and were subsequently analyzed independently for radiocarbon and stable isotope signature. PCGC isolated standards were found to have lower $\delta^{13}\text{C}$ than their bulk parent counterparts by 0.2 to 2.2‰, and $\Delta^{14}\text{C}$ signatures 4.3 to 9.0‰ greater than the bulk material. PCGC isolation was therefore not a significant source of fractionation.

3.2.4 Additional fraction analyses

In addition to *n*-alcohols isolated from each core-top, corresponding bulk sediment, bulk TLE, and acid-insoluble fractions from each core were also isolated and analyzed for radiocarbon content by NOSAMS. TLE was extracted as described above using smaller replicate sediment amounts of roughly 300 mg. A subsample (roughly 1.0 to 1.5 g) of lipid-extracted sediments were treated with acid hydrolysis by immersion in 20 ml of 6N HCl, covered with nitrogen headspace, capped, and maintained at 100°C for 19 hours to remove hydrolysable amino acids and some carbohydrates and obtain an ‘acid-insoluble’ fraction. It has been shown that hydrolysis with strong H_2SO_4 rather than HCl is a more effective method to remove carbohydrates from organic matter (Pakulski and Benner, 1992; Wang and Druffel, 2001). However, given that both acids would encourage the hydrolysis of polymeric carbohydrates into monomers (Mopper and Furton, 1991; Benner, 2002), it is likely that at least some carbohydrates were also mobilized into the acid layer during hydrolysis. After hydrolysis, the acid layer (containing amino acids and some carbohydrates) was pipetted off, and samples were rinsed and centrifuged x3 with Milli-Q water to remove acid residue. Sample that remained after both TLE extraction and acid hydrolysis treatment contained a mixture of protokerogen and mineral material (Wang and Druffel, 2001), and gives insight to the nature of material that may be preserved long term in Lake Malawi sediments.

3.2.5 Water column

In January 2014 water column samples were collected from Lake Malawi during a second sampling event in the central basin of the lake approximately 122 km due south

from the most offshore sediment core 11MC. Dissolved organic carbon (DOC), total inorganic carbon (TIC), and particulate organic carbon (POC) were collected from 350m water depth at this location, in addition to TIC from 30m water depth. POC was collected by gravity filtration of 800 mL of lake water from depth through a combusted GFF filter, which was then wrapped in combusted foil and frozen. Filtrate from that sampling was collected in a sterile ashed 1L glass bottle as the DOC sample, which was acidified to pH 2 with 6M HCl (ACS reagent grade). TIC samples were collected by transfer of whole lake water to sterile ashed 500 mL amber glass bottles (with ground glass stopper fittings) until the bottle overflowed for half the time it took to fill the bottle. Headspace (5 mL) was removed from these bottles and 100 μ L of saturated HgCl₂ was added. Apeizon-M grease was added to the seal of the ground glass stoppers in the bottles, and stoppers were secured in the bottle via 2 rubber bands. All samples were transported back to the Large Lakes Observatory (USA) and submitted to NOSAMS for radiocarbon analysis.

3.3 Results

3.3.1 Bulk elemental analysis and biomarker relative abundance

Substantial shifts in bulk surface sediment (0 – 4 cm) composition occur as distance from shore and water depth at coring location increase (Fig. 3.2). Along this transect, both %TOC and %TON nearly double between the most nearshore core 2MC (82 m) and the most distal core 11MC (386 m). Concurrently, C/N decreases and $\delta^{15}\text{N}$ becomes more depleted, showing rapid drops along the first three to four core locations, then remaining low throughout the remainder of the transect. Concerning the *n*-alcohols of focus for this study, 67% are terrestrial in origin (long chain, C28 and C30) in the most nearshore core, and 33% are aquatic (short chain, C20, C22, and C24) (Fig. 3.3a). Terrestrial *n*-alcohol relative abundance subsequently decreases with water depth and distance from shore, showing rapid drop off in the first three cores, then slight increase, and further decline at the most offshore coring location. Concurrently, aquatic *n*-alcohols relative abundance increases across the first few cores, decline slightly, and increase

again- ultimately resulting in clear dominance (~96%) of aquatic *n*-alcohols at the most distal 386 m core. Alcohol concentrations per g of sediment organic carbon are shown for select cores in Fig. 3.3b. While all alcohols increase in concentration at least slightly as water depth at coring location increases, the short chain C20 and C24 alcohols become much more abundant than other by core 9MC (220 m water depth).

3.3.2 Multi-fraction stable carbon isotope

The stable carbon isotope signature differs between fractions isolated from homogenized 0-4 cm surface sediment at each core location (Fig. 3.4). Throughout the suite of cores, bulk sediment and protokerogen fractions show very similar values that are the most ^{13}C -enriched (heaviest) of the analyzed fractions. Values range from -22 to -26.0‰ and become slightly more ^{13}C -depleted (lighter) as distance from shore and water depth increase. Total lipids extracted from the same sediment are more depleted in ^{13}C than the bulk and protokerogen fractions in all cores, with values from -29 to -31‰ and no obvious trend across the transect. Aquatic *n*-alcohols are the most ^{13}C depleted fraction at all locations with successful measurement, ranging from -32 to -38‰. This fraction also shows the most variability in $\delta^{13}\text{C}$ among cores across the sampling line, with wide variation in values between adjacent cores. Values seem to become lighter (^{13}C depleted) at more offshore locations. The $\delta^{13}\text{C}$ of water column isolated carbon fractions are shown in Fig. 3.5. TIC $\delta^{13}\text{C}$ is -0.7 and -2.5‰ at 30 m and 350 m water depth, respectively, while $\delta^{13}\text{C}$ of POC from 350 m water depth is -28‰.

3.3.3 Multi-fraction radiocarbon

There is a less clear-cut distinction between sediment fractions based upon radiocarbon signatures than that observed for stable carbon isotope signatures (Fig. 3.6). Bulk sediment shows consistently greater than modern $\Delta^{14}\text{C}$ values across the transect, ranging from +10 to 46‰. A steady decline is observed from 46‰ in core 2MC (the most nearshore) to 10‰ in 6MC (157 m water depth), at which point $\Delta^{14}\text{C}$ again increases and stabilizes around 37‰ in the most offshore cores. Protokerogen trends

most similarly to the bulk sediment fraction, though this fraction is slightly more aged than the bulk material at all core locations (Fig. 3.6). Protokerogen $\Delta^{14}\text{C}$ ranges from -21 to +27‰ across the transect, decreasing from 0‰ at 2MC to -21‰ at 4MC, then steadily increasing and stabilizing around +20‰ at the most offshore cores. Radiocarbon content of lipid fractions is extremely varied among core locations. Total lipid extracts encompass a wide range of $\Delta^{14}\text{C}$ values, -91 to +28‰, over the whole transect. The oldest TLE values occur at the most nearshore cores, with $\Delta^{14}\text{C} = -91‰$ at core 2MC, increasing to +28‰ by core 6MC, declining again to -13‰ at core 8MC, and finally stabilizing around +18‰ in the three most offshore cores. Aquatic and terrestrial *n*-alcohols isolated from the same surface sediment show an even wider range of $\Delta^{14}\text{C}$ values in all samples, ranging from -75 to +107‰ overall, but appear generally more ^{14}C -depleted nearshore than offshore. Radiocarbon signatures of water column fractions are shown in Fig. 3.7. DOC from 350 m water depth shows the most depleted $\Delta^{14}\text{C}$ of the measured water carbon fractions at +27‰, while POC from the same water depth is extremely enriched at 186‰. TIC $\Delta^{14}\text{C}$ is intermediate between the two at both water depths, with 67‰ at 30 m; 92‰ at 350 m.

3.4 Discussion

3.4.1 Bulk elemental analysis and biomarker relative abundance

Trends in bulk elemental and isotopic signatures of surface sediment (0 – 4 cm) from nearshore core 2MC to the most offshore core 11MC indicate an increased influence of aquatic (autochthonous) organic matter sources as distance from shore and water depth increase, and a concurrent decrease in terrestrial influence. The overall level of ^{13}C depletion in surface sediment of all cores, combined with concurrently low C/N from each core, indicates that organic carbon input to surface sediment of all cores is dominated by lacustrine algae sources (Meyers, 1997). Subsequently, the decreasing $\delta^{13}\text{C}$ and concurrently decreasing C/N of surface sediment as water depth and distance from shore increase indicates an increasing contribution of lacustrine algae and reduced influence from terrestrial inputs (Meyers, 1997; Tenzer et al., 1997; Talbot and Laerdal,

2000). These results are consistent with bulk elemental and isotopic analysis of surface sediment (0 – 1 cm) for this same suite of cores, as reported by Kruger et al. (in prep). In that study, the positive relationship between surface sediment biogenic silica content (as indicated by Si:Ti) and water depth beyond the chemocline was an additional indicator of increasing aquatic influence on surface sediment, and helped eliminate the possibility of significant microbial influence on C/N sediment values. In recent decades, the incidence of agriculture has increased in the Lake Malawi basin, with more small operations clearing land for conversion to tobacco or maize crops (Orr, 2000). Maize fixes carbon through the C4 biochemical pathway, in which carbon isotope fractionation is reduced relative to the more common C3 carbon fixation pathway, and has a resulting stable carbon isotopic signature more ^{13}C enriched ($\delta^{13}\text{C}$: -10 to -16‰) than C3 plants ($\delta^{13}\text{C}$: -25 to -35‰) (Meyers, 1997). Therefore the greater $\delta^{13}\text{C}$ observed for both bulk and protokerogen fractions at the most nearshore cores could reflect the incorporation of a small amount of ^{13}C enriched maize carbon, or naturally occurring C4 plant matter, and subsequent $\delta^{13}\text{C}$ decline as distance from shore increases supports our interpretation of reduced terrestrial influence.

This interpretation of increasing aquatic influence on sediment with distance from shore is supported by the relative abundance of aquatic and terrestrial *n*-alcohol biomarkers isolated from surface sediments (Fig. 3.3), which shows clear aquatic biomarker dominance at the most offshore core locations. However, this record must be interpreted carefully, as lipids of different carbon chain length can undergo differential sedimentation and preservation efficiency due to their differing reactivity. Lipid analysis of sequentially deeper sediment traps in Lake Michigan has revealed that the relative contribution of both alkanols and alkanoic acids decreases with water depth during sedimentation (Meyers et al., 1984). However, shorter chain species have been shown to degrade at faster rates than their longer chain counterparts during sinking for those and other lipids (Meyers and Eadie, 1994; Meyers et al., 1984). This is supported by comparison of the lipid composition of water column organisms (bacteria, rotifers, protozoans) versus that of the underlying lake sediments in a eutrophic lake, which found

more degradation of autochthonous short chain alkanols than long chain species prior to deposition (Robinson et al., 1984). This unequal loss of short chain alkanols while sinking is likely due to preferential microbial remineralization of those more recently synthesized compounds. Combined, this evidence does not dispute interpretation of our *n*-alcohol biomarker abundance record in Lake Malawi but rather indicates that, if anything, the dominance in contribution of aquatic *n*-alcohols to the sediment at depth that we observe is likely under-representative of the actual aquatic contribution and thus, the observed trends are conservative estimates.

Similarly, lipid compounds of varying chain length also undergo unequal diagenesis after sedimentation, though *n*-alcohols seem more resistant to such degradation relative to other compounds. Kawamura and Ishiwatari (1985) compared the *n*-alcohol, *n*-alkane, and fatty acid carbon chain length distribution in surface sediment of Japanese lakes with varying trophic status. They found the *n*-alcohol carbon chain length to correspond to the expected OM source for each lake. Sedimentary *n*-alcohols in the most oligotrophic lake were dominated by long chain species reflective of the high contribution of terrigenous OM to the lake. Predominance of short chain *n*-alcohols was found in the most eutrophic lake sediments, reflecting high levels of algal productivity, and *n*-alcohol carbon chain length distribution in mesotrophic lakes were intermediate between the two end members. However, fatty acids, whose chain length distribution would also be expected to reflect varying OM source did not, in fact, do so; they instead showed only a predominance of shorter chain compounds in all lakes, indicating high microbial reworking of that lipid class. These findings corroborate similar studies on separate Japanese lakes, where *n*-alcohol chain length distribution was also confirmed to reflect known dominant OM sources to the lakes (Fukushima and Ishiwatari, 1984). These findings, combined with the sinking particle diagenetic effects discussed above, confirm that the increasing dominance of aquatic *n*-alcohol relative abundance observed in our data is a reliable indication of increased contribution of autochthonous organic matter to sediments as water depth and distance from shore increase.

It is important to note that lipid degradation in both water column and sediment environments is heavily influenced by the presence of oxygen, with more rapid lipid breakdown occurring in the presence of oxygen than in anoxic environments (Sun et al., 1997; Sun and Wakeham, 1998). The zone of permanent anoxia in Lake Malawi occurs below ~250 m water depth, though both the upper and lower chemocline boundaries are believed to be non-static. Samples collected in this study begin in a nearshore zone of water column mixing and enter the permanently anoxic zone of the lake, crossing through the chemocline zone. This transfer from oxygenated to anoxic conditions means the likelihood of sediment lipid degradation is higher in the nearshore cores where exposure to oxygen is likely, although this can be offset to a degree by increased preservation resulting from higher nearshore sedimentation rates (Burdige, 2007). Combined with the preferential degradation of short chain saturated alcohols over long chain ones as described above, this could indicate that the decreased aquatic biomarker predominance in nearshore surface sediment is partially due to decreased short chain lipid preservation. Again, however, the saturated *n*-alcohol lipid class has been shown to be less reactive in sediments relative to other lipid classes, both in oxygenated sediment (Fukushima and Ishiwatari, 1984; Kawamura and Ishiwatari, 1985) and anoxic sediment (Grossi et al., 2001). We therefore believe the differential preservation effects between permanently anoxic and variably oxic surface sediment to be minimal.

3.4.2 $\delta^{13}\text{C}$ of multiple sediment fractions

$\delta^{13}\text{C}$ signatures of sedimentary organic carbon fractions are influenced by many factors, including the carbon source pool utilized, fractionation resulting from differential metabolic pathways, and fractionation associated with carbon uptake (Hayes, 1993). As described above, in this study $\delta^{13}\text{C}$ and C/N signatures of bulk surface sediment OC (in conjunction with other parameters) are consistent with high autochthonous carbon input throughout the sample suite, as well as an increase in contribution from aquatic sources and reduced influence of terrigenous carbon inputs as water depth and distance from

shore increase. This bulk $\delta^{13}\text{C}$ signature reflects the combined influence of fractionation and source effects imparted to its different molecular constituents.

Sub-fractions isolated from the bulk sediment whose $\delta^{13}\text{C}$ signatures differ from the bulk signature represent unique carbon sources and/or fractionation pathways. Lipids are known to be depleted in ^{13}C relative to other biogenic compounds, due to fractionation that occurs when glucose is oxidized to acetyl coenzyme A, which then serves as the main carbon source in lipid biosynthesis (DeNiro and Epstein, 1977). Thus, ^{13}C depletion in lipids is sufficient to affect the bulk $\delta^{13}\text{C}$ signature of the tissue (i.e., lipid reserves in zooplankton) or structure (i.e., wax coatings on leaves) into which the lipids are incorporated en masse (Tieszen et al., 1983). The $\delta^{13}\text{C}$ of TLE fractions in this study are shown to be 3 to 7‰ more ^{13}C -depleted than the bulk sediment signature at all core locations. While the magnitude of difference in isotopic signature between the bulk and TLE fractions is not universal, this offset is consistent with multi-fraction stable carbon isotope data from surface sediment reported for various locations including Lake Malawi's north basin (Castaneda et al., 2011) and the Southern Ocean (Wang and Druffel, 2001). The existence of this offset illustrates the relatively small proportion of total bulk sedimentary carbon that consists of lipids. A comparison of surface sediment (0 – 2 cm) from the NE Pacific and Southern Oceans showed lipids to constitute 3 and 14% of total organic carbon, respectively (Wang and Druffel, 2001). The sum of the most dominant lipid classes in four Japanese lakes of varying trophic statuses was just 1.7 to 2.7% of total organic carbon (Kawamura and Ishiwatari, 1985).

It follows, then, that the *n*-alcohol compound class is even more ^{13}C depleted than the total lipid fraction, given the high percentage of these compounds that is derived from saturated carbon groups of the ^{13}C depleted acetyl CoA. These lipid compounds also constitute a correspondingly low percentage of the total extractable lipids. This study shows a 3 to 10‰ ^{13}C depletion of *n*-alcohols relative to TLE at all core locations with successful measurement, meaning some *n*-alcohol groups are extremely depleted in ^{13}C , between -32 and -39‰ for aquatic *n*-alcohols. This is more ^{13}C depleted than previous $\delta^{13}\text{C}$ measurements of *n*-alcohols of similar chain length in surface sediment of Lake

Malawi (Castaneda et al., 2011) and in the Santa Monica Basin (Pearson et al., 2001); however, it is still within the assumed possible range of -26 to -47‰ for organic matter produced exclusively by phytoplankton (Leng et al., 2005). Bacterial utilization of methane has been shown to account for baseline carbon fixation independent of photoautotrophic production in food webs in some freshwater systems (Kiyashko et al., 2001; Pasche et al., 2011; Naeher et al., 2014). Strong carbon isotope fractionation is imparted during thermogenic and biogenic formation of methane, and further (but smaller) fractionation occurs during microbial oxidation of that already very ^{13}C -depleted methane. The result is bacterial biomass with extremely low $\delta^{13}\text{C}$ signatures, -74 to -45‰, which can then be incorporated into the aquatic food chain (Hanson and Hanson, 1996). Methane is not known to exist in significant amounts in the deep water of Lake Malawi, although there has been little research focus on its measurement. It is likely that methane exists in the sediments, due to OM degradation, and therefore may exist in the hypolimnion as well. The constant temperature profile observed in the permanently anoxic zone indicates a low likelihood of abiogenic geothermal methane contribution to the water column, although the rift basin nature of the lake suggests there may be some level of hydrothermal input. Some methane production may occur biogenically, derived from acetate or CO_2 . The possibility of methanotrophically fixed carbon cannot be ruled out as a ^{13}C depleted source of carbon in Lake Malawi. Such contribution could contribute to the very low lipid $\delta^{13}\text{C}$ values, however the lack of significantly measured methane from the lake and the absence of extremely low $\delta^{13}\text{C}$ signatures in independently measured parameters (such as TIC or DOC) suggests this is not a major contribution to the carbon cycle in the lake. Rather, it is likely that the very low *n*-alcohol $\delta^{13}\text{C}$ signatures reflect phytoplanktonic production. The typical assumption is that phytoplankton produce organic matter that is approximately 20‰ more depleted than $\delta^{13}\text{C}$ of DIC in lake systems (Leng and Marshal, 2004), though this is not a fixed offset and, as discussed previously, the very saturated nature of *n*-alcohols could result in greater fractionation during their production than other lipid compounds. $\delta^{13}\text{C}$ of TIC measured in Lake Malawi's central basin in 2014 was roughly -1‰ at 30 m water depth

and -2.5‰ at 350 m water depth (Fig. 3.6). It is not assumed that these values would have changed significantly in the five years between sediment and water column sampling. A final possibility is that extremely low *n*-alcohol $\delta^{13}\text{C}$ values shown in this study may indicate some degree of fractionation as a result of compound isolation or analysis. This is unlikely during the initial compound class isolation, as minimal fractionation is expected with the organic isolation methods employed here. As a control, the $\delta^{13}\text{C}$ of bulk and the L5/L6 fraction were measured from both corn leaves grown in 2012, and from a sample of Devonian shale. Only slight fractionation was observed and can be attributed to the expected ^{13}C depletion of the lipid fraction relative to the bulk material. To test possible fractionation imparted by PCGC analysis, three alcohol standards (C19, 24, and 28) were isolated from a standard mixture via PCGC following methods used for all samples, and were subsequently analyzed independently for radiocarbon and stable isotope signature. PCGC isolated standards were found to have lower $\delta^{13}\text{C}$ than their bulk parent counterparts by 0.2 to 2.2‰. Therefore, the very ^{13}C depleted *n*-alcohol values may reflect some fractionation from PCGC isolation. However, application of even the greatest offset measured to the *n*-alcohol values imparts relatively minimal change with respect to their $\delta^{13}\text{C}$ offset from TLE, and *n*-alcohols would remain much more ^{13}C depleted than TLE at all points.

The acid insoluble (AI) fraction has been shown to account for 43 – 57% of total sedimentary organic carbon in NE Pacific and Southern Oceans (Wang and Druffel, 2001), and between 13 – 67% (average = 45%, $n = 21$) of carbon recovered from sequentially deeper sediment traps at three near-continent sites in the Atlantic and Pacific (Roland et al., 1998). The similarity of $\delta^{13}\text{C}$ between the bulk sediment and the AI fraction in this study is not surprising, given the seemingly universal predominance of this fraction, and is consistent with other reported values for both fractions (Wang and Druffel, 2001; Roland et al., 2008).

3.4.3 Radiocarbon signatures of multiple sediment fractions

The consistently modern (younger than 1950) age of Lake Malawi bulk surface sediment throughout the sample transect, as indicated by enriched $\Delta^{14}\text{C}$ signatures, is supported by ^{210}Pb dating performed on the same suite of cores by Kruger et al. (in prep). Linear sedimentation rates and mass accumulation rates calculated in that study for cores 2MC, 5MC, 8MC, and 9MC averaged from $0.34 - 0.5 \text{ cm}\cdot\text{yr}^{-1}$ and $0.007 - 0.32 \text{ g}\cdot\text{cm}^{-2}\cdot\text{yr}^{-1}$, respectively, for 0 – 4 cm sediment. Modern surface sediment radiocarbon signatures would be expected with these correspondingly high sedimentation values if no significant input of highly aged material is occurring.

While modern throughout, there is structure apparent in this nearshore to offshore bulk $\Delta^{14}\text{C}$ record. Multiple factors can cause differences in $\Delta^{14}\text{C}$ between sampling locations, including differentially aged carbon source material and/or unique cycling dynamics before sedimentation. Large differences in bulk sediment $\Delta^{14}\text{C}$ between locations are often interpreted as distinct shifts in major sedimentary organic carbon source, e.g, recently synthesized material versus significantly aged resuspended sedimentary or rock-scoured material (Roland et al., 2008). Alternatively, shifts in bulk signature can also reflect variable preservation of unique sediment fractions, each of which has a distinct source and subsequently unique $\Delta^{14}\text{C}$ (Eglinton et al., 1997; Pearson et al., 2001; Wang and Druffel, 2001). The slight decline in bulk sediment $\Delta^{14}\text{C}$ across the first five core locations (2MC – 6MC) occurs in the shallowest water where sedimentation rate is highest. Average MAR and TOC-MAR for the 0 – 4 cm horizon in core 2MC were found to be $0.33 \text{ g}\cdot\text{cm}^{-2}\cdot\text{yr}^{-1}$ and $0.007 \text{ g}\cdot\text{cm}^{-2}\cdot\text{yr}^{-1}$, respectively, twice as high as the same parameters in core 5MC (Kruger et al., in prep). As outlined in this study and in Kruger et al. (in prep), organic carbon in surface sediment at all core locations is largely reliant on aquatic production, however terrestrial influence on sediment composition is most prominent at nearshore core locations, as indicated by bulk elemental, isotopic, biogenic silica, and *n*-alcohol biomarker relative abundance analyses. In this study, all sediment fractions analyzed at nearshore locations are more depleted in ^{14}C than the bulk sediment, including the acid insoluble fraction (AIF) which could likely constitute a significant proportion of the bulk sediment (Wang and Druffel, 2001, Roland

et al., 2008). This suggests the presence of a sediment component with an enriched $\Delta^{14}\text{C}$ signature that was not characterized in this study. Studies of abyssal sediment from the North East Pacific and Southern Oceans have found the acid soluble fraction of sediment, composed mainly of amino acids, to compose a relatively large percentage of bulk OC (20-30%) and be ‘younger’ than bulk material according to $\Delta^{14}\text{C}$ signature (i.e., more positive) (Wang and Druffel, 2001). Marine coastal POC from highly productive areas in the NE Pacific and NW Atlantic Oceans, as well as an Eastern Subtropical Atlantic open ocean site, were all also found to be composed of a high percentage of acid soluble organic material (30-54%, including amino acid and carbohydrate content as calculated by mass balance) which was consistently more enriched in $\Delta^{14}\text{C}$ than the bulk particulate matter (Roland et al. 2008). This acid soluble fraction, unmeasured in this study, could be an enriched $\Delta^{14}\text{C}$ source to Lake Malawi bulk sediments. Aluwihare and Repeta (1999) showed that some marine phytoplankton exude high molecular weight (HMW) DOM rich in polysaccharides (carbohydrate macromolecules), the composition of which is similar to that found to be a major component of seawater HMW DOM. Carbohydrates were also found to be a major component (53 – 65%) of HMW DOM from Lake Superior, which was modern in $\Delta^{14}\text{C}$ signature (Zigah et al., 2014). It is also possible that carbohydrates can be sourced to the lake in the form of cellulose from land plant material. However, if such acid soluble compounds are also abundantly produced by phytoplankton in Lake Malawi, they would be expected to have $\Delta^{14}\text{C}$ signatures similar to that of the DIC pool from which the carbon was fixed. DIC measured in Lake Malawi in 2014 had high $\Delta^{14}\text{C}$ at both 30 m and 350 m water depth, at roughly 60 and 90‰, respectively. While the acid soluble fraction was not analyzed in this study, this level of DIC enrichment could mean that photosynthetically fixed acid soluble compounds constitute the major enriched $\Delta^{14}\text{C}$ end member in Lake Malawi sediment. The mixture of this radiocarbon enriched fraction with other $\Delta^{14}\text{C}$ depleted fractions (reported here) could produce the observed bulk radiocarbon signatures. It follows, then, that shifts in production or preservation of this major acid soluble sediment fraction would cause shifts in the bulk sediment $\Delta^{14}\text{C}$, and could explain the elevated nearshore

bulk $\Delta^{14}\text{C}$ and subsequent decline. The propensity of the polar acid-soluble molecules to sorb onto mineral surfaces decreases their likelihood of degradation, and this sorption would be highest at the most nearshore core locations where riverine input of mineral particulates would be highest (Keil et al., 1994). In addition, the high sedimentation rates measured at the most nearshore core (Kruger et al, in prep) would encourage quick burial of these sorbed compounds, further decreasing their degradation despite the oxygenated nature of the area and resulting in an enrichment of overall bulk sediment $\Delta^{14}\text{C}$. The subsequently declining bulk sediment $\Delta^{14}\text{C}$ from 2MC to 6MC could then represent a shift in preservation of the acid soluble sediment fraction. As distance from shore increases sedimentation rate declines (Kruger et al., in prep), allowing more opportunity for labile amino acid and carbohydrate compounds to be consumed before sedimentation, thus causing bulk sediment $\Delta^{14}\text{C}$ to decrease. The subsequent rise and stabilization of bulk $\Delta^{14}\text{C}$ values at depth could then reflect a decline in post-sedimentary diagenesis of these labile acid soluble compounds in the permanently anoxic bottom waters.

Applying assumptions about this lake system allows us to calculate estimations of contribution to surface sediment from the different source pools. Phytoplankton are known to produce OM with C/N ranging from 4-10, while that of vascular plants is often 20 or higher (Meyers and Teranes, 2002). As previously described at length in this document, the application of all other bulk sediment analyses indicates that surface sediment OM at the most offshore location, 11MC, is highly aquatic in nature. The OM at that location has a C/N of 8.7. We can therefore estimate that OM produced in the lake has a C/N value of 8, toward the high end of the known scale. We can also assume a conservative value of 20 for vascular land plant OM production, though it could in reality be higher. Given these assumptions, and ignoring possible diagenetic alterations to the C/N ratio upon sedimentation, the surface sediment sources at site 11MC are determined to be 94% aquatic, and 6% terrestrial in origin. Similarly, the surface sediment at site 2MC, the closest to shore, is determined to be 82% aquatic and 18% terrestrial in origin.

At 11MC, the radiocarbon values of aquatic and terrestrially sources *n*-alcohols are 113‰ and -27‰, respectively. Using these values as representative of the entire bulk

aquatic and terrestrial sources (which is likely not truly applicable to this system) and applying the above calculated ratio of terrestrial to aquatic source, the predicted bulk surface sediment $\Delta^{14}\text{C}$ at 11MC would be 105‰. This is far from the actual bulk surface sediment $\Delta^{14}\text{C}$ of 38‰ measured at that location in this study. Furthermore, at location 2MC, both terrestrial and aquatic *n*-alcohol fractions have $\Delta^{14}\text{C}$ signatures significantly older than the bulk material, -34 and -73‰, making a mass balance calculation using just those two end members impossible. The far offshore locations seem to be ‘low’ on radiocarbon-depleted lipids with regard to mass balance calculated bulk sediment signatures (under the assumptions stated here), while the nearshore locations seems to have an overabundance of radiocarbon depleted lipids. This could be the result of aged terrestrial fraction lipid contribution nearshore, and possibly transport and accumulation of aged aquatic lipids along the shoreline. Further assuming that at the nearshore 2MC location the radiocarbon depleted *n*-alcohol lipids constitute 40% of the bulk OM radiocarbon signature in their respective terrestrial vs. aquatic input ratios calculated above, and that the radiocarbon signature of other 60% of the total OM pool is composed of an uncharacterized radiocarbon-enriched source as postulated above, and giving that uncharacterized source the $\Delta^{14}\text{C}$ of the most radiocarbon enriched fraction measured in this study (113‰, measured for aquatic *n*-alcohols at 11MC), the predicted bulk surface sediment $\Delta^{14}\text{C}$ would be 41‰. That value is similar to the actual bulk surface sediment $\Delta^{14}\text{C}$ of 46‰ measured in this study. Therefore, under the assumptions stated here, it is reasonable to estimate that the uncharacterized radiocarbon enriched source at location 2MC constitutes roughly 60% of the bulk OM signal and has a $\Delta^{14}\text{C}$ signature near 113‰.

The nearshore depletion of total lipid $\Delta^{14}\text{C}$ and its enrichment as distance from shore increases also suggests shifting carbon source or composition within the lipid pool, a trend that seems mirrored by individually analyzed *n*-alcohol groups though with more variability. DOC measured at 350 m water depth was also somewhat radiocarbon depleted relative to other water column fractions, though not to the extent seen in the lipid fractions. However this single data point from the central basin of the lake may not

be representative of DOC radiocarbon signatures across the lake. As previously described, highest decomposition of the most labile lipid classes would be expected in the oxygen rich nearshore environment, where oxygen also likely penetrates the surface sediment (Wakeham et al., 1997; Sun et al., 1997; Sun and Wakeham, 1998). Bacterial membrane lipids are more resistant to degradation than less saturated lipids and could be selectively preserved in nearshore sediments, and bacterial incorporation of aged DOC into membrane lipids has been proposed as a possibility to explain aged lipid fractions in other studies (Wang and Druffel, 2001; Roland et al., 2008). However, such studies have been located in marine locations with significantly aged sediment and DOC pools, and sediment resuspension was also named as a more likely contributor to aged lipid fractions. This scenario does not apply in Lake Malawi, where surface sediments are modern at all sites measured.

Additionally, with $\Delta^{14}\text{C} = 25\text{‰}$, DOC at depth is still much more enriched than the most nearshore total lipids at -95‰ , and assuming this DOC value is representative of lake wide deep water DOC, suggests either a mechanism other than DOC incorporation or a large fractionation associated with DOC incorporation is occurring. Nucleic acids of bacteria assumed to incorporate DOC in marine systems have been shown to be equal to or more radiocarbon enriched than corresponding DOC at two locations, suggesting no significant carbon fractionation during bacterial DOC incorporation (Cherrier et al., 1999). Similarly, Pearson et al., (2001) found bacterial C31 hopanol isolated from surface sediment of the Santa Monica Basin to exhibit moderate $\Delta^{14}\text{C}$ relative to other lipids, and a similar $\Delta^{14}\text{C}$ to phytoplanktonic carbon, indicating a dominantly heterotrophic sedimentary environment. Without radiocarbon analysis of bacterial specific lipid biomarkers in Lake Malawi sediment we cannot speculate as to the potential radiocarbon content of those compounds, however evidence from these marine based studies does not suggest the occurrence of a bacterial fractionation mechanism sufficient to correspond to the highly depleted $\Delta^{14}\text{C}$ of nearshore total lipids.

Another possible explanation is influence from aged carbon originating from soils within Lake Malawi's watershed. It is known that deforestation for conversion of land to

agricultural space has increased around Lake Malawi in recent decades, and it has also been shown that this land conversion causes increased erosion and sediment loading to the lake since many of the converted plots are on hilly slopes (Orr, 2000; Hecky et al., 2003). Overall, the modern ages of the bulk surface sediment seen in all cores indicates the input of soil organic carbon, if aged, is not sufficient to affect the modern radiocarbon signatures. It is therefore unlikely that this potentially aged soil carbon accounts for the low $\Delta^{14}\text{C}$ of lipids nearshore, though it is possible that lipids synthesized in soil environments using older sources of organic C could be preferentially transported to the lake. While many lipids found in soils (including *n*-alcohols) are synthesized by land plants (Al-mutlaq et al., 2007, Diefendorf et al., 2011), which would cause them to have a modern radiocarbon signature reflective of atmospheric levels, lipids are also produced microbially in soils utilizing different carbon source pools. Bardgett et al. (2007) found heterotrophic soil microbes to be the first colonizers of terrain exposed after glacial retreat in the Austrian Alps, and showed those microbes consumed ancient, recalcitrant carbon as an energy source well before the establishment of an autotrophic community. They also showed that more than 50 years of organic matter accumulation occurred before the soil microbial community was predominately supported by modern carbon sources. While this not only supports the assumption that microbes can consume old and recalcitrant organic carbon, it also suggests that very old soil carbon exposed during land use changes in the Lake Malawi basin could be similarly colonized by heterotrophic microbes capable of feeding on aged carbon.

As previously described, the incidence of new agricultural plots in the Malawi basin being created on sloped hillsides is increasing, and the initial land clearing combined with subsequent erosion may expose very old soil horizons. Heterotrophic microbial consumption of old carbon from those soils would result in the production of radiocarbon depleted microbial biomass. While the modern radiocarbon signatures of bulk sediment does not indicate high bulk input of aged organic carbon in general, the relative proportion of autochthonous lipids preserved in the nearshore oxic zone may be low enough that only slight input of such terrestrially sourced and highly radiocarbon

depleted microbial lipids may skew the bulk lipid pool to reflect that aged source. The increase in lipid fraction $\Delta^{14}\text{C}$ as distance from shore increases could reflect the reduced contribution from such microbial sources with distance from river outflow. However, while this scenario may partially explain the total lipid trends, it does not necessarily explain the seemingly similar trend observed for specific *n*-alcohols. The heterotrophic colonizing microbes reported by Bardgett et al. (2007) were largely bacterial but included some fungal species. Bacterially produced membrane lipids are predominantly phospholipids and fatty acids, and neutral lipids such as *n*-alcohols are rarely produced by bacteria (Cronan, 1978; Boschker and Middleburg, 2002). Similarly, lipids produced by fungal species are mostly phospholipid fatty acids and sterols, with very little neutral lipid production reported (Brennan and Losel, 1978; Boschker and Middleburg, 2002).

The low nearshore $\Delta^{14}\text{C}$ of both TLE and *n*-alcohols may also indicate the occurrence of lipid sorption onto particles and subsequent redistribution. Sorption of organic matter onto mineral surfaces is a prevalent process in the sedimentation of most marine organic carbon, and can protect the organic molecules, delaying remineralization (Keil et al., 1994). Greater association of organic carbon has been demonstrated for mineral molecules with large surface areas, such as clays, and ultrafine particles that exhibit high buoyancy (Hedges and Keil, 1995; Coppola et al., 2007). The small relative grain size of such clays and ultrafine materials results in a high likelihood of suspension in the water column and transport. This typically results in a sorting of sediment grain size whereby average grain size decreases and %TOC increases as distance from shore increases (Thompson and Eglinton, 1978; Burdige, 2007), a trend also observed in surface sediments from this transect within Lake Malawi (Kruger et al., in prep). Following this logic, one would assume lipids sorbed onto fine-grained mineral molecules would be preferentially transported offshore. While this is likely true to an extent, the very high sedimentation rate observed nearshore in this sample transect (discussed previously) could also cause increased nearshore preservation of particle-sorbed lipids. If aged lipids, possibly sourced from resuspended aged material or aged terrestrial sources, become sorbed onto highly mobile fine grain sediments, various

lateral transport mechanisms could result in their transport to the nearshore region (Hwang et al., 2009), where the high sedimentation rate might preferentially preserve that material. Other studies have concluded that such resuspension and lateral transport mechanisms might explain the highly radiocarbon aged alkenone lipids extracted from bulk sediments with much younger ages in marine systems (Ohkouchi et al., 2002; Mollenhauer, 2003). The subsequent increase in TLE and *n*-alcohol $\Delta^{14}\text{C}$ as distance from shore increases might reflect the reduced sedimentation rate and higher remineralization of the sorbed lipid fraction, as the amount of mineral-sorbed OC has been shown to decrease as a function of oxygen exposure time in offshore settings (Coppola et al., 2007).

3.5 Conclusion

Bulk sediment elemental and isotopic analysis combines with *n*-alcohol relative abundance trends to confirm conclusions reached in chapter two; that influence from aquatic sources on sedimentary organic matter increases as distance from shore and water depth increase. The stable carbon isotopic signature of bulk sediment is similar in value and trends to that of the protokerogen fraction. That material is likely to be preserved long term in the sedimentary record due to the recalcitrant nature of its organic compounds, and the $\delta^{13}\text{C}$ of that material may be reflective of the $\delta^{13}\text{C}$ of the bulk organic carbon pool as it was deposited. Lipid fractions isolated from the bulk material are much more depleted in ^{13}C , as expected. Bulk sediment throughout this nearshore to offshore sampling are modern in age with respect to radiocarbon content, but the presence of several highly radiocarbon depleted fractions at the most nearshore locations indicates an unidentified radiocarbon enriched carbon source to the sediment. While not isolated in this study, the acid soluble sediment fraction, composed of amino acids and carbohydrates, is the likely source of this assumed radiocarbon-rich material. The extreme depletion of the lipid classes at the nearshore locations is somewhat puzzling. It is possible that the radiocarbon depleted total lipid signal is reflecting basin-level land use changes, as disturbed sloped terrain is colonized by heterotrophic bacterial and fungal

communities that feed on recently exposed aged soils. However this scenario does not necessarily explain the concurrent lipid depletion of isolated *n*-alcohols, as bacteria and fungi have both been shown to produce only very low relative amounts of these compounds. Alternatively, the depleted nearshore lipid fractions could represent the lateral transport of aged lipid material sorbed onto mineral particles and sedimented in the zone of elevated mass accumulation rate nearshore. The ultimate source of these extremely radiocarbon depleted lipids remains unclear.

Table 3.1. Cores collected from the northern basin of Lake Malawi in 2009 for this study, the associated water depth at the coring location (m) for each, and the distance from each coring location to the nearest lake shoreline (km).

Core	Water Depth at Coring Location (m)	Distance from Nearest Lakeshore (km)
2MC	82	2.2
3MC	98	3.0
4MC	116	4.5
5MC	141	6.4
6MC	¹⁵ 7	7.8
7MC	181	9.7
8MC	197	10.8
9MC	220	12.4
10MC	301	20.4
11MC	386	21.3

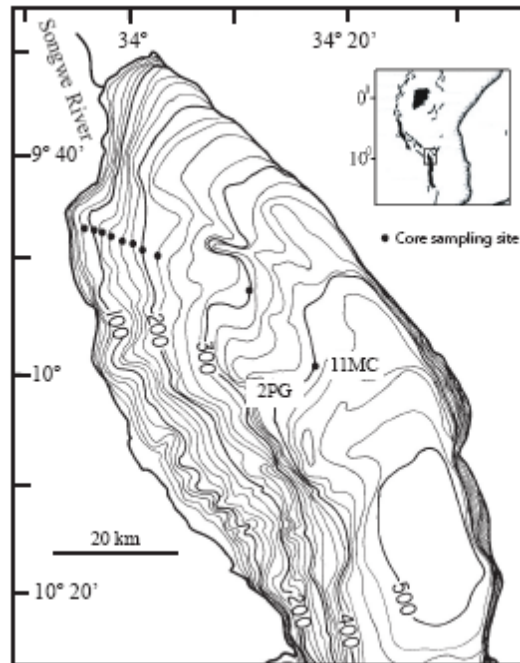


Figure 3.1. Coring locations in Lake Malawi's northern basin, core 2MC is the most nearshore core in the sampling line (82 m water depth), and core names increase numerically until core 11MC (demarked) at 386 m water depth.

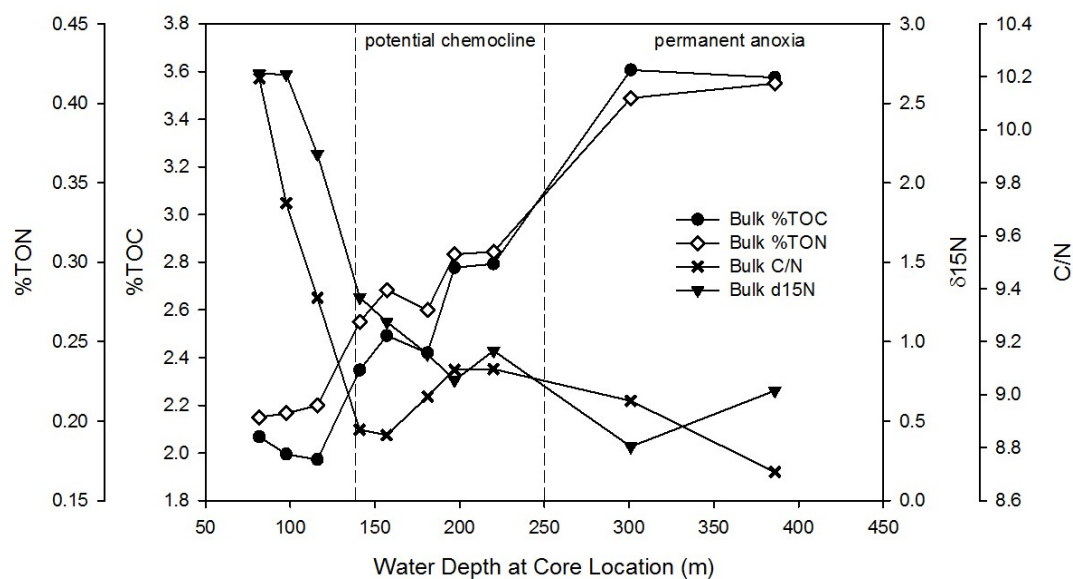


Figure 3.2. Bulk sediment parameters as measured for the 0-4 cm homogenized horizons used for subsequent fraction isolation. $\delta^{15}\text{N}$ is reported in units of per mil (‰) as described in the text.

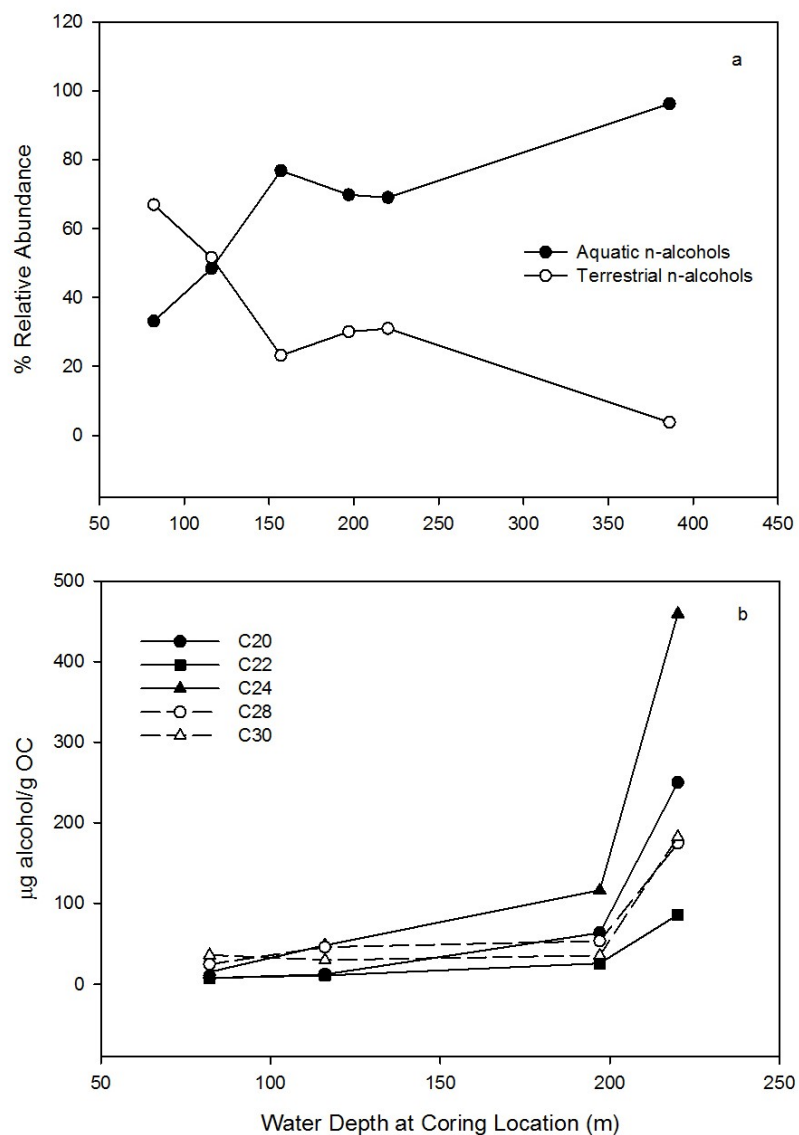


Figure 3.3. Percent relative abundance of aquatic (C20, 22, and 24) and terrestrial (C28 and 30) *n*-alcohols analyzed after polar lipid isolation from TLE (a), and the concentration of each alcohol normalized to g OC of the analyzed sediment.

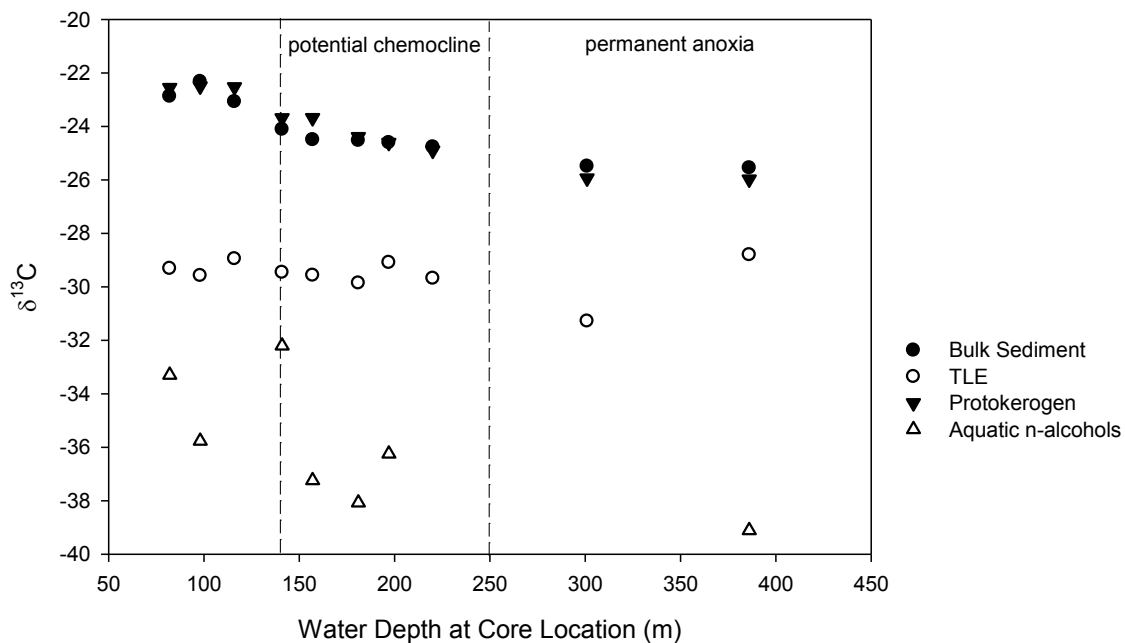


Figure 3.4. Stable carbon isotopic ratio in units of per mil (‰) for bulk sediment (0-4 cm) and fractions isolated from that sediment including protokerogen, total lipid extract (TLE), and aquatic *n*-alcohols (C20, 22, and 24). The approximate boundary of permanent anoxia and the potential extent of the chemocline zone are noted, although these boundaries are highly mobile and affected by numerous parameters (see text).

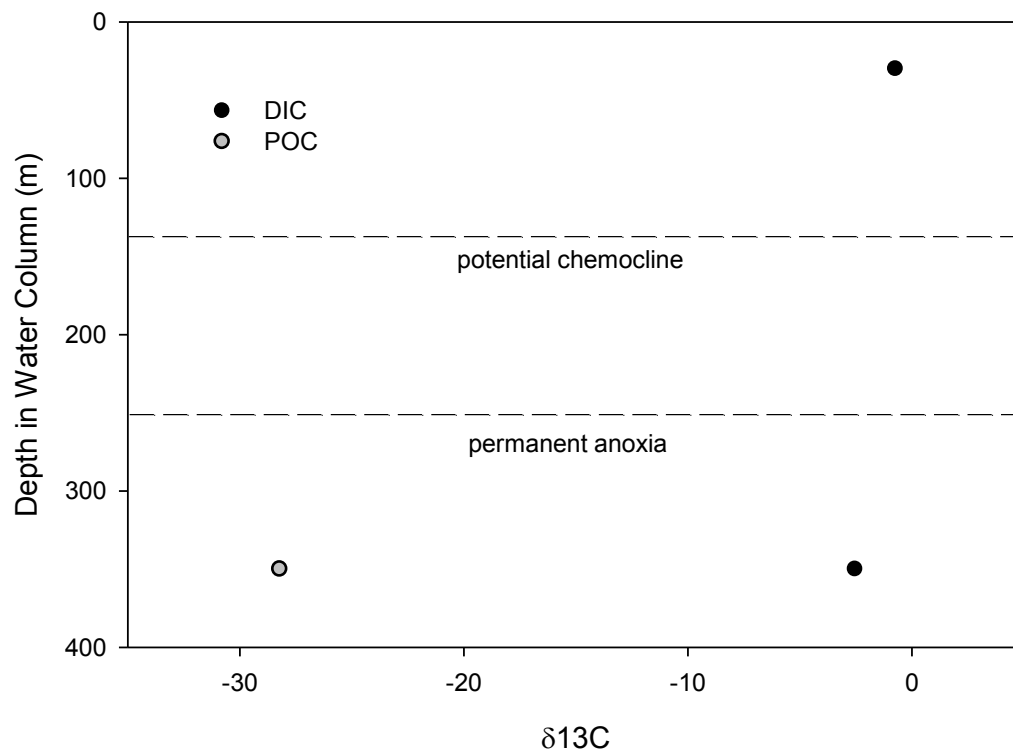


Figure 3.5. Stable carbon isotopic ratio in units of per mil (‰) of water column organic carbon fractions DIC and POC from 30 and 350 m water depth where successful. The approximate boundary of permanent anoxia and the potential extent of the chemocline zone are noted, although these boundaries are highly mobile and affected by numerous parameters (see text).

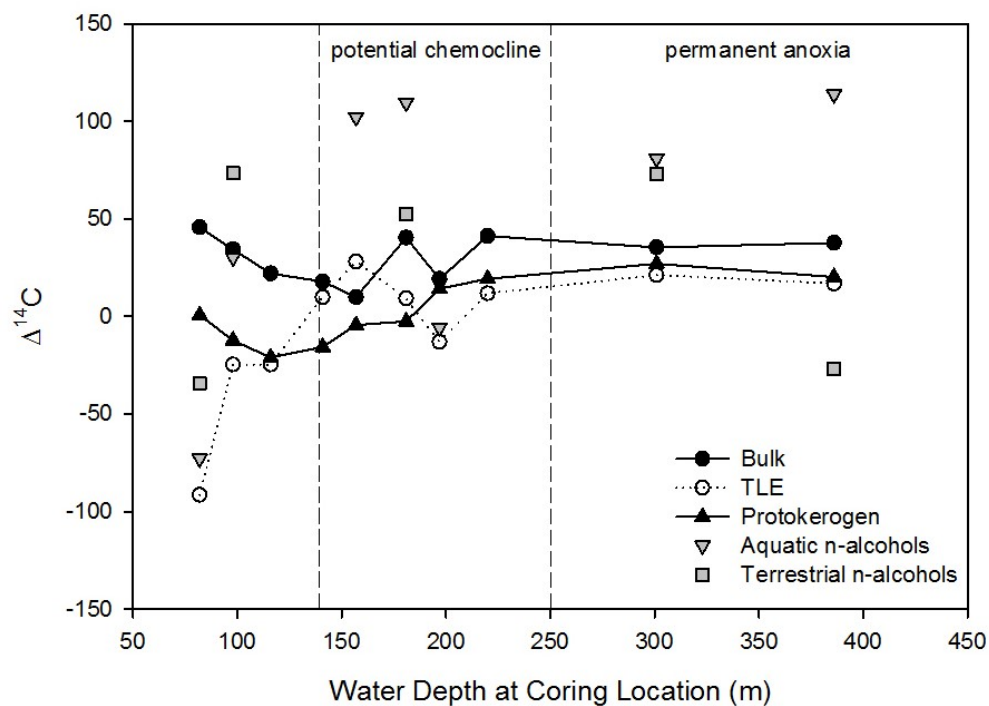


Figure 3.6. Radiocarbon signatures presented as $\Delta^{14}\text{C}$ (units of per mil, ‰) for bulk sediment (0-4 cm) and fractions isolated from that sediment including protokerogen, total lipid extract (TLE), aquatic *n*-alcohols (C20, 22, and 24), and terrestrial *n*-alcohols (C28 and 30). The approximate boundary of permanent anoxia and the potential extent of the chemocline zone are noted, although these boundaries are highly mobile and affected by numerous parameters (see text).

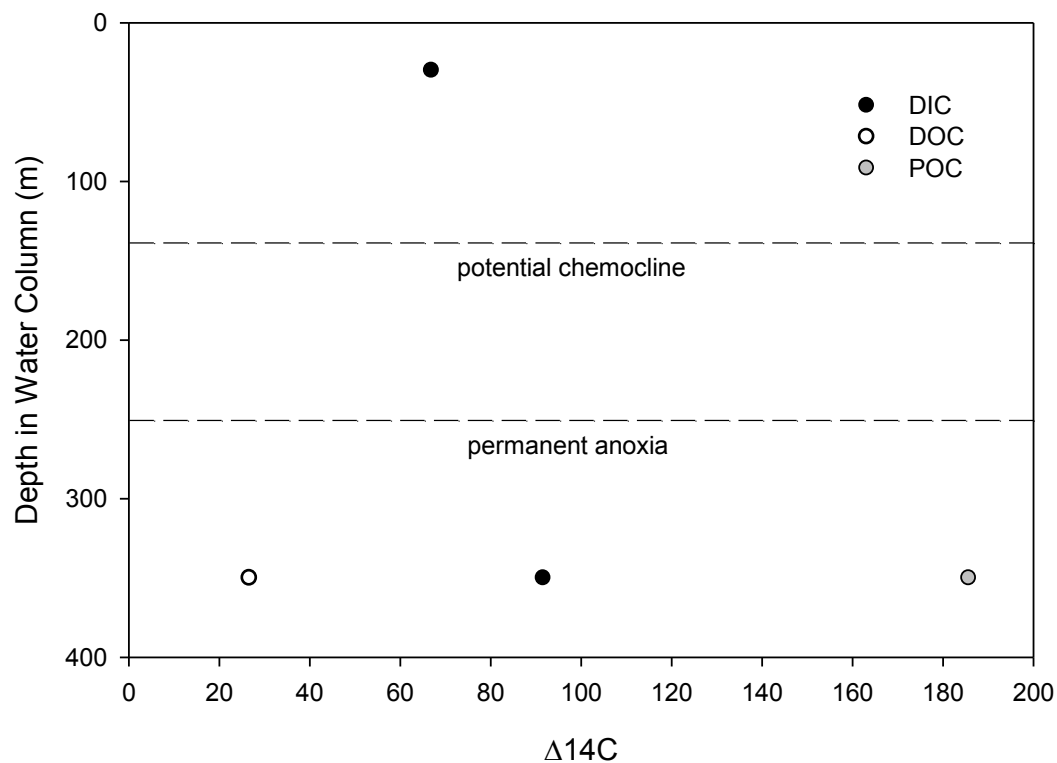


Figure 3.7. Radiocarbon signatures presented as $\Delta^{14}\text{C}$ (units of per mil, ‰) of water column organic carbon fractions DIC, DOC and POC from 30 and 350 m water depth where successful. The approximate boundary of permanent anoxia and the potential extent of the chemocline zone are noted, although these boundaries are highly mobile and affected by numerous parameters (see text).

Chapter 4: Organic Matter Transfer in Lake Superior's Food Web: Insights from Bulk and Molecular Stable Isotope and Radiocarbon Analyses

This chapter combines a suite of isotopic methods to provide a uniquely comprehensive investigation of organic matter transfer through an aquatic food web. We apply the compound specific nitrogen isotope analysis (CSNIA) of amino acids in organisms, a relatively new method and one not yet widely applied to large lake systems, to determine the discrete trophic level at which species are operating. Comparison of this trophic designation to those calculated by traditional bulk stable carbon and nitrogen isotope signature, as well as gut content analyses, revealed *Limnocalanus macrurus*, an omnivorous copepod, to have a trophic position one whole level above those previously assumed. This is likely due to slightly different diet constituents than previously assumed. We also applied radiocarbon analysis of bulk tissue to learn about the relative ages of carbon sources to the organisms, a method not commonly applied to the study of trophic level relationships. We found the benthic amphipod *Diporeia* to have an aged carbon source unique from other species, a trait that was not detectable by either CSNIA of amino acids or traditional stable isotope or gut content analysis studies. Fish in this system seem to integrate the radiocarbon signature of the system throughout their lifetime.

4.1 Introduction

Large lakes of the world ($>500 \text{ km}^2$) provide excellent environments for the study of carbon cycling in both the geologic and biologic realms. Globally, large lakes accumulate $\sim 10\%$ of the amount of organic carbon contained in marine sediments, despite occupying an area just 0.4% as large as that of marine waters (Alin and Johnson, 2007). Additionally, biodiversity and food chain length can be very high in large lakes regardless of lake productivity level (Post et al., 2000), creating opportunity to study energy transfer pathways in the relatively isolated environment the lake provides. Despite the high carbon accumulation and potentially high biodiversity within large

lakes, many characteristics of the carbon cycle within these systems remain unresolved. For example, in Lake Superior (USA and Canada), the degree to which allochthonous carbon inputs support the aquatic food web is unclear. Carbon budget imbalance suggests carbon in the lake is supplemented by an uncharacterized source (Cotner et al., 2004; Urban et al. 2005). Preliminary work by Zigah et al. (2011) found that radiocarbon signatures of mesozooplankton ($> 300 \mu\text{m}$) seem to track those of simultaneously sampled dissolved inorganic carbon (DIC) rather than particulate organic matter (POM). Since the atmospherically sourced DIC pool is the primary carbon source for photosynthesis by aquatic autotrophic organisms such as phytoplankton (Ingalls and Pearson, 2005; McNichol and Aluwihare, 2011) this result suggests the preferential consumption of recently photosynthesized material by mesozooplankton, rather than indiscriminant feeding on POM of varied age signatures.

Few studies have attempted to trace the flow of organic matter through trophic levels utilizing radiocarbon signatures in conjunction with traditional bulk stable isotope analysis (Hajdas, 2009), and furthermore, never have the compound specific nitrogen isotope analysis (CSNIA) food web structure methods developed by Chikaraishi et al. (2009) been combined with extensive radiocarbon analysis of the species under investigation. This food web structure is developed by assigning each sampled species a discrete trophic level value, based on the ratio of stable nitrogen isotopes in the amino acids phenylalanine and glutamine (Chikaraishi et al, 2009). This method was found to be robust in aquatic food webs, and is due to the low fluctuation of phenylalanine $\delta^{15}\text{N}$ and the concurrent enrichment of glutamine $\delta^{15}\text{N}$ with increasing trophic level (Chikaraishi, 2009). Though the radiocarbon and bulk isotope analysis can elucidate energy transfer pathways within the food web, such bulk isotope work cannot indicate actual trophic levels. The addition of this CSNIA approach therefore allows the carbon transfer pathways to be linked to discrete trophic levels, providing an unprecedented analysis of food web structure. Together these methods allow novel insight into how the food web of Lake Superior is supported and which carbon pools provide source material that is propagated up the food web.

The goal of this study was to trace carbon as it moves through the aquatic food web by applying bulk radiocarbon and stable carbon isotope analysis to multiple species of varied trophic levels (including higher zooplankton and fish) as well as particulate and dissolved organic carbon. Additionally, compound specific nitrogen isotope analysis (CSNIA) of amino acids was used to assign specific trophic levels to zooplankton and fish studied after the methods of Chikaraishi et al. (2009). If in fact the base of the food web relies largely on fresh photosynthetically produced material as hypothesized, that radiocarbon signature of ‘new’ material will be evident as it is propagated to higher trophic levels.

4.2 Methods

4.2.1 Sample Collection

In August 2012 fish and zooplankton were collected from three Lake Superior sampling locations aboard the R/V Kiyi (fish) and the R/V Blue Heron (zooplankton). Additional fish samples were collected near the Baptism and Ontonogan River sites using small vessels that deployed gillnets near each river to augment fish collections taken using R/V Kiyi. Two sampling locations were adjacent to large perennial river inputs, while the third was a deep water mid-lake location (Fig. 4.1). Fish were captured aboard the R/V Kiyi using a 39 ft Yankee bottom trawl net towed at 2-3 knots during daylight hours (see Stockwell et al. 2007 for detailed description of R/V Kiyi bottom trawl sampling protocol). To augment fish collections made using bottom trawls, experimental gillnets of sizes 2.5 (2 x 33-m panel), 7.5, 9, 11.5, 12.5 and 15.2 cm stretch mesh (2x 73-m panels) were fished adjacent to each river at depths ranging from 30 to 80 m for 16-20 hours between August 6th and August 15th 2012. Fish representing three distinct feeding strategies were targeted: piscivorous Siscowet Lake Trout (*Salvelinus namaycush*), planktivorous Coregonid species (either Kiyi (*Coregonus kiyi*) or Lake Herring (*Coregonus artedii*)), and benthic Deep Water Sculpin (*Myoxocephalus thompsonii*) (Table 1). Specimens were sorted by species aboard the vessel and ten representatives were collected for each target species (where possible), then frozen. Zooplankton were

collected using vertical net tows for planktonic species or grab sampling for benthic species. Zooplankton targeted included species or appropriate groups to represent dominant species at different trophic level positions: predatory *Mysis relicta*, the benthic amphipod *Diporeia*, the omnivorous copepod *Limnocalanus macrurus*, and the herbivorous cladoceran group *Daphnia spp* (Table 1). Vertical tows were conducted with a Puget Sound net with a 0.785 m² bridle opening (4m length, 153 µm mesh size). Tows were conducted during the night to facilitate maximum capture of vertically migrating species. After zooplankton were recovered from the net, they were incubated in a dark refrigerator for two hours in a large beaker of Milli-Q water to allow gut evacuation. Species were then carefully decanted into a new container, leaving the bottom 10 cm of beaker water as waste. *Mysis* were picked from the mixed zooplankton samples by hand, placed on nitex mesh filters, and frozen in combusted foil. The remaining mixed sample, containing predominantly a mix of cladoceran and copepod species, was collected on nitex mesh filters by handpump and glass filtering apparatus. Filters were folded in half and wrapped in combusted foil, then frozen. Benthic *Diporeia* were collected by deploying an Ekman Dredge to collect surface sediments at each site. The dredge was emptied into a large pan aboard the ship and specimens were collected with forceps and placed in sterile Milli-Q water for gut-evacuation incubation, then transferred onto nitex mesh filters, wrapped in sterile foil and frozen. Frozen samples were transported to the Large Lakes Observatory and remained frozen until analysis.

At each site, water column fractions were also collected from 5 m water depth and from ~ 5 m above the sediment (45 m water depth at BR2 and ONT2, and 120 m water depth at WM2) through deployment of a Niskin bottle rosette. Total inorganic carbon samples, which consist overwhelmingly of dissolved inorganic carbon (DIC) as the lake is undersaturated with respect to calcium carbonate, were collected by transfer of whole lake water directly from Niskin bottles to sterile ashed amber glass bottles (with ground glass stopper fittings) until the bottle overflowed for half the time it took to fill the bottle. Headspace (5 mL) was removed from these bottles and 100 µL of saturated HgCl₂ was added. Apeizon-M grease was used to seal the ground glass stoppers in the bottles, and

stoppers were further secured in the bottle via rubber bands. Particulate organic carbon (POC) and dissolved organic carbon (DOC) samples were obtained by transferring sample water into modified stainless-steel canisters and passing the sample through 0.7 μm pore size combusted GFF filters in stainless-steel housings by pressurizing the canisters with nitrogen gas. Filtrate was collected and acidified to pH 2 for DOC samples. Water was filtered until the filter ‘clogged’ or flow was significantly slowed to obtain sufficient material for POC analysis. Filters were collected, placed in combusted foil, and frozen.

4.2.2 Sample Processing

Tissue samples were collected from 10 fish per species per site (or as many as were recovered) by taking muscle plugs. Plugs were placed in combusted glass vials (which were covered loosely with aluminum foil) and dried in a 60° C oven. To obtain an isotope signature representative of the overall species, all muscle plugs for each species at each site were ground with sterilized mortar and pestle and homogenized. This resulted in one discrete sample for each fish species collected from each site. These homogenized samples were split, with ~10mg of each submitted to the National Ocean Sciences Accelerator Mass Spectrometry (NOSAMS) facility for radiocarbon analysis, and the rest saved for CSNIA performed at the Japan Agency for Marine-Earth Science and Technology (JAMSTEC).

Zooplankton samples were thawed and separated with forceps into groups of interest under a dissection microscope. Samples were rinsed with Milli-Q water prior to collection in combusted glass vials (for large species, *Diporeia* and *Mysis*) or onto combusted GFF filters (for small species, *Limnocalanus* and *Daphnia*). Large zooplankton (*Diporeia* and *Mysis*) were separated into distinct size classes (large, L; medium, M; and small, S), as different feeding strategies occur at different life stages for many zooplankton. Size classes were as follows: *Diporeia*: L \geq 5mm; M <5mm, *Mysis*: L \geq 15mm; M <15, >10; S \leq 10mm. For these larger species, total size class samples were dried and homogenized, and a subsample of the large size class was sent to NOSAMS for

radiocarbon analysis, while the remainders of all size classes were saved for CSNIA. For *Limnocalanus* and *Daphnia*, at least n = 50 individuals were collected on GFF filters for radiocarbon analysis, and at least n = 150 individuals were combined for CSNIA. All zooplankton samples were dried in a 55°C oven and samples for CSNIA were homogenized. A small split from each homogenized CSNIA sample was analyzed on a ThermoFinnigan Delta^{plus} XP isotope ratio mass spectrometer coupled to a ThermoFinnigan Flash EA1112 elemental analyzer at JAMSTEC to obtain bulk stable isotope signatures and elemental composition. Stable isotope ratios are reported as $\delta^{13}\text{C}$ and $\delta^{15}\text{N}$ and represent the ratio of isotopes in the sample relative to a standard, which was VPD Belemnite carbonate for $\delta^{13}\text{C}$ and atmospheric air for $\delta^{15}\text{N}$. Standard deviation relative to standards for measurement of $\delta^{13}\text{C}$ and $\delta^{15}\text{N}$ was 0.37 and 0.40‰, respectively (n = 14 and n = 18).

DIC and DOC samples were submitted to NOSAMS as collected for radiocarbon analysis. POC filters were thawed, dried, and also submitted, and underwent acid fumigation at NOSAMS to remove inorganic C prior to analysis as part of standard radiocarbon analysis protocol.

4.2.3 Radiocarbon Analysis

AMS analyses were performed at the National Ocean Sciences Accelerator Mass Spectrometry (NOSAMS) facility at Woods Hole Oceanographic Institute (WHOI) as described in Pearson et al. (2001). Radiocarbon results are reported here as $\Delta^{14}\text{C}$, defined as:

$$\Delta^{14}\text{C} = (f_m * e^{\lambda * (1950 - yc)} - 1) * 1000 \quad (1)$$

where f_m = fraction modern value reported by NOSAMS, $\lambda = 1/8267$, and yc = year collected, following the convention of Stuiver and Polach (1977). The $\Delta^{14}\text{C}$ value is $\delta^{13}\text{C}$ corrected, and corrected for decay time between year of collection and year of analysis.

4.2.4 CSNIA

Amino acids were extracted from homogenized organism samples at JAMSTEC as described in Chikaraishi et al (2007). Briefly, samples were subjected to 12 hours of acid hydrolysis at 110°C with 12N HCl. Hydrolysate was filtered and de-fatted by removing lipids with three liquid-liquid extractions using 3:2 v/v hexane:dichloromethane (DCM), followed by three rinses with methanol and drying under a gentle stream of nitrogen. Amino acids were esterified using 1:4 thionyl chloride:2-propanol at 110°C for 2 hours, and pivaloylated using 1:4 pivaloyl chloride:DCM at 110°C for 2 hours. Samples were rinsed with DCM then dried three times after each derivatization to completely remove remaining derivative agents. Water was added to the dried, derivatized sample, and amino acids were extracted via liquid-liquid extraction with 2x addition 3:2 hexane:DCM. Amino acid samples were dried, brought to appropriate volumes for analysis, and were injected on a ThermoFinnigan Delta^{Plus} XP isotope ratio mass spectrometer coupled to an Agilent Technologies 6890N gas chromatograph via combustion and reduction furnaces for N isotope measurement of amino acids. From these isotope measurements trophic level (TL_{Glu/Phe}) values were calculated following Chikaraishi et al. (2009) as described in the following section.

4.2.5 Trophic Level Calculations

Traditional trophic level based on bulk tissue isotope signature was calculated for each species as:

$$TL_{bulk} = ((\delta^{15}N_{consumer} - \delta^{15}N_{producer})/3.4) + 1 \quad (2)$$

where $\delta^{15}N_{consumer}$ is the bulk $\delta^{15}N$ signature of the species in question, and $\delta^{15}N_{producer}$ is the $\delta^{15}N$ of primary producers in the system. $\delta^{15}N_{producer}$ was estimated by averaging the $\delta^{15}N$ of 39 particulate organic nitrogen measurements performed by Zigah et al., (2012a) at seven lake-wide locations in Lake Superior and at three water depths at most sites, measured in both June and August, 2009. This gave a value of -0.60‰. In that study PON was collected by passing sample water across a 0.7 µm GF filter and subsequent filter analysis. Zooplankton biomass could have influenced those PON values, as all filter-trapped particulates were analyzed without removal of filtered zooplankton,

however bulk zooplankton (>300 µm) collected from the same sites were typically ~3-6‰ more enriched than the corresponding PON (Zigah et al., 2012b), indicating that mesozooplankton biomass contribution to filter particles was likely minimal. This value therefore can be assumed to represent a multi-season lake-wide integrated estimation of primary producer $\delta^{15}\text{N}$ in Lake Superior, and others have used bulk filtered seston to infer information about primary producers in Lake Superior (Harvey and Kitchell, 2000). Using such an integrated value for $\delta^{15}\text{N}_{\text{producers}}$ in the above equation increases the accuracy of trophic level estimations, since the animal biomass measured for each species also represents an integration of primary producer organic matter across multiple seasons. A lake-wide average is also appropriate, as higher trophic level fishes are highly mobile and can assimilate organic matter from prey at many locations. However, the assumed trophic ^{15}N enrichment of 3.4‰ is most applicable when investigating food webs with many trophic transfers, and is less reliable in systems with just a few linkages (Post, 2002). For example, Adams and Sterner (2000) demonstrated that the ^{15}N enrichment between algae and *Daphnia* varies from 0 to 5‰ depending on algal C/N, and was around 2‰ for algal C/N of 7-10. For this reason Post (2002) concluded that a more appropriate equation for defining trophic level from bulk-organism isotope signatures is:

$$\text{TL}_{\text{bulk-zoop}} = ((\delta^{15}\text{N}_{\text{zooplankton}} - \delta^{15}\text{N}_{\text{POM}})/2.2) + 1 \quad (3)$$

C/N of POM in Lake Superior was found to average ~8.3 by Zigah et al. (2012b) at 8 lake-wide sampling locations in June and August 2009, and therefore equation 3 was also used to estimate trophic level of zooplankton from bulk isotopic signature.

Quantified trophic level (TL) was calculated for each species as in Chikaraishi et al. (2009), defined as:

$$\text{TL}_{\text{Glu/Phe}} = (\delta^{15}\text{N}_{\text{Glu}} - \delta^{15}\text{N}_{\text{Phe}} - 3.4)/7.6 + 1 \quad (4)$$

where $\delta^{15}\text{N}_{\text{Glu}}$ = the compound specific $\delta^{15}\text{N}$ signature of glutamic acid from the sample, and $\delta^{15}\text{N}_{\text{Phe}}$ = the compound specific $\delta^{15}\text{N}$ signature of phenylalanine from the sample.

4.3 Results

4.3.1 Bulk Isotope Signatures

Bulk $\delta^{15}\text{N}$ and $\delta^{13}\text{C}$ signatures of all species and size classes from all sampling locations are plotted in Figure 4.2a. Lipids are known to be more ^{13}C depleted than other biogenic compounds as a result of fractionation during synthesis (DeNiro and Epstein, 1977), and many zooplankton rely on lipid content for energy reserves and flotation assistance (Lee et al., 1971). A mass balance lipid normalization model refined for lacustrine systems by Smyntek et al., (2010) can be applied to remove the isotopic influence of lipids on bulk $\delta^{13}\text{C}$ and allow for direct comparison of stable isotope values between zooplankton and higher organisms such as fish. This model uses bulk atomic C/N of the sample (C:N_{bulk}) and bulk sample $\delta^{13}\text{C}$ to estimate $\delta^{13}\text{C}$ of the sample if lipids had been extracted prior to analysis ($\delta^{13}\text{C}_{\text{ex}}$) as:

$$\delta^{13}\text{C}_{\text{ex}} = \delta^{13}\text{C}_{\text{bulk}} + 6.3((\text{C:N}_{\text{bulk}} - 4.2)/\text{C:N}_{\text{bulk}}) \quad (5)$$

In this equation 6.3 represents the average estimated per mil difference between $\delta^{13}\text{C}$ of the sample lipids and proteins (+/- 1.3‰) and 4.2 represents the estimated C/N of the extracted sample (+/- 0.4), based on comparison of model predictions and actual extracted sample results for lacustrine copepods and cladocerans (Smyntek et al., 2010). Figure 2b shows the same bulk isotope data after this isotope correction has been applied to the $\delta^{13}\text{C}$ signatures of zooplankton.

Most species group relatively near to each other in isotopic signature regardless of sample location. Regarding the bulk isotope data without lipid correction, *Daphnia* are the most depleted in ^{15}N , -0.1 to +0.6‰, and exhibit one of the widest intra-species ranges in $\delta^{13}\text{C}$, from -29.5 to -25.5‰. *Mysis* and *Diporeia* overlap in both $\delta^{15}\text{N}$ and $\delta^{13}\text{C}$, with $\delta^{15}\text{N}$ ranging from 2.1 to 6.0‰ and 3.3 to 4.0‰, respectively, and $\delta^{13}\text{C}$ from -27.9 to -24.6‰ and -26.8 to -24.6‰, respectively. Coregonid fish species range in $\delta^{15}\text{N}$ from 6.4 to 8.9‰, and in $\delta^{13}\text{C}$ from -26.0 to -25.2‰. Deep Water Sculpin range in $\delta^{15}\text{N}$ from 9.7 to 10‰ and in $\delta^{13}\text{C}$ from -25.4 to -25.0‰. Lake Trout range in $\delta^{15}\text{N}$ from 9.1 to 12.5‰, and in $\delta^{13}\text{C}$ from -25.1 to -25.5‰. *Limnocalanus* copepods are the only species that plot separately from other groups, with high $\delta^{15}\text{N}$ ranging from 8.0 to 9.6‰ coupled with a very low $\delta^{13}\text{C}$ signature ranging from -31.7 to -31.0‰. Lipid correction

of zooplankton $\delta^{13}\text{C}$ values resulted in a positive shift for almost all species (Fig. 4.4a.2b). Greatest changes were seen for *Limnocalanus* ($\delta^{13}\text{C}$ increases of 3.3 to 3.7‰) and *Daphnia* ($\delta^{13}\text{C}$ increases of 0.9 to 3.0‰). Corrections for *Mysis* and *Diporeia* resulted in both slight positive and negative shifts in $\delta^{13}\text{C}$, though not over a magnitude of 1.7‰ in the positive direction or 1.1‰ in the negative direction.

For each water column carbon fraction, the stable carbon isotope signature did not differ between shallow and deep water, and $\delta^{13}\text{C}$ values were similar across all sampling locations (Fig. 3). The $\delta^{13}\text{C}$ of DOC ranged from -26.6 to -26.3‰ in surface waters across all sites, and from -26.5 to -26.3‰ in deep waters across all sites. The $\delta^{13}\text{C}$ of POC ranged from -29.1 to -26.0‰ in surface waters and from -29.8 to -26.3‰ in deep waters across all sites. For DIC, the $\delta^{13}\text{C}$ in surface waters ranged from 0.15 to 1.36‰ and in deep waters, from -0.14 to 0‰.

4.3.2 Calculated Trophic Positions

Results for the three separate trophic level calculations (equations 2-4) are presented in Table 2 and $\text{TL}_{\text{Glu-Phe}}$ are plotted in Fig. 4.4a and Fig. 4.4b. For all species, calculated trophic level is similar regardless of sample location, indicating homogenization within the lake area sampled (Fig. 4.4a). *Daphnia* were consistently the lowest TL organism, with TL_{bulk} from 0.9 – 1.4, $\text{TL}_{\text{bulk-zoop}}$ from 0.8 – 1.6, and $\text{TL}_{\text{Glu-Phe}}$ from 1.9 – 2.1. *Limnocalanus* copepods, which would be assumed to fall near to *Daphnia* in trophic position according to other analyses of calanoid copepods (Harvey and Kitchell, 2000) were found to occupy at least one complete trophic level higher with $\text{TL}_{\text{Glu-Phe}}$ from 3.0 – 3.2. TL_{bulk} and $\text{TL}_{\text{bulk-zoop}}$ estimate their trophic position to be even higher, at 3.5 – 4.0 and 5.3 – 6.1, respectively. Large size classes of *Mysis* and *Diporeia* occupy trophic positions intermediate between TL 2 and 3 according to all TL calculations, with TL_{bulk} from 2.7 – 3.2 and 2.2 – 2.3, $\text{TL}_{\text{bulk-zoop}}$ from 3.0 – 4.6 and 3.0 – 3.3, and $\text{TL}_{\text{Glu-Phe}}$ from 2.6 – 2.7 and 2.3 – 2.4, respectively. Coregonid species were found to be near trophic level 3 with TL_{bulk} from 2.7 – 3.8 and $\text{TL}_{\text{Glu-Phe}}$ from 3.1 – 3.3. Deep water sculpin measured near trophic level 4, with $\text{TL}_{\text{bulk}} = 4.1$ at all locations, and

TL_{Glu-Phe} between 3.7 – 3.9. Lake trout were also found near to TL 4, with TL_{bulk} from 3.9 – 4.9, while TL_{Glu-Phe} values were between 3.8 – 3.9. TL_{bulk} values tended to encompass a wider range of values per species than did TL_{Glu-Phe}, which was especially true at higher trophic levels. Additionally, the TL_{bulk-zoop} indicated drastically higher trophic levels than the other calculation methods for all species above *Daphnia*. Calculated trophic level was similar between different size classes of *Diporeia* and *Mysis* according to TL_{Glu-Phe} (Fig. 4.4b) but *Mysis* showed slight trophic level enrichment with increasing size according to TL_{bulk} (Table 2).

4.3.3 Radiocarbon Signatures

Species-specific radiocarbon signatures were very similar at all sampling locations (Fig. 4.5). *Diporeia* showed clearly distinct $\Delta^{14}\text{C}$ (ranging from 17.3 and 22.5‰) relative to other species at each location collected. There is also an obvious decline in $\Delta^{14}\text{C}$ between higher order fish and lower order zooplankton. Lake trout $\Delta^{14}\text{C}$ ranged from 63.1 to 77.8‰ at all locations, 63.5 to 68.9‰ for Coregonids, 63.6 to 69.4‰ for DW Sculpin, 53.0 to 57.8‰ for large *Mysis*, 40.5 to 53.4‰ for *Limnocalanus*, and 31.2 to 45.6‰ for *Daphnia*.

Water column fractions showed some $\Delta^{14}\text{C}$ variability both between and within fractions and water depths measured (Fig. 3). DOC radiocarbon signature was roughly 53 - 60‰ at all sites and water depths, except for the deep water measurement at WM2 which was the highest measured water column $\Delta^{14}\text{C}$ value at 77‰. Of all water column fractions POC was the most variable. In particular, the $\Delta^{14}\text{C}$ of surface water POC measured at Ont2 was very low, 0.5‰, while Bap2 and WM2 surface water were 45.5 and 41.9‰, respectively. Deep water POC was similar at Bap2 and Ont2 at 28.7 and 25.4‰, respectively, but was 42.0‰ at WM2. DIC $\Delta^{14}\text{C}$ was slightly variable between both sites and depths, though less so than POC. DIC $\Delta^{14}\text{C}$ values in surface water ranged from 38.0 to 49.1‰, and were similar at Bap2 and WM2 (at around 49‰). In deeper water measurements, DIC $\Delta^{14}\text{C}$ ranged from 35.7 – 45.9‰ and was lowest at WM2 at 35.7‰.

4.4 Discussion

4.4.1 Food Web Structure from Bulk Stable Isotopes

The ratios of stable nitrogen isotopes ($\delta^{15}\text{N}$) and stable carbon isotopes ($\delta^{13}\text{C}$) in organisms have long been used to investigate trophic relationships in aquatic systems by exploiting the fractionation that occurs between consumer and food source. The $\delta^{15}\text{N}$ of consumers is typically 3 – 4‰ enriched relative to their diet and 3.4‰ is the generally accepted shift in $\delta^{15}\text{N}$ between trophic levels (DeNiro and Epstein, 1981; Peterson and Fry 1987; Post, 2002). Carbon isotope fractionation during food web transfer is smaller, with a 1‰ or less enrichment of consumers over source carbon (DeNiro and Epstein, 1978; Peterson and Fry, 1987). This means the $\delta^{13}\text{C}$ of organic carbon within an aquatic system can preserve the unique isotope signature imparted to it from its carbon source (Meyers, 1997; Leng and Marshall, 2004) with little influence from organic matter transfer fractionation. As a result, plotting the $\delta^{15}\text{N}$ versus $\delta^{13}\text{C}$ signature of bulk animal tissue has become a common method to investigate trophic structure and potential carbon sources in aquatic systems (Post, 2002). Examination of this plot reveals lake trout as the top predator at all locations sampled in Lake Superior, while *Daphnia* consistently occupy the lowest trophic level measured in this study. According to known diet compositions (Table 2) the general organization of lowest to highest trophic position of organisms in this study would be assumed to follow *Daphnia* → larger zooplankton → small planktivorous fish → larger piscivorous fish. Bulk $\delta^{15}\text{N}$ and $\delta^{13}\text{C}$ organism signatures generally support this assumption, and are consistent with other stable isotope analyses of the same species in Lake Superior (Harvey and Kitchell, 2000).

Daphnia spp. in the Laurentian Great Lakes are known to be efficient filter feeders, consuming algae, diatoms, or acceptable POM, while some have also evolved the capability to temporarily attach to large algae or macrophytes and scrape off surface-adhered diatoms or POM (Balcer et al., 1984). While *Daphnia* are an obvious gateway to incorporate primary production into food web biomass, the extent of ^{15}N fractionation during nitrogen assimilation by *Daphnia mendotae*, a common Lake Superior species,

can vary from 0 to 5‰ and is dependent on C/N of the algal material being consumed (Adams and Sterner, 2000). Therefore the isotopic signature of *Daphnia* is not a direct indication of the isotopic signature of primary production, but the assumption can be made that *Daphnia* operate near $TL = 2$ as the major consumers of primary productivity in the system. Radiocarbon results, described further below, showing the $\Delta^{14}C$ of *Daphnia* to overlap with that of water column DIC, also indicate that *Daphnia* are consumers of recently produced in-lake production. *Daphnia* consumption by the higher order zooplankton *Mysis* is likely as this omnivorous species employs predacious feeding strategies, consuming both algae and other pelagic crustacean zooplankton (Grossnickle et al., 1982). While *Limnocalanus* also exhibits omnivorous feeding strategies, it is more likely their diet focuses on nauplii and small copepodites in the Great Lakes, though small or immature *Daphnia* may also be consumed (Warren 1993; Warren 1995). *Daphnia* consumption by *Diporeia* is also unlikely given their predominantly benthic life cycle, and it is likely their diet consists mostly of benthic zooplankton and sedimented algae (Sierszen et al., 2006). This is reflected by *Diporeia* $\delta^{15}N$ values slightly lower than that of *Mysis* and much lower than *Limnocalanus*, which suggests their reduced reliance on predatory consumption of zooplankton (Fig. 4.2).

Coregonid spp. fishes in the Great Lakes are planktivorous feeders, though the two species of focus in this study have different preferred prey. Kiyi, found at sites WM2 and Ont2, focus on *Mysis* as a prey item, and though they also feed to a lesser extent on *Daphnia*, *Mysis* constitute nearly 100% of their diet by biomass in spring, summer, and fall (Gamble et al., 2011). Their $\delta^{15}N$ values reflect this preference, with an evident 3.4‰ enrichment over *Mysis* $\delta^{15}N$. Lake herring, the *Coregonid* found at Bap2, prefers Calanoid copepods as its main diet source in the spring, *Bythotrephes* in the summer, and *Bythotrephes* and *Mysis* in the fall (Gamble et al., 2011). This diet pattern, distinct from that of Kiyi, is mirrored in a distinctly lower $\delta^{15}N$ for this species, reflecting the lower $\delta^{15}N$ influence from copepods (Fig. 4.2). However, the $\delta^{15}N$ of the calanoid copepod *Limnocalanus macrurus* measured in this study is higher than that of Lake Herring, indicating low consumption of that species by Lake Herring.

Furthermore, the copepod *Limnocalanus* also seems to be an exception to the otherwise ordered food web structure indicated by bulk stable isotopes; according to their very low $\delta^{13}\text{C}$ and elevated $\delta^{15}\text{N}$ they do not fall within the grouped food web species as expected. Others have also found this particular copepod species to be very depleted in ^{13}C and enriched in ^{15}N (Chetelat et al., 2012; Branstrator, University of Minnesota, Duluth, personal communication), implying these unique signatures might be a relatively unreported hallmark of the species. This also implies that the influence of *Limnocalanus* on the bulk isotopic signatures of total calanoid copepods might be minimal, as measurements on that general copepod group have not produced similarly unique isotopic results (Harvey and Kitchell, 2000). Brown and Branstrator (2004) found that *Limnocalanus* composed an average of 20% and 11% of major calanoid copepods at 10 coastal sites in Lake Superior's western arm during May and August, respectively, and an average of 31% and 15% at four offshore locations during May and August. However, *Limnocalanus* biomass was more than double and triple that of the next most abundant crustacean zooplankton, *Diaptomus* (another calanoid copepod), in May and August, respectively, which could effectively make it the most abundant metazoan in Lake Superior's western arm. The bulk isotopic signature of bulk calanoid copepods was not measured in this study, but Harvey and Kitchell (2000) found that the isotope signatures of bulk calanoid copepods in Lake Superior were seemingly unaffected by the unique signatures of *Limnocalanus*. This could imply that, at the time of their sampling, other major calanoid species dominated (e.g. *Epsichura*, *Diaptomus* (Brown and Branstrator, 2004)), that do not show such extreme isotopic signatures. Another possibility is the calanoid copepods species other than *Limnocalanus* have their own oppositely unique isotopic signatures that may effectively 'cancel out' the *Limnocalanus* signature. To our knowledge there has not been extensive species-specific isotopic investigation of calanoid copepods in Lake Superior. Possible explanations for the unique stable isotope signatures of *Limnocalanus* are explored in the following section.

4.4.2 Unique Stable Isotopic Signatures of Limnocalanus macrurus

Several possibilities exist that could explain the $\delta^{15}\text{N}$ enrichment and $\delta^{13}\text{C}$ depletion of *Limnocalanus macrurus*. This species has arctic marine origins, and is believed to have first colonized freshwater during the Pleistocene glaciation. It has retained a high lipid content, up to 67% by dry weight, composed mainly of wax ester reserves that may facilitate early season egg production during times of low prey abundance (Vanderploeg et al., 1995). The low $\delta^{13}\text{C}$ of *Limnocalanus* samples is therefore likely a reflection of their high lipid content, and a large increase (3.5‰) is observed for *Limnocalanus* $\delta^{13}\text{C}$ after application of lipid correction. While lipid correction places *Limnocalanus* nearer to the range of $\delta^{13}\text{C}$ values measured for other zooplankton species in this study (Fig 2b) they are still the most ^{13}C depleted organisms studied here. This could indicate a unique carbon source relative to other species, or that the general algorithm for lipid correction does not completely correct for the high lipid concentrations of *Limnocalanus*.

Isotopic influence of lipids does not, however, explain the $\delta^{15}\text{N}$ enrichment or elevated trophic level (TL) calculated for that species. Others have measured enriched $\delta^{15}\text{N}$ for this copepod species in lake systems (Chetelat et al., 2012, Branstrator, personal communication). *Limnocalanus* were found to have an average $\delta^{15}\text{N}$ of 7.2‰ across ten small arctic lakes, and were 8‰ or higher in at least one sampling in 4 of 10 lakes (Chetelat et al., 2012). After normalizing $\delta^{15}\text{N}$ of *Limnocalanus* to that of a primary consumer to minimize effects of $\delta^{15}\text{N}$ baseline differences among lakes, those researchers concluded that % adult biomass was the best predicting factor for $\delta^{15}\text{N}$ enrichment. An average enrichment of 3.3‰ between the copepodite and adult stages was measured. Changing trophic position was ruled out to explain the $\delta^{15}\text{N}$ enrichment, as no evidence of zooplankton predation was found in stomachs of large individuals (Chetelat et al., 2012). However, *Limnocalanus* have been shown to exhibit predatory behavior in other lakes, including heavy feeding on copepod nauplii in Lake Michigan (Warren, 1983; Warren, 1985). In two of the Arctic lakes described above where their $\delta^{15}\text{N}$ was very enriched (8.4 and 8.7‰) *Limnocalanus* were feeding heavily on diatoms according to gut

analyses, and in the lake with the highest measured $\delta^{15}\text{N}$ (10.6‰) stomachs contained high amounts of algae (Chetelat et al., 2012). It has been shown that *Limnocalanus* exhibit seasonal changes in diet (Vanderploeg et al., 1995), and it is possible that naupliar and microzooplankton abundances were lowest during the summer gut sampling (July and August) described by Chetelat et al. (2012). Bulk organism $\delta^{15}\text{N}$ would reflect all previous nitrogen integration, and predation on smaller zooplankton species could be one explanation for *Limnocalanus* $\delta^{15}\text{N}$ enrichment in Lake Superior.

Vanderploeg et al. (1995) found naupliar abundance to be greatest in late winter to early spring in Lake Michigan. In Lake Superior *Limnocalanus* nauplii begin to increase in abundance in February and peak in late May, while naupliar abundance of other copepod species begins increasing in late May and peaks in June or July (Selgeby, 1975). In Lake Superior *Limnocalanus* adults may reach peak abundance in late winter and early spring (Selgeby, 1975) or into the summer (Brown and Branstrator, 2004) and therefore overlap with periods of high naupliar abundance from other copepod species. This presents the opportunity for carnivory, which could partially explain their $\delta^{15}\text{N}$ enrichment. Furthermore, Zigah et al. (2012a) showed the $\delta^{15}\text{N}$ of POM to be heavier and less variable in June than in August by roughly 3.3 to 4.3‰ (-1.7 to 1.7‰ in June vs. -3.7 to +3.0‰ in August). However, feeding on nauplii alone would not be expected to account for *Limnocalanus* $\delta^{15}\text{N}$ values of 7.9 and 9.6‰ measured in this study. If nauplii are assumed to graze predominantly on phytoplankton, they would be expected to have $\delta^{15}\text{N}$ signatures near to 0‰, as did *Daphnia* grazers in this study. Consumer $\delta^{15}\text{N}$ signatures of ~3.4‰ would be expected from reliance on nauplii consumption, given the ~3.4‰ $\delta^{15}\text{N}$ enrichment that occurs with each trophic transfer (DeNiro and Epstein, 1981; Post, 2002). A plausible scenario to explain enrichments as measured here include the consumption of nauplii by a microzooplankton intermediate, perhaps other small copepods or late stage copepedids, which are then consumed by adult *Limnocalanus*. These two separate trophic transfers of nitrogen could create $\delta^{15}\text{N}$ signatures around 7‰, which are nearer to the *Limnocalanus* values reported here, particularly taking into account the higher early season $\delta^{15}\text{N}$ of POM in Lake Superior (Zigah et al., 2012a) when

such intermediate feeding is likely to occur. Late copepodid and adult stages of the *Diaptomus* copepod family, which are common in the Laurentian Great Lakes (Balcer et al., 1984) and one of the most dominant species in Lake Superior's western arm (Brown and Branstrator, 2004), are known to have wide-ranging diets which can include large algae, rotifers, and small crustacean zooplankton (Balcer et al., 1984) which could include nauplii. Both *Diaptomids* and Cyclopoid copepods, also a dominant copepod group in Lake Superior (Brown and Branstrator, 2004), are considerably smaller as adults (~0.9 – 1.3 mm and 0.5 to 1.5 mm, respectively) than *Limnocalanus* (~2.2 – 3.2 mm) (Balcer et al., 1984). It is therefore morphologically possible for adults or copepodid stages of these groups to be preyed upon by *Limnocalanus*, based on body size, and they could represent an intermediate between nauplii and adult *Limnocalanus* consumption. However, Warren (1985) found that *Limnocalanus* in Lake Michigan exhibit limited predacious feeding behavior on copepodites of both *Diaptomous* spp. and *Cyclops* spp. (a cyclopoid copepod genera), instead preferentially selecting nauplii for consumption when available. This implies that the $\delta^{15}\text{N}$ enrichment in adult *Limnocalanus* is more likely a result of predation on isotopically enriched nauplii rather than the influence of an intermediate consumer. Studies have shown the nauplii of *Calanus* spp., an arctic calanoid copepod genus, to feed predaciously on heterotrophic protists rather than grazing on phytoplankton to the extent that their dominant dietary component was phagotrophic ciliates and dinoflagellates (Turner et al., 2001). Others have found nauplii of multiple copepod species to feed on bacterioplankton in marine environments (Turner and Tester, 1992; Roff et al., 1995). It is also known that nauplii are in fact able to detect prey and employ either feeding-current or ambush mechanisms to selectively obtain their prey (Bruno et al., 2012). It is plausible then that nauplii of some Great Lakes species employ similar mechanisms to feed predaceously on heterotrophic or autotrophic organisms, thus enriching their $\delta^{15}\text{N}$ signatures, and causing further enrichment to their adult copepod predators, including *Limnocalanus*. It follows that the most likely cause of enriched *Limnocalanus* $\delta^{15}\text{N}$ in Lake Superior is a combination of their direct feeding on

nauplii that are themselves $\delta^{15}\text{N}$ enriched, and feeding on small microzooplankton omnivores.

4.4.3 A Comparison of Trophic Level Calculation Methods and Implications for Food Web Structure

Clear discrepancies exist between the predicted trophic level for each organism depending on the calculation method used. Particularly for higher order organisms, TL calculations based on bulk isotopic data show wider ranging results for the same organism between lake locations than does the CSNIA method. The $\text{TL}_{\text{bulk-zoop}}$ calculation method, which used a smaller $\delta^{15}\text{N}$ enrichment factor, drastically overestimated the trophic position of all organisms beyond *Daphnia* with consideration to known gut content analyses. Based on these values, the $\text{TL}_{\text{bulk-zoop}}$ method was not considered as a viable approach for TL calculation in this system. One complication inherent in the application of bulk stable isotope signatures to infer actual organism trophic level is the need to quantify the baseline nitrogen isotopic signature of the food web (Post, 2002). Baselines of aquatic systems are often highly variable. The stable isotopic signature of POM has been measured in Lake Superior's western arm as a representation of baseline nitrogen isotope values for trophic level evaluation (Harvey and Kitchell, 2000), and these values were found to exhibit high spatial heterogeneity with $\delta^{15}\text{N}$ ranging 0 - 4‰. Zigah et al., (2012a) found even more variable $\delta^{15}\text{N}$ of PON in Lake Superior during their extensive lake-wide sampling, with values from -3.9 to +3.7‰. Furthermore, variable baseline signatures can combine with nitrogen integration time lags to further complicate apparent trophic structure. For example, O'Reilly et al. (2002) found the $\delta^{15}\text{N}$ of phytoplankton in Lake Tanganyika to be very ^{15}N enriched and equal to values measured for zooplankton (6 to 8‰), due to an upwelling event of ^{15}N -enriched bottom waters in the days prior to sampling. This heavy nitrogen isotope signature had already been incorporated into the phytoplankton bulk isotope signature, but was not yet evident in the zooplankton consumers. Hannides et al., (2004) found the

bulk $\delta^{15}\text{N}$ of primary copepod consumers to shift 5 to 9‰ between seasons, indicating a large temporal shift in the isotope composition of the nitrogen source. Finally, the typically accepted trophic transfer $\delta^{15}\text{N}$ increase of 3.4‰ can actually vary from 0 to 9‰, dependent on species and metabolism mechanisms (DeNiro and Epstein, 1981; McCutchan et al., 2003). Lower trophic level transfers in particular, such as the assimilation of primary productivity by primary consumers, has been shown to occur with a fractionation much lower than the standard 3.4‰ in some aquatic systems, often nearer to 2‰ (Adams and Sterner, 2000; McCutchan et al., 2003). The CSNIA of amino acids method mitigates these issues by removing the need for an independent characterization of isotopic baseline and automatically reflecting an integrated signal of primary producer $\delta^{15}\text{N}$ (Chikaraishi et al., 2009).

The CSNIA of amino acid method for TL determination is robust due to the observations first reported by McClelland and Montoya (2002) that some amino acids (e.g., glutamic acid, leucine, alanine, and others) experience ^{15}N enrichment with trophic transfer, while others (e.g., phenylalanine, glycine, serine and others) seem to undergo little nitrogen fractionation. It was proposed by Chikaraishi et al. (2007) that this differential ^{15}N enrichment between amino acids was the result of different metabolic pathways, whereby amino acids that exhibit large ^{15}N enrichment with trophic transfer (such as glutamic acid) do so as a result of transamination reactions which cleave a C-N bond, while amino acids that do not show nitrogen fractionation (such as phenylalanine) undergo metabolisms independent of nitrogen-cleaving or bonding reactions. Chikaraishi et al. (2007) also determined phenylalanine to be the amino acid that exhibited $\delta^{15}\text{N}$ values most representative of the source material in a marine food web, while glutamic acid was the most regularly enriched between trophic transfers ($7.6\text{‰} \pm 1.4\text{‰}$). Furthermore, each of these two amino acids (and others) exhibited ^{15}N fractionation of similar magnitude and direction from bulk organism material whether isolated from green algae or cyanobacteria species, indicating similar amino acid biosynthesis and metabolism pathways of all photoautotrophs (Chikaraishi et al., 2007). Continuing their work to investigate $\delta^{15}\text{N}$ of amino acids from multiple algae, zooplankton, and fish

species, Chikaraishi et al. (2009) proposed that use of the $\delta^{15}\text{N}$ of glutamic acid and phenylalanine gave the most reliable calculation of specific trophic levels of species by following $\text{TL}_{\text{Glu/Phe}} = (\delta^{15}\text{N}_{\text{Glu}} - \delta^{15}\text{N}_{\text{Phe}} - 3.4)/7.6 + 1$, with this equation also resulting in the lowest associated error of all amino acid pairs investigated. A similar equation was used by Hannides et al., (2009) to investigate the trophic position of zooplankton in the North Pacific Subtropical Gyre, concluding that this CSNIA method efficiently differentiated between primary and secondary consumer copepods, producing $\text{TL}_{\text{Glu-Phe}}$ values that were mostly consistent with TL_{bulk} values, but that were preferred over bulk measurement due to reduced variability, smaller required sample size, and the decoupling of bulk method reliance on isotopic characterization of primary producers.

Generally, the calculated trophic levels for organisms in this study (Fig. 4.4a) are also consistent with the trophic positions as indicated by bulk $\delta^{13}\text{C}$ and $\delta^{15}\text{N}$ (Fig. 4.2), though discrepancies are evident between $\text{TL}_{\text{Glu-Phe}}$ and TL_{bulk} for certain organisms. While the elevated $\text{TL}_{\text{Glu-Phe}}$ of the copepod *Limnocalanus* is an unexpected overall finding in this study, it is consistent with their previously discussed bulk $\delta^{13}\text{C}$ and $\delta^{15}\text{N}$ signatures. This consistency indicates that the elevated $\delta^{15}\text{N}$ in that species is likely the result of increased trophic transfers, however it cannot rule out a unique species-specific nitrogen metabolism or fractionation effect. TL_{bulk} values calculated for *Limnocalanus* are almost a full trophic level greater than the $\text{TL}_{\text{Glu-Phe}}$ values. This phenomenon is also observed for lake trout at two of three locations. Another example of discrepancy comes from DW sculpin, which show slight difference between trophic level indicated by bulk $\delta^{13}\text{C}$ and $\delta^{15}\text{N}$ versus calculated by CSNIA. Calculated $\text{TL}_{\text{Glu/Phe}}$ for that species is at or above that of lake trout at all sampling locations, while bulk $\delta^{15}\text{N}$ signature of DW sculpin indicates a trophic position below that of lake trout at two of three locations, but above at one (Fig. 4.2). However, $\text{TL}_{\text{Glu-Phe}}$ for lake trout at all locations are very similar. Gut content analyses have shown *Mysis* and *Diporeia* to constitute roughly 40 – 75% and 10 – 40% of DW sculpin diet respectively, across spring, summer, and fall seasons (Harvey and Kitchel, 2000; Gamble et al., 2012). This dependence on the highly predatory *Mysis* indicates that a $\text{TL}_{\text{Glu-Phe}}$ near to 4 is in fact expected for that species.

Both of these cases further highlight the issues in analyzing food web structure based on either bulk $\delta^{15}\text{N}$ values or TL_{bulk} calculations that incorporate those values, which stem from the inherent variability in those methods due to $\delta^{15}\text{N}$ baseline variations. These measurements are, to our knowledge, the first application of CSNIA of amino acids in a large lake system, and support work done in smaller lakes, thus further confirming that this method of TL determination is appropriate in lake environments.

Because of the reduction in baseline uncertainty and consistency with gut content analysis studies, we judge these $\text{TL}_{\text{Glu-Phe}}$ values to be the most representative of actual trophic positions for organisms in this study. Extensive gut content analysis of Lake Superior fish (Table 4.1) sheds light on actual feeding strategies for these organisms. Feeding interactions illustrated by gut content studies are consistent with the isotopically determined $\text{TL}_{\text{Glu-Phe}}$ positions of fish species, validating this technique as the most accurate method for trophic level determination of the methods examined here.

4.4.4 Carbon Pool Interactions as Indicated by Radiocarbon Signatures

The record of food web interactions as indicated by radiogenic carbon content differs from that inferred from bulk stable isotope analyses or CSNIA of amino acids. From this analysis, it is clear that *Diporeia* have a unique carbon source from other organisms in this study. The relatively depleted bulk $\Delta^{14}\text{C}$ of that species, while still ‘modern’ in age, indicates the incorporation of carbon sources older than the most recently photosynthesized material. *Diporeia* $\Delta^{14}\text{C}$ values are well below the $\Delta^{14}\text{C}$ of DIC in all seasons, and could be the result of carbon assimilation from aged sedimentary sources. An estimated 58% of external sediment loading to the lake comes from erosion of the clay cliffs of Wisconsin, while riverine input accounts for roughly 30% (Kemp et al., 1978), and both can be a source of aged carbon to the system. Inflow from tributaries to Lake Superior can contribute ^{14}C depleted DOC and/or POC at different levels of flow (Zigah et al., 2011), and direct sloughing of cliff faces to the lake can be a source of aged particulate organics typically sequestered in deeper soil horizons. Particulates from both

sources can end up deposited as sediment older than material originating in the lake. The benthic life history and feeding strategy of *Diporeia* makes its ingestion of aged sedimentary carbon likely, either directly through detrital grazing or during feeding on epilithic or benthic algae (Sierszen et al., 2006). The $\delta^{13}\text{C}$ signature of POC is similar to that of *Diporeia*, which does not dispute the incorporation of sedimented POC to their diet, though the range of $\delta^{13}\text{C}$ measured for all zooplankton overlap, particularly after lipid correction (Fig. 4.2). Furthermore, since the $\delta^{13}\text{C}$ of organic matter produced by land plants overlaps with that produced by phytoplankton it cannot be assumed that the POC has either allochthonous or autochthonous origins, and likely represents a mixture of both sources. It should also be noted that there may be a lag time in equilibration between atmospheric $\Delta^{14}\text{C}$ and the DIC pool of Lake Superior. Atmospheric $\Delta^{14}\text{C}$ has been declining since the spike from bomb material in the 1950s, and Zigah et al. (2012a) attributed offshore $\Delta^{14}\text{C}$ of DIC that were 12 - 27‰ higher than co-occurring atmospheric $\Delta^{14}\text{C}$ to reflect exchange time for the atmospheric carbon and DIC pools. Thus, recently fixed terrestrial plant material transported into the lake may have radiocarbon signatures with lower $\Delta^{14}\text{C}$ than material recently produced within the lake. This could indicate that *Diporeia* is consuming ^{14}C -depleted sedimentary material that was actually sourced from recent land plant grown.

The $\Delta^{14}\text{C}$ of POC in this study is highly variable between locations and water depths, which could also reflect varying contributions from aged suspended sediment particles or terrestrial carbon inputs. Zigah et al. (2012a) also found POC radiocarbon content to be highly variable across lake wide sites, during both spring mixing and summer stratification. Moreover, those researchers found that the $\Delta^{14}\text{C}$ signature of mixed pelagic mesozooplankton (>300 μm) tracked that of DIC rather than POC in all seasons and locations sampled, despite the high availability of POC, indicating a zooplankton preference for recently synthesized autochthonous material (Zigah et al., 2012). With the exception of the unique *Diporeia* $\Delta^{14}\text{C}$ signatures, zooplankton in this study also exhibit $\Delta^{14}\text{C}$ signatures similar to that of DIC. However, despite the higher variability, POC $\Delta^{14}\text{C}$ values are also similar to that of DIC at multiple locations and

water depths in this study. Therefore, with this data from a single time-point, we cannot conclude that the radiocarbon content of zooplankton distinctively tracks either water column carbon pool.

Radiocarbon content of DOC is also variable between sites, with the most ^{14}C -enriched measurement found in deep water DOC from the mid-lake location (Fig. 4.3). This variability could reflect multiple DOC sources. DOC can be released extracellularly from phytoplankton (Baines and Pace, 1991), although $\Delta^{14}\text{C}$ of that material should still track that of DIC in Lake Superior. Variability in DOC $\Delta^{14}\text{C}$ could also reflect the variability of DOC cycling time within the water column. DOC that is aged by a few decades but still younger than the 1950's bomb spike would have higher $\Delta^{14}\text{C}$ values than recently synthesized DOC. Primary production incorporation of this slightly ^{14}C enriched DOC pool at WM2 could contribute to the elevated *Daphnia* and *Limnocalanus* ^{14}C signatures also seen at the deep water site. However, the WM2 POC fraction does not show concurrently elevated ^{14}C signatures, which would be expected if DOC was being used as a primary carbon source and if those consumers constituted a large proportion of the POC fraction. It is possible that such DOC consumers may not constitute a significant portion of the POC pool. Additionally, DIC $\Delta^{14}\text{C}$ is not elevated at this location, at roughly 49 and 36‰ in surface and deep water, respectively.

The general decline in $\Delta^{14}\text{C}$ observed between fishes and zooplankton (Fig. 4.5) likely reflects the multi-year carbon incorporation by fishes versus the relatively newly fixed carbon of zooplankton with shorter life cycles. Zigah et al. (2011) estimated the $\Delta^{14}\text{C}$ of DIC in Lake Superior to be declining by roughly 11‰ yr⁻¹ as a result of declining $\Delta^{14}\text{C}$ of atmospheric CO₂ following the spike resulting from nuclear testing in the 1950's and 60's (Hsueh et al., 2007). In Lake Superior, *Daphnia* life cycles are less than one year, *Limnocalanus* exhibit life cycles lasting roughly one year, and *Diporeia* and *Mysis* exhibit roughly 2-year life cycles (Carpenter and Mansey, 1974; Selgeby, 1975; Balcer et al., 1984; Sierszen, 2006). Lake trout, on the other hand, have even longer life spans in large clear-water lakes than in smaller lakes, and can reach 25 years of age in Lake Superior, though ~15 is more typical (Shuter et al., 1998). It is also

possible for Coregonid fish of Lake Superior to live longer than 10 years, and they are considered mature at 3-4 years (Ebener et al., 2008). Deep water sculpin have the shortest life spans of fish measured here, reaching maturity at ~3 years and usually not living past 7 years in the wild (Selgeby, 1988). To determine elemental turnover rate in fish muscle, Hesslein et al. (1993) fed growing *Coregonus nasus* isotopically labeled food. They determined the time required for complete muscle mass carbon turnover in wild populations of that freshwater Arctic Coregonid would be years. Similar studies on shorter-lived fish species from a small lake have shown carbon half-lives in muscle mass during periods of initial rapid growth to be 1 – 2 weeks, but were 116 – 171 days for mature fish (Weidel et al., 2011). Therefore, the natural abundance isotopic signatures of wild fish beyond the fast growing early life stages should represent long-term averages of food sources. Thus, the elevated $\Delta^{14}\text{C}$ of the long life-span fish species in this study are likely a relict signature reflecting the incorporation of organic matter synthesized during previous years when $\Delta^{14}\text{C}$ of DIC was also higher.

Although the radiocarbon signatures of fish in this study are ‘greater than modern’, we can make rough estimations of their age by estimating how many years of carbon incorporation would be required to result in the measured radiocarbon values. This study shows that in 2012 the average $\Delta^{14}\text{C}$ of surface water DIC at the three sites sampled was 45‰, while in 2009 it was 54‰ (n = 6, Zigah et al., 2012). This indicates the rate of decline in surface water DIC is not consistently 11‰ per year as postulated by Zigah et al. (2011). The $\Delta^{14}\text{C}$ of atmospheric CO_2 in 2009 and 2012 as determined by corn leaf analysis was 38‰ and 25‰, respectively. Thus, the Lake Superior surface water DIC pool at the three sampling locations in question was, on average, 16‰ and 20‰ more enriched than atmospheric $\Delta^{14}\text{C}$ in 2009 and 2012, respectively. Because these two offsets are fairly consistent over that three year time span, we can average those values to obtain a standard offset of 18‰ between atmospheric and DIC $\Delta^{14}\text{C}$. Since the $\Delta^{14}\text{C}$ of northern hemisphere atmospheric CO_2 in 2007 was 50‰, the corresponding $\Delta^{14}\text{C}$ of surface water DIC can be assumed at 68‰. Average $\Delta^{14}\text{C}$ of Lake Trout, Coregonid, and Sculpin fish tissue as determined in this study (fish captured in 2012) was 72, 65, and

66‰, respectively. This indicates that muscle tissue of all fish species studied here reflect carbon incorporation over many years. Lake Trout have the longest life cycle of fish studied and exhibit the highest average muscle tissue $\Delta^{14}\text{C}$ at 72‰. Again applying the calculated 18‰ offset from atmospheric $\Delta^{14}\text{C}$, lake DIC would have been 72‰ in approximately 2005 according to published northern hemisphere $\Delta^{14}\text{C}$ (Graven et al., 2012). Assuming that at least some carbon turnover has occurred since its hatching, Lake Trout in this study must have hatched prior to 2005 and are therefore older than 7 years in age. Applying similar logic to the Coregonids and Scuplin, whose tissue $\Delta^{14}\text{C}$ were very similar at 65 and 66‰, indicated that those fish were born before the year 2007, and are more than 5 years in age. Exact rates of carbon turnover in muscle tissue of these specific species are not known. However, the assumed minimum age for these Coregonids seems consistent with the ‘multiple year’ carbon turnover rates determined in other Coregonid species by Hesslein (1992).

4.5 Conclusion

We found the CSNIA of amino acids method of trophic level determination to support previously assigned trophic positions (based on bulk stable isotope signatures and gut content analyses) of organisms investigated in this study. An obvious exception is that of the copepod *Limnocalanus macrurus*, whose trophic position was found to be almost an entire position higher than previously assumed. This suggests that CSNIA of amino acids is a powerful tool to apply in large lake systems, particularly for lower order organisms whose feeding habits are harder to infer. This method can be used to shed light on previously unrecognized microbial loops or additional prey incorporation of these lower order organisms. Radiocarbon analysis of these food web components revealed a different picture, indicating that the benthic amphipod *Diporeia* consumed a unique, more radiocarbon depleted carbon source not significantly incorporated by other organisms examined here, including a benthic feeding fish. We conclude that the

combination of these two methods, CSNIA of amino acids and bulk radiocarbon analysis, is a powerful way to examine organic matter transfers in aquatic systems.

Table 4.1. Scientific and common name of species studied, and predominant diet items for each.

Species/Group	Common Taxon Name	Diet ^a
<i>Daphnia spp.</i>	<i>Daphnia</i>	Phytoplankton, diatoms, POM (1)
<i>Limnocalanus macrurus</i>	<i>Limnocalanus</i>	Algae, nauplii, crustacean zooplankton (2)
<i>Diporeia</i>	<i>Diporeia</i>	Sedimented phytoplankton, benthic algae (3)
<i>Mysis relicta</i>	<i>Mysis</i>	Phytoplankton, crustacean zooplankton (4)
<i>Coregonus kiyi</i>	Kiyi	^b Mysis, Daphnia (5,6)
<i>Coregonus artedii</i>	Lake Herring	^b Calanoid copepods, Bythotrephes, Mysis (5,6)
<i>Myoxocephalus thompsonii</i>	Deep Water Sculpin (DW Sculpin)	^b Diporeia, Mysis (5)
<i>Salvelinus namaycush</i>	Siscowet Lake Trout (Lake Trout)	^b Deep Water Sculpin, Coregonids, fish eggs (5,6)

^aBased on gut content analysis studies, references in parentheses: 1, Balcer et al., (1984); 2, Warren (1983, 1985); 3, Sierszen et al., (2006); 4, Grossnickle et al., (1982); 5, Gamble et al. (2011); 6, Ahrenstorff et al. (2013)

^bFish diets include top three items constituting $\geq 10\%$ of total mass percent consumed, and are ordered from greatest to least contribution taking overall consumption into account across spring, summer, and fall seasons as in Gamble et al. (2011). The combination of top three prey items consistently represented $>90\%$ of total biomass consumed across spring and summer sampling.

Table 4.2. Calculated trophic levels for each species at each location, and of each size for those divided into size classes. N/a represents no animals recovered from that sampling location

Common Taxon Name	TL_{bulk}	TL_{bulk-zoop}	TL_{Glu/Phe}
BAP2			
<i>Daphnia</i>	1.3	1.6	2
<i>Limnocalanus</i>	3.5	5.3	3.0
<i>Diporeia-M</i>	2.3	3.2	2.2
<i>Diporeia-L</i>	2.3	3.3	2.4
<i>Mysis-S</i>	2.2	3.0	3.0
<i>Mysis-M</i>	2.4	3.3	2.7
<i>Mysis-L</i>	2.7	4.0	2.7
Kiyi	n/a		n/a
Lake Herring	3.1		3.1
DW Sculpin	4.1		3.9
Lake Trout	3.9		4.1
WM2			
<i>Daphnia</i>	1.4	1.6	1.9
<i>Limnocalanus</i>	4.0	6.1	3.2
<i>Diporeia-M</i>	n/a	n/a	n/a
<i>Diporeia-L</i>	n/a	n/a	n/a
<i>Mysis-S</i>	2.7	4.0	2.8
<i>Mysis-M</i>	2.9	4.2	2.9
<i>Mysis-L</i>	3.2	4.6	2.6
Kiyi	2.7		3.2
Lake Herring	n/a		n/a
DW Sculpin	4.1		3.7
Lake Trout	4.6		3.8
ONT2			
<i>Daphnia</i>	0.9	0.8	2.1
<i>Limnocalanus</i>			
<i>Diporeia-M</i>	2.3	3.1	2.7
<i>Diporeia-L</i>	2.2	3.0	2.4
<i>Mysis-S</i>	1.9	2.5	2.5
<i>Mysis-M</i>	1.8	2.4	2.4
<i>Mysis-L</i>	2.7	3.0	2.7
Kiyi	3.8		3.3
Lake Herring	n/a		n/a
DW Sculpin	4.1		3.9
Lake Trout	4.9		3.8

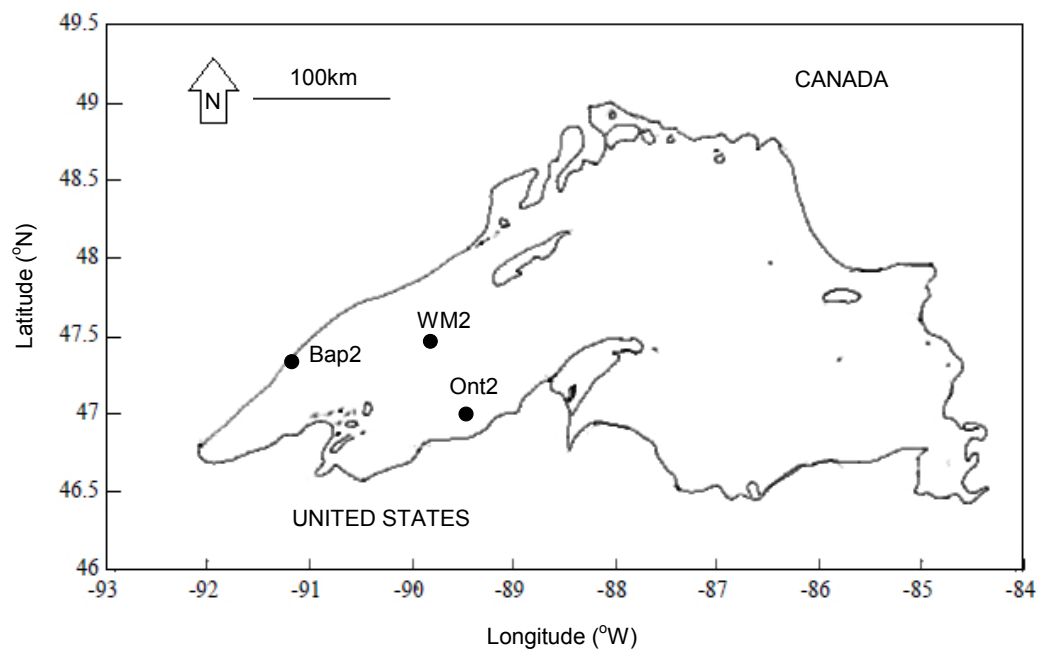


Figure 4.1. Sampling map reflecting the three sampling locations in the western arm of Lake Superior.

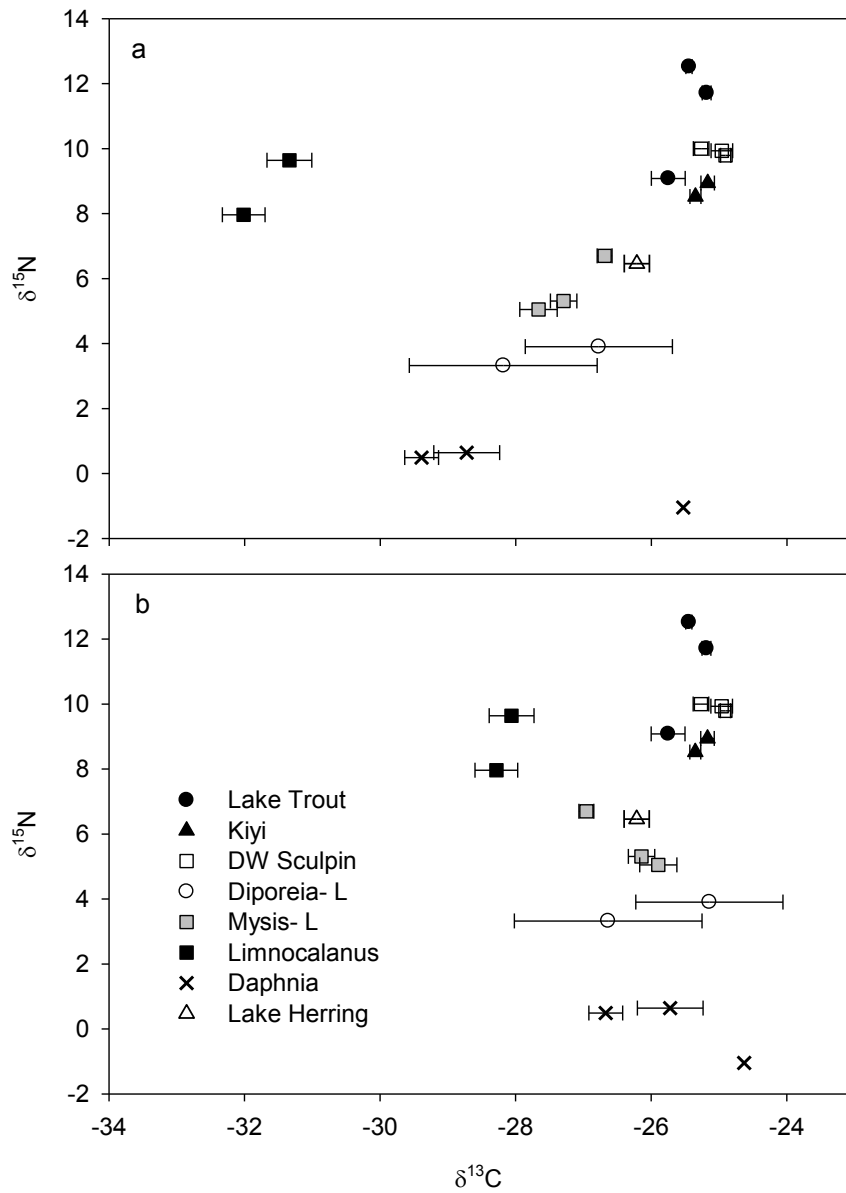
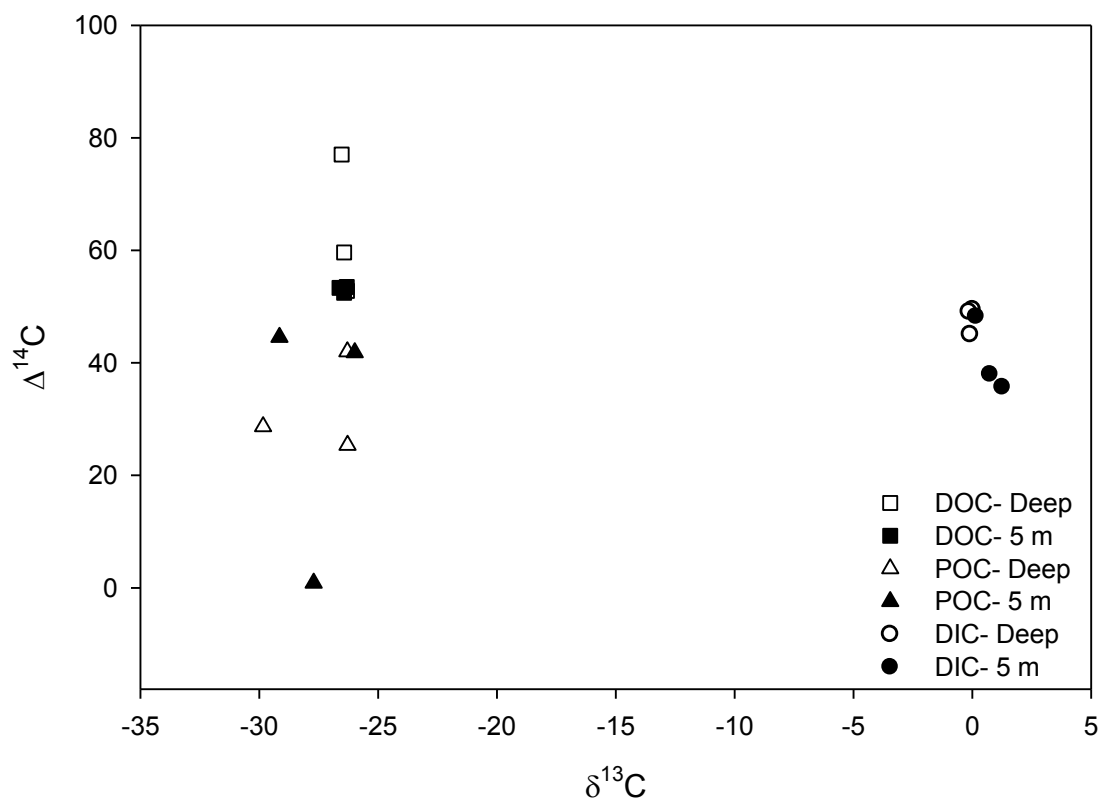


Figure 4.2. Stable isotope signatures (all in units of per mil (‰)) of all organisms at all sites a) as measured without sample pre-treatment, and b) with post-analysis lipid correction applied to zooplankton species using $\delta^{13}\text{C}_{\text{ex}} = \delta^{13}\text{C}_{\text{bulk}} + 6.3((\text{C}:\text{N}_{\text{bulk}} - 4.2)/\text{C}:\text{N}_{\text{bulk}})$ as refined by Smyntek et al. (2007) and described in text. Horizontal error bars represent average error in $\delta^{13}\text{C}$ between bulk analyses with no pre-treatment and analyses with acid pre-treatment to remove inorganics as a preparative step for

radiocarbon analysis and may also represent error associated with separate instrumentation.



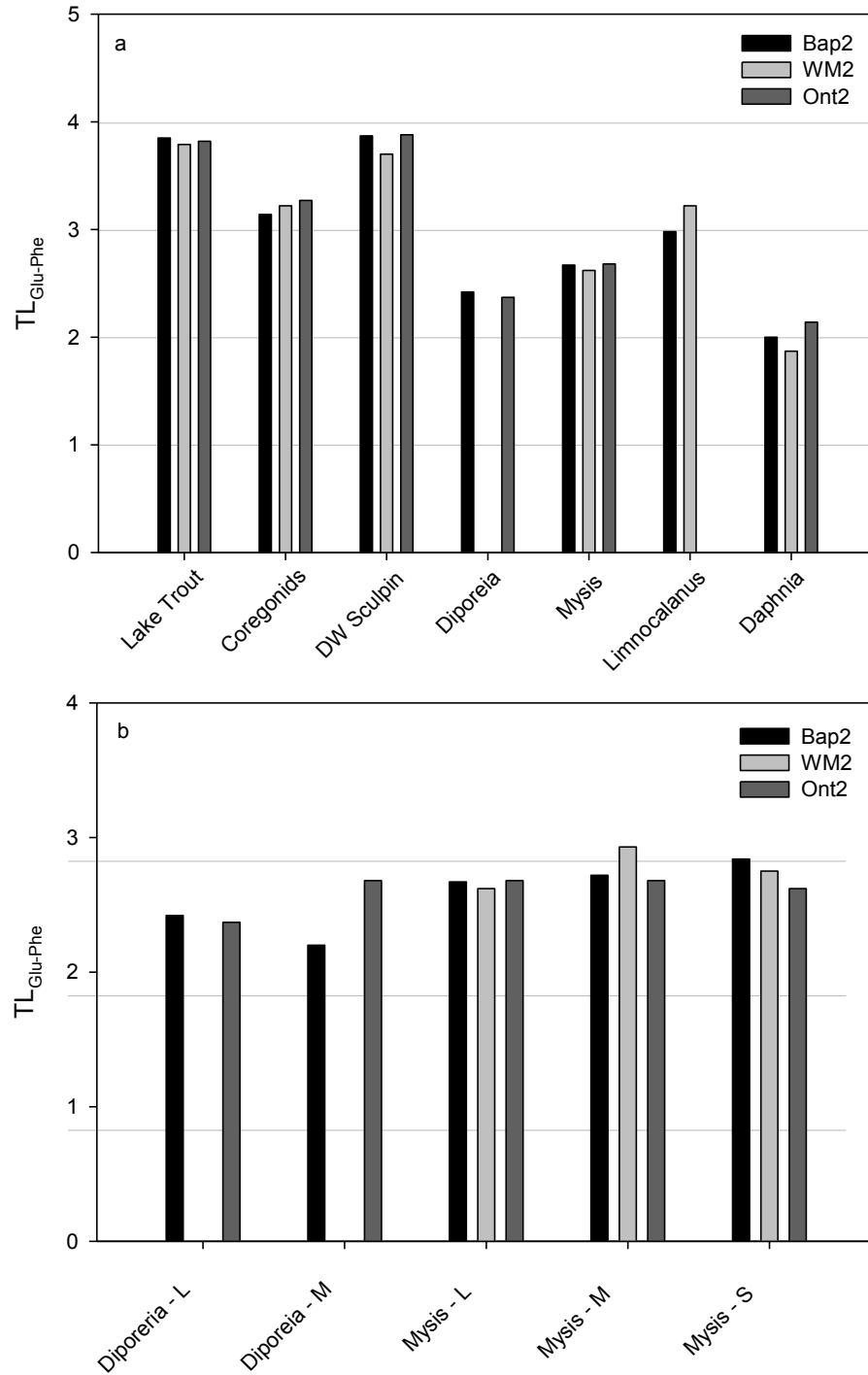


Figure 4.4. Organism trophic levels from all sampling locations (a) and of multiple size classes for *Mysis* and *Diporeia* (b) as calculated by: $TL_{(Glu/Phe)} = (\delta^{15}N_{Glu} - \delta^{15}N_{Phe} - 3.4)/7.6 + 1$ from Chikaraishi et al. 2009.

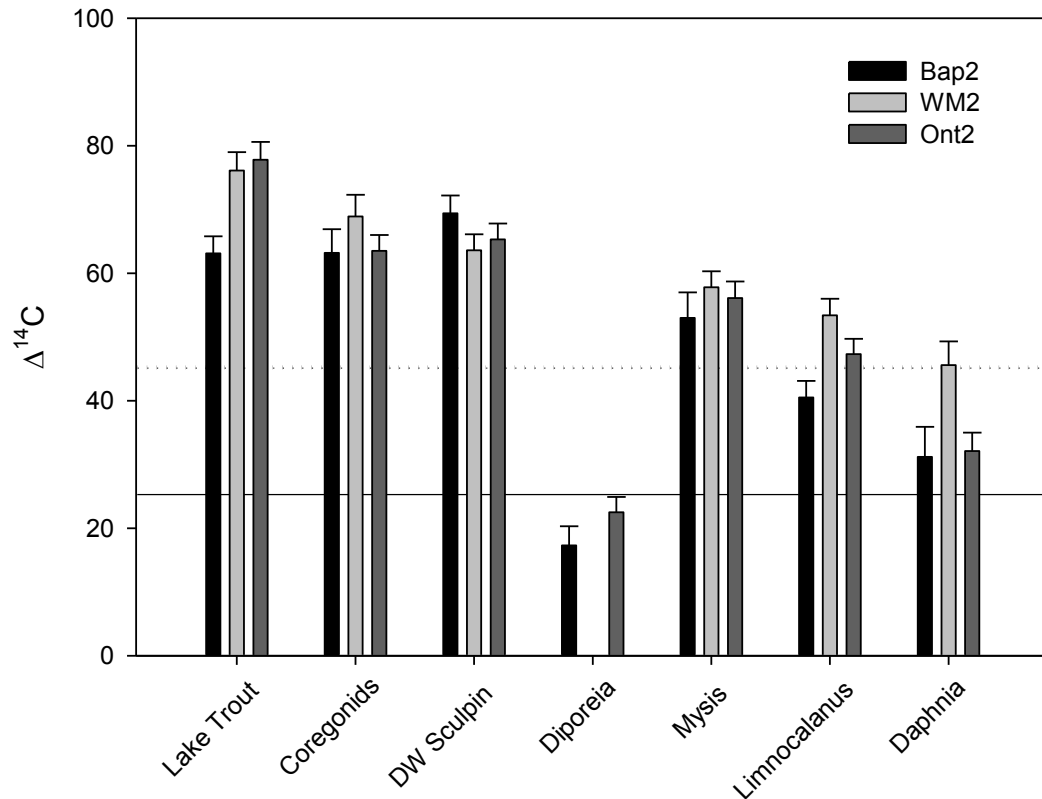


Figure 4.5. Radiocarbon signature of organisms sampled at all locations including only large size classes of Mysis and Diporeia, in units of per mil (‰). Error bars represent cumulative error associated with radiocarbon measurement techniques. Solid horizontal line represents the atmospheric $\Delta^{14}\text{C}$ signature (‰) as measured from annual corn leaves grown the same year as sampling occurred. Dotted horizontal line represents the average ($\pm 3\%$) of all surface and deep water DIC $\Delta^{14}\text{C}$ measurements made (reference text for measurement specifics).

Chapter 5: System Comparison

Although this research sought to investigate independent systems in two very different large lakes of the world, brief comparisons of organic matter components can be made between the two. In terms of abundance in the water column, DIC dominates over DOC in both systems although data from Lake Malawi was limited. Average DOC concentration was $106.9 \mu\text{M}$ ($n = 6$, $\pm 12 \mu\text{M}$) during August at the study locations in Lake Superior, while DOC was measured to be 44.9 at a single, deepwater (350 m) location in the central basin of Lake Malawi. The DIC pool was much larger, with an average concentration of $870 \mu\text{M}$ ($n = 6$, $\pm 36 \mu\text{M}$) at the Lake Superior locations, and an average of 2.3 mM ($n = 2$, $\pm 0.18 \text{ mM}$) between the surface (30 m) and deep water (350 m) at the Lake Malawi location. Isotopic signatures of these water column pools also differ between the lakes, as described at length in previous chapters. In brief, Lake Superior DOC $\delta^{13}\text{C}$ averaged -26.4‰ between all locations and depths, ($n = 6$, standard deviation (stdev) = 0.12‰), while DIC averaged 0.3‰ ($n = 6$, $\pm 0.6\text{‰}$). In Lake Malawi, stable carbon isotope signature of the single measured DOC point was not measured, though the $\delta^{13}\text{C}$ of DIC was quite different between the surface and deep water at the single water column sampling location, -0.7‰ and -2.5‰ , respectively. Though not quantified in these systems, POC at the sampled locations and depths was similar in $\delta^{13}\text{C}$ between the two lakes; -27.5‰ ($n = 6$, stdev = 1.6) in Lake Superior, and -28.2‰ ($n = 1$, water depth = 350 m). With regard to radiocarbon content of these water column fractions, $\Delta^{14}\text{C}$ signatures for each fraction were quite different between lakes. In Lake Superior, the DOC, DIC, and POC fractions had average ($n = 6$ for all) $\Delta^{14}\text{C}$ signatures of 58.1‰ (stdev = 9.6‰), 44.3‰ (stdev = 6.0‰), and 30.6‰ (stdev = 16.6‰), respectively. In Lake Malawi, the same fractions had $\Delta^{14}\text{C}$ signatures of 26.7‰ ($n = 1$, water depth = 350 m), 79.3‰ ($n = 2$, stdev = 17.5‰), and 185.7‰ ($n = 1$, water depth = 350 m), respectively. Collectively, these values give a picture of a water column OM system where the stable isotopic signatures are relatively consistent between these two unique systems, but the radiocarbon signatures seem unique to each. Though water column data from Lake Malawi is limited in this study, it points to a very different

temporal cycling of water column carbon fractions than that of Lake Superior. This is to be expected given the drastically different mixing and circulation mechanisms occurring between the lakes.

With regard to sedimentary organic carbon, this study found roughly 2.1% of the nearshore surface sediment in Lake Malawi to be organic carbon, increasing to 3.5% in the deep, open-lake basin. In Lake Superior, an extensive lake-wide study also found similar surface sediment organic carbon levels, ranging roughly 2-4% throughout the lake (Li et al., 2012). Sedimentation rate was found to be relatively high in Lake Malawi, with mass accumulations of roughly $0.3 \text{ g cm}^{-2}\text{yr}^{-1}$ nearshore and dropping to roughly $0.07 \text{ g cm}^{-2}\text{yr}^{-1}$ in the deep water location. In Lake Superior, four open lake sites had surface sedimentation rates ranging roughly $0.01 - 0.02 \text{ g cm}^{-2}\text{yr}^{-1}$ (Li et al., 2012). This is likely a reflection of climate differences between systems; the year-round tropical climate in which Lake Malawi is found could facilitate more constant OM input to the lake year round, as well as more consistent autochthonous production year round.

The CSNIA method of organism trophic level investigation undertaken in Lake Superior could easily be applied to Lake Malawi. However, complications could occur with regard to the sheer number of macro-organism species present in the Lake. With over 400 species of endemic cichlid fish alone (Moran et al., 1994), it would be necessary to focus on applying trophic level determination methods to specific known or suspected chains of feeding interaction to actually ascertain specific OM flow pathways. However, an equally interesting approach may in fact be to determine the trophic level of as many fish species as possible, from as many of the known feeding strategies as possible, simply to look at the distribution of consumer trophic levels. This approach may in fact shed light on feeding interactions that are radically different, isotopically, from most.

REFERENCES

- Abbott, M. B., & Stafford Jr, T. W. (1996). Radiocarbon geochemistry of modern and ancient Arctic lake systems, Baffin Island, Canada. *Quaternary Research*, 45(3), 300-311.
- Abraham, W. R., Hesse, C., & Pelz, O. (1998). Ratios of carbon isotopes in microbial lipids as an indicator of substrate usage. *Applied and Environmental Microbiology*, 64(11), 4202-4209.
- Adams, T. S., & Sterner, R. W. (2000). The effect of dietary nitrogen content on trophic level ^{15}N enrichment. *Limnology and Oceanography*, 45(3), 601-607.
- Ahrenstorff, T. D., Hrabik, T. R., Stockwell, J. D., Yule, D. L., & Sass, G. G. (2011). Seasonally dynamic diel vertical migrations of *Mysis diluviana*, coregonine fishes, and Siscowet lake trout in the pelagia of western Lake Superior. *Transactions of the American Fisheries Society*, 140(6), 1504-1520.
- Albertson, R. C., Markert, J. A., Danley, P. D., & Kocher, T. D. (1999). Phylogeny of a rapidly evolving clade: the cichlid fishes of Lake Malawi, East Africa. *Proceedings of the National Academy of Sciences*, 96(9), 5107-5110.
- Bakun, A. 1990. Global climate change and intensification of global coastal upwelling. *Science*.247: 198-201.
- Albertson, R. C., Streelman, J. T., & Kocher, T. D. (2003). Directional selection has shaped the oral jaws of Lake Malawi cichlid fishes. *Proceedings of the National Academy of Sciences*, 100(9), 5252-5257.
- Alin, S. R., and A.S. Cohen. (2003). Lake-level history of Lake Tanganyika, East Africa, for the past 2500 years based on ostracode-inferred water-depth reconstruction. *Palaeogeography, Palaeoclimatology, Palaeoecology*. 199(1): 31-49.
- Alin, S.R., and T.C. Johnson. (2007). Carbon cycling in large lakes of the world: A synthesis of production, burial and lake-atmosphere exchange estimates. *Global Biogeochemical Cycles*. 21:doi:10.1029/2006GB002881.
- Al-Mutlaq, K., Rushdi, A. I., & Simoneit, B. R. (2007). Organic compound tracers of fine soil and sand particles during summer in the metropolitan area of Riyadh, Saudi Arabia. *Environmental geology*, 52(3), 559-571.
- Aluwihare, L. I., Repeta, D. J., (1999). A comparison of the chemical characteristics of oceanic DOM and extracellular DOM produced by marine algae. *Marine Ecology Progress Series*, 186, 105-117.

- Austin, J. A., & Colman, S. M. (2007). Lake Superior summer water temperatures are increasing more rapidly than regional air temperatures: A positive ice-albedo feedback. *Geophysical Research Letters*, 34(6).
- Austin, J., & Colman, S. (2008). A century of temperature variability in Lake Superior. *Limnology and Oceanography*, 53(6), 2724.
- Aycard, M., Derenne, S., Largeau, C., Mongenot, T., Tribovillard, N., & Baudin, F. (2003). Formation pathways of proto-kerogens in Holocene sediments of the upwelling influenced Cariaco Trench, Venezuela. *Organic geochemistry*, 34(6), 701-718.
- Bahr, A., F. Lamy, H. Arz, H. Kuhlmann, G. Wefer. (2005). Late glacial to Holocene climate and sedimentation history in the NW Black Sea. *Marine Geology*. 214: 309-322.
- Baines, S. B., & Pace, M. L. (1991). The production of dissolved organic matter by phytoplankton and its importance to bacteria: patterns across marine and freshwater systems. *Limnology and Oceanography*, 36(6), 1078-1090.
- Balcer, M. D., Korda, N. L., & Dodson, S. I. (1984). *Zooplankton of the Great Lakes: a guide to the identification and ecology of the common crustacean species*. Univ of Wisconsin Press.
- Bardgett, R. D., Richter, A., Bol, R., Garnett, M. H., Bäumler, R., Xu, X. & Wanek, W. (2007). Heterotrophic microbial communities use ancient carbon following glacial retreat. *Biology letters*, 3(5), 487-490.
- Beadle, L.C. (1981). *The inland waters of tropical Africa. An introduction to tropical limnology*. Longman, London.
- Benner, R. (2002). Chemical composition and reactivity. In: *Biogeochemistry of marine dissolved organic matter*, p. 59-90.
- Benner, R., Benitez-Nelson, B., Kaiser, K., & Amon, R. M. (2004). Export of young terrigenous dissolved organic carbon from rivers to the Arctic Ocean. *Geophysical Research Letters*, 31(5).
- Bennett, E. B. (1978). Characteristics of the thermal regime of Lake Superior. *Journal of Great Lakes Research*, 4(3), 310-319.
- Bootsma, H. A. and R. E. Hecky. (1993). Conservation of the African Great Lakes: a limnological perspective. *Conservation Biology*. 7(3): 644-656.

- Bootsma, H. A., R.E. Hecky, T.C. Johnson, H.J. Kling, & J. Mwita. (2003). Inputs, outputs, and internal cycling of silica in a large, tropical lake. *Journal of Great Lakes Research*. 29: 121-138.
- Bootsma, H.A., and R.E. Hecky. (2003). A comparative introduction to the biology and limnology of the African Great Lakes. *J. Great Lakes Res.* 29(supplement 2): 3-18.
- Boschker, H. T. S., & Middelburg, J. J. (2002). Stable isotopes and biomarkers in microbial ecology. *FEMS Microbiology Ecology*, 40(2), 85-95.
- Brown, E. T., L. Le Callonnec, and C.R. German. (2000). Geochemical cycling of redox-sensitive metals in sediments from Lake Malawi: A diagnostic paleotracer for episodic changes in mixing depth. *Geochimica et Cosmochimica Acta*. 64(20): 3515-3523.
- Brown, M. E., & Branstrator, D. K. (2004). A 2001 survey of crustacean zooplankton in the western arm of Lake Superior. *Journal of Great Lakes Research*, 30(1), 1-8.
- Bruland, K. W., Koide, M., Bowser, C., Maher, L. J., & Goldberg, E. D. (1975). Lead-210 and pollen geochronologies on Lake Superior sediments. *Quaternary Research*, 5(1), 89-98.
- Bruno, E., Borg, C. M. A., & Kiørboe, T. (2012). Prey detection and prey capture in copepod nauplii. *PloS one*, 7(10), e47906.
- Burdige, D. J. (2007). Preservation of organic matter in marine sediments: controls, mechanisms, and an imbalance in sediment organic carbon budgets. *Chemical reviews*, 107(2), 467-485.
- Carpenter, G. F., Mansey, E. L., & Watson, N. H. F. (1974). Abundance and life history of *Mysis relicta* in the St. Lawrence Great Lakes. *Journal of the Fisheries Board of Canada*, 31(3), 319-325.
- Castaneda, I. S. (2007). Paleoenvironmental variability in the southeast African tropics since the Last Glacial Maximum: Molecular and isotopic records from Lake Malawi (Doctoral dissertation, UNIVERSITY OF MINNESOTA).
- Castañeda, I. S., & Schouten, S. (2011). A review of molecular organic proxies for examining modern and ancient lacustrine environments. *Quaternary Science Reviews*, 30(21), 2851-2891.
- Castañeda, I. S., Werne, J. P., Johnson, T. C., & Filley, T. R. (2009). Late Quaternary vegetation history of southeast Africa: the molecular isotopic record from Lake Malawi. *Palaeogeography, Palaeoclimatology, Palaeoecology*, 275(1), 100-112.

- Castañeda, I. S., Werne, J. P., Johnson, T. C., & Powers, L. A. (2011). Organic geochemical records from Lake Malawi (East Africa) of the last 700 years, part II: Biomarker evidence for recent changes in primary productivity. *Palaeogeography, Palaeoclimatology, Palaeoecology*, 303(1), 140-154.
- Castaneda, I.S., J.P. Werne, and T.C. Johnson. (2007). Wet and arid phases in the southeast African tropics since the Last Glacial Maximum. *Geology*. 35(9): 823-826.
- Cherrier, J., Bauer, J. E., Druffel, E. R., Coffin, R. B., & Chanton, J. P. (1999). Radiocarbon in marine bacteria: Evidence for the ages of assimilated carbon. *Limnology and Oceanography*, 44(3), 730-736.
- Chetelat, J., Amyot, M., & Cloutier, L. (2012). Shifts in elemental composition, methylmercury content and $\delta^{15}\text{N}$ ratio during growth of a High Arctic copepod. *Freshwater Biology*, 57(6), 1228-1240.
- Chikaraishi, Y., N.O. Ogawa, Y. Kashiyama, H. Suga, A. Tomitani, H. Miyashita, H. Kitazato, and N. Ohkouchi. (2009). Determination of aquatic food web structure based on compound specific nitrogen isotope composition of amino acids. *Limnology and Oceanography: Methods*. 7: 740-750.
- Chikaraishi, Y., Y. Kashiyama, N.O. Ogawa, H. Kitazato, and N. Ohkouchi. (2007). Metabolic control of nitrogen isotope composition of amino acids in macroalgae and gastropods: implications for aquatic food web studies. *Marine Ecology Progress Series*. 342: 85-90.
- Cohen, A. S., Soreghan, M. J., & Scholz, C. A. (1993). Estimating the age of formation of lakes: an example from Lake Tanganyika, East African Rift system. *Geology*, 21(6), 511-514.
- Collister, J. W., Rieley, G., Stern, B., Eglinton, G., & Fry, B. (1994). Compound-specific $\delta^{13}\text{C}$ analyses of leaf lipids from plants with differing carbon dioxide metabolisms. *Organic Geochemistry*, 21(6), 619-627.
- Conley, D. J., & Schelske, C. L. (2001). Biogenic silica. In *Tracking environmental change using lake sediments* (pp. 281-293). Springer Netherlands.
- Coppola, L., Gustafsson, Ö., Andersson, P., Eglinton, T. I., Uchida, M., & Dickens, A. F. (2007). The importance of ultrafine particles as a control on the distribution of organic carbon in Washington Margin and Cascadia Basin sediments. *Chemical geology*, 243(1), 142-156.

- Cotner, J.B., B.A. Biddanda, W. Makino, and E. Stets. 2004. Organic carbon biogeochemistry of Lake Superior. *Aquatic Ecosystem Health and Management*. 7(4): 451-464.
- Cronan Jr, J. E. (1978). Molecular biology of bacterial membrane lipids. *Annual review of biochemistry*, 47(1), 163-189.
- Danley, P. D., & Kocher, T. D. (2001). Speciation in rapidly diverging systems: lessons from Lake Malawi. *Molecular Ecology*, 10(5), 1075-1086.
- Degnbol, P., & Mapila, S. (1982). Limnological observations on the pelagic zone of Lake Malawi from 1970 to 1981. *Fisheries Expansion Project Malawi: Biological studies on the pelagic ecosystem of Lake Malawi*. FAO FI: DP/ML/W/75/019, 5-47.
- DeNiro, M. J., & Epstein, S. (1977). Mechanism of carbon isotope fractionation associated with lipid synthesis. *Science*, 197(4300), 261-263.
- DeNiro, M. J., & Epstein, S. (1978). Influence of diet on the distribution of carbon isotopes in animals. *Geochimica et cosmochimica acta*, 42(5), 495-506.
- DeNiro, M. J., & Epstein, S. (1981). Influence of diet on the distribution of nitrogen isotopes in animals. *Geochimica et Cosmochimica Acta*, 45(3), 341-351.
- Desai, A. R., Austin, J. A., Bennington, V., & McKinley, G. A. (2009). Stronger winds over a large lake in response to weakening air-to-lake temperature gradient. *Nature Geoscience*, 2(12), 855-858.
- Diefendorf, A. F., Freeman, K. H., Wing, S. L., & Graham, H. V. (2011). Production of n-alkyl lipids in living plants and implications for the geologic past. *Geochimica et Cosmochimica Acta*, 75(23), 7472-7485.
- Dryer, W. R., Erkkila, L. F., & Tetzloff, C. L. (1965). Food of lake trout in Lake Superior. *Transactions of the American Fisheries Society*, 94(2), 169-176.
- Ebener, M. P., Stockwell, J. D., Yule, D. L., Gorman, O. T., Hrabik, T. R., Kinnunen, R. E., ... & Sitar, S. P. (2008). Status of cisco (*Coregonus artedii*) in Lake Superior during 1970-2006 and management and research considerations. *Great Lakes Fishery Commission Special Publication*. Available at: <http://www.glfco.org/pubs/SpecialPubs/Cisco.pdf>.
- Ebinger, C. J., Deino, A. L., Tesha, A. L., Becker, T., & Ring, U. (1993). Tectonic controls on rift basin morphology: evolution of the Northern Malawi (Nyasa) Rift. *Journal of Geophysical Research: Solid Earth*. 98(B10), 17821-17836.

- Eccles, D.H. (1974). An outline of the physical limnology of Lake Malawi (Lake Nyasa). *Limnology and Oceanography*. 19(5): 730-742.
- Eglinton, G., and R.J. Hamilton. 1967. Leaf epicuticular waxes. *Science*. 156: 1322-1335.
- Eglinton, T. I., Aluwihare, L. I., Bauer, J. E., Druffel, E. R., & McNichol, A. P. (1996). Gas chromatographic isolation of individual compounds from complex matrices for radiocarbon dating. *Analytical Chemistry*, 68(5), 904-912.
- Eglinton, T. I., Benitez-Nelson, B. C., Pearson, A., McNichol, A. P., Bauer, J. E., & Druffel, E. R. (1997). Variability in radiocarbon ages of individual organic compounds from marine sediments. *Science*, 277(5327), 796-799.
- Evershed, R. P., Crossman, Z. M., Bull, I. D., Mottram, H., Dungait, J. A., Maxfield, P. J., & Brennand, E. L. (2006). ¹³C-Labeling of lipids to investigate microbial communities in the environment. *Current opinion in biotechnology*, 17(1), 72-82.
- Fahnenstiel, G. L., Sicko-Goad, L., Scavia, D., & Stoermer, E. F. (1986). Importance of picoplankton in Lake Superior. *Canadian Journal of Fisheries and Aquatic Sciences*, 43(1), 235-240.
- Filippi, M.L. and M.K. Talbot. (2005). The paleolimnology of northern Lake Malawi over the last 25 ka based upon the elemental and stable isotopic composition of sedimentary organic matter. *Quaternary Science Reviews*. 24:1303-1328.
- Finney, B.P., and T.C. Johnson. (1991). Sedimentation in Lake Malawi (East Africa) during the past 10,000 years: a continuous paleoclimatic record from the southern tropics. *Palaeogeography, Palaeoclimatology, and Palaeoecology*. 85: 351-366.
- Finney, B.P., C.A. Scholz, T.C. Johnson, and S. Trumbore. (1996). Lake quaternary lake level changes of Lake Malawi. P495-508. In: Johnson, T.C. and E.O. Odada. 1996. *The limnology, climatology and paleoclimatology of the East African Great Lakes*. Gordon and Breach Publishers. The Netherlands.
- Fogel, M. L., and L.A. Cifuentes. (1993). Isotope fractionation during primary production. In *Organic geochemistry*. Springer, U.S. p. 73-98.
- Frostick, L.E., and I. Reid. 1990. Structural control of sedimentation patterns and implication for the economic potential of the East African rift basins. *Journal of African Earth Sciences*. 10(1/2): 307-318.
- Fritz, S.C. (1996). Paleolimnological records of climate change in North America. *Limnology and Oceanography*. 41(5): 882-889.

- Fry, B. (1991). Stable isotope diagrams of freshwater food webs. *Ecology* 72: 2293–2297.
- Fukushima, K., & Ishiwatari, R. (1984). Acid and alcohol compositions of wax esters in sediments from different environments. *Chemical geology*, 47(1), 41-56.
- Gaebler, O. H., Vitti, T. G., & Vukmirovich, R. (1966). Isotope effects in metabolism of ^{14}N and ^{15}N from unlabeled dietary proteins. *Canadian Journal of Biochemistry*, 44(9), 1249-1257.
- Gamble, A. E., Hrabik, T. R., Stockwell, J. D., & Yule, D. L. (2011a). Trophic connections in Lake Superior Part I: the offshore fish community. *Journal of Great Lakes Research*, 37(3), 541-549.
- Gamble, A. E., Hrabik, T. R., Yule, D. L., & Stockwell, J. D. (2011b). Trophic connections in Lake Superior Part II: the nearshore fish community. *Journal of Great Lakes Research*, 37(3), 550-560.
- Gasse, F., and F.A. Street. (1978). Late quaternary lake level fluctuations and environments of the Northern rift valley and Afar region (Ethiopia and Djibouti). *Palaeogeography, Palaeoclimatology, Palaeoecology*. 24: 279-325.
- Gasse, F., P. Barker, and T.C. Johnson. (2002). A 24,600 yr diatom record from the northern basin of Lake Malawi. In: *The East African Great Lakes: Limnology, Palaeoclimatology and Biodiversity*. E. O. Odada and D. O. Olago. Dordrecht, Kluwer Academic Publishers: 393-414.
- Grossnickle, N. E. (1982). Feeding habits of *Mysis relicta*—an overview. *Hydrobiologia*, 93(1-2), 101-107.
- Guildford, S. J., & Hecky, R. E. (2000). Total nitrogen, total phosphorus, and nutrient limitation in lakes and oceans: Is there a common relationship. *Limnology and Oceanography*, 45(6), 1213-1223.
- Guildford, S. J., R.E. Hecky, W.D. Taylor, R. Mugidde, & H.A. Bootsma. (2003). Nutrient enrichment experiments in tropical great lakes Malawi/Nyasa and Victoria. *Journal of Great Lakes Research*. 29: 89-106.
- Hajdas, I. (2009). Applications of radiocarbon dating method. *Radiocarbon*. 51(1): 79-90.
- Halfman, J. D. (1993). Water column characteristics from modern CTD data, Lake Malawi, Africa. *Journal of Great Lakes Research*. 19(3): 512-520.
- Hannides, C. C., Popp, B. N., Landry, M. R., & Graham, B. S. (2009). Quantification of zooplankton trophic position in the North Pacific Subtropical Gyre using stable nitrogen isotopes. *Limnology and oceanography*, 54(1), 50.

- Hanson, R. S., & Hanson, T. E. (1996). Methanotrophic bacteria. *Microbiological reviews*, 60(2), 439-471.
- Harvey, C. J., Schram, S. T., & Kitchell, J. F. (2003). Trophic relationships among lean and siscowet lake trout in Lake Superior. *Transactions of the American Fisheries Society*, 132(2), 219-228.
- Harvey, C.J., and J.F. Kitchell. (2000). A stable isotope evaluation of the structure and spatial heterogeneity of the Lake Superior food web. *Can. J. Fish. Aquat. Sci.* 57: 1395-1403.
- Hayes, J. M. (1993). Factors controlling $\delta^{13}\text{C}$ contents of sedimentary organic compounds: Principles and evidence. *Marine Geology*, 113(1), 111-125.
- Healey, F.P. and L.L. Hendzel. (1980). Physiological indicators of nutrient deficiency in lake phytoplankton. *Can. J. Fisheries Aquatic Sci.* 37: 442-453.
- Hecky, R. E. (2000). A biogeochemical comparison of Lakes Superior and Malawi and the limnological consequences of an endless summer. *Aquatic Ecosystem Health & Management*, 3(1), 23-33.
- Hecky, R. E., & Kilham, P. (1988). Nutrient limitation of phytoplankton in freshwater and marine environments: a review of recent evidence on the effects of enrichment. *Limnology and Oceanography*, 33(4), 796-822.
- Hecky, R. E., Bootsma, H. A., & Kingdon, M. L. (2003). Impact of land use on sediment and nutrient yields to Lake Malawi/Nyasa (Africa). *Journal of great lakes research*, 29, 139-158.
- Hecky, R. E., H.A. Bootsma, R.M. Mugidde, and F.W.B. Bugenyi. (1996). Phosphorus pumps, nitrogen sinks, and silicon drains: plumbing nutrients in the African Great Lakes. In: *The limnology, climatology and paleoclimatology of the East African lakes*. Editors: T.C. Johnson and E.O. Odada. Gordon and Breach p. 205-233.
- Hecky, R.E. (1993). The eutrophication of Lake Victoria. *Verh. Internat. Verein. Limnol.* 25: 39-48.
- Hesslein, R. H., Hallard, K. A., & Ramlal, P. (1993). Replacement of sulfur, carbon, and nitrogen in tissue of growing broad whitefish (*Coregonus nasus*) in response to a change in diet traced by $\delta^{34}\text{S}$, $\delta^{13}\text{C}$, and $\delta^{15}\text{N}$. *Canadian Journal of Fisheries and Aquatic Sciences*, 50(10), 2071-2076.
- Hofmann, W. (1998). Cladocerans and chironomids as indicators of lake level changes in north temperate lakes. *Journal of Paleolimnology*. 19: 55-62.

- Hsueh, D. Y., Krakauer, N. Y., Randerson, J. T., Xu, X., Trumbore, S. E., & Southon, J. R. (2007). Regional patterns of radiocarbon and fossil fuel-derived CO₂ in surface air across North America. *Geophysical Research Letters*, 34(2).
- Huang, Y., Freeman, K. H., Eglinton, T. I., & Street-Perrott, F. A. (1999A). $\delta^{13}\text{C}$ analyses of individual lignin phenols in Quaternary lake sediments: A novel proxy for deciphering past terrestrial vegetation changes. *Geology*, 27(5), 471-474.
- Huang, Y., Street-Perrott, F. A., Perrott, R. A., Metzger, P., & Eglinton, G. (1999B). Glacial–interglacial environmental changes inferred from molecular and compound-specific $\delta^{13}\text{C}$ analyses of sediments from Sacred Lake, Mt. Kenya. *Geochimica et Cosmochimica Acta*, 63(9), 1383-1404.
- Hulme, M., R. Doherty, T. Ngara, M. New, and D. Lister. 2001. African climate change: 1900-2100. *Climate Research*. 17: 145-168.
- Hwang, J., & Druffel, E. R. (2003). Lipid-like material as the source of the uncharacterized organic carbon in the ocean. *Science*, 299(5608), 881-884.
- Hwang, J., Manganini, S. J., Montluçon, D. B., & Eglinton, T. I. (2009). Dynamics of particle export on the Northwest Atlantic margin. *Deep Sea Research Part I: Oceanographic Research Papers*, 56(10), 1792-1803.
- Ingalls, A. E., Shah, S. R., Hansman, R. L., Aluwihare, L. I., Santos, G. M., Druffel, E. R., & Pearson, A. (2006). Quantifying archaeal community autotrophy in the mesopelagic ocean using natural radiocarbon. *Proceedings of the National Academy of Sciences*, 103(17), 6442-6447.
- Ingalls, A.E. and A.N. Pearson. (2005). Ten years of compounds specific radiocarbon analysis. *Oceanography*. 18(3): 18-31.
- Irvine, K., & Waya, R. (1999). Spatial and temporal patterns of zooplankton standing biomass and production in Lake Malawi. In *From Limnology to Fisheries: Lake Tanganyika and Other Large Lakes* (pp. 191-205). Springer Netherlands.
- Ivanikova, N. V., Popels, L. C., McKay, R. M. L., & Bullerjahn, G. S. (2007). Lake Superior supports novel clusters of cyanobacterial picoplankton. *Applied and environmental microbiology*, 73(12), 4055-4065.
- Jaffé, R., Mead, R., Hernandez, M. E., Peralba, M. C., & DiGuida, O. A. (2001). Origin and transport of sedimentary organic matter in two subtropical estuaries: a comparative, biomarker-based study. *Organic Geochemistry*, 32(4), 507-526.
- Jansen, B., Nierop, K. G., Hageman, J. A., Cleef, A. M., & Verstraten, J. M. (2006). The straight-chain lipid biomarker composition of plant species responsible for the

- dominant biomass production along two altitudinal transects in the Ecuadorian Andes. *Organic Geochemistry*, 37(11), 1514-1536.
- Jansen, J.H.F., Van der Gaast, S.J., Koster, B., Vaars, A.J., (1998). CORTEX, a shipboard XRF-scanner for element analyses in split sediment cores. *Mar. Geol.* 151, 143–153.
- Jensen, O. P., Yurista, P. M., Hrabik, T. R., & Stockwell, J. D. (2009). Densities and diel vertical migration of *Mysis relicta* in Lake Superior: a comparison of optical plankton counter and net-based approaches. *Verh. Int. Ver. Limnol*, 30, 957-963.
- Johns, T.C., J.M. Gregory, W.J.Ingram, C.E. Johnson, A. Jones, J.A. Lowe, J.F.B. Mitchell, D.L. Roberts, D.M.H. Sexton, D.S. Stevenson, S.F.B. Tett, and M.J. Woodage.(2003). Anthropogenic climate change for 1860-2100 simulated with the HadCM3 model under updated emissions scenarios. *Climate Dynamics*. 20: 583-612.
- Johnson, T. B., Hoff, M. H., Trebitz, A. S., Bronte, C. R., Corry, T. D., Kitchell, J. F., ... & Schreiner, D. R. (2004). Spatial patterns in assemblage structures of pelagic forage fish and zooplankton in western Lake Superior. *Journal of Great Lakes Research*, 30, 395-406.
- Johnson, T. C., E.T. Brown, J. McManus, S. Barry, P. Barker, & F. Gasse, (2002). A high-resolution paleoclimate record spanning the past 25,000 years in southern East Africa. *Science*. 296(5565): 113-132.
- Johnson, T.C. (1996). Sedimentary processes and signals of past climate change in the Large Lakes of the East African Rift Valley. P367-412. In: Johnson, T.C. and E.O. Odada. 1996. *The limnology, climatology and paleoclimatology of the East African Great Lakes*. Gordon and Breach Publishers. The Netherlands.
- Johnson, T.C., E.T. Brown, and J. Shi. 2011. Biogenic silica deposition in Lake Malawi, East Africa over the past 150,000 years. *Palaeogeography, Palaeoclimatology, and Palaeoecology*. 303(1-4): 103-109.
- Jones, B. F., & Bowser, C. J. 1978. The mineralogy and related chemistry of lake sediments. In *Lakes*. pp. 179-235. Springer New York.
- Kawamura, K., & Ishiwatari, R. (1985). Distribution of lipid-class compounds in bottom sediments of freshwater lakes with different trophic status, in Japan. *Chemical Geology*, 51(1), 123-133.
- Kendall, C., Elliott, E. M., & Wankel, S. D. (2007). Tracing anthropogenic inputs of nitrogen to ecosystems. In: *Stable isotopes in ecology and environmental science*, 2, 375-449.

- Keil, R. G., Montluçon, D. B., Prahl, F. G., & Hedges, J. I. (1994). Sorptive preservation of labile organic matter in marine sediments. *Nature*. 370: 549-552.
- Kemp, A. L. W., Dell, C. I., & Harper, N. S. (1978). Sedimentation rates and a sediment budget for Lake Superior. *Journal of Great Lakes Research*, 4(3), 276-287.
- Killops, S., and V. Killops. (2005). *Introduction to organic geochemistry*. Blackwell Publishing, Victoria, Australia. p 217.
- Kiyashko, S. I., Narita, T., & Wada, E. (2001). Contribution of methanotrophs to freshwater macroinvertebrates: evidence from stable isotope ratios. *Aquatic Microbial Ecology*, 24(2), 203-207.
- Lee, R. F., Nevenzel, J. C., & Paffenhöfer, G. A. (1971). Importance of wax esters and other lipids in the marine food chain: phytoplankton and copepods. *Marine Biology*, 9(2), 99-108.
- Lehman, J. T. (1996). Pelagic food webs of the East African great lakes. *The Limnology, Climatology and Paleoclimatology of the East African Lakes*, 281-301.
- Lehmann, M. F., Bernasconi, S. M., Barbieri, A., & McKenzie, J. A. (2002). Preservation of organic matter and alteration of its carbon and nitrogen isotope composition during simulated and in situ early sedimentary diagenesis. *Geochimica et Cosmochimica Acta*, 66(20), 3573-3584.
- Leng, M. J., and J. D. Marshall. 2004. Palaeoclimate interpretation of stable isotope data from lake sediment archives. *Quaternary Science Reviews*. 23(7): 811-831.
- Matheson, D. H., & Munawar, M. (1978). Lake Superior basin and its development. *Journal of Great Lakes Research*, 4(3), 249-263.
- McCarthy, M. D., Lehman, J., & Kudela, R. (2013). Compound-specific amino acid $\delta^{15}\text{N}$ patterns in marine algae: Tracer potential for cyanobacterial vs. eukaryotic organic nitrogen sources in the ocean. *Geochimica et Cosmochimica Acta*, 103, 104-120.
- McClelland, J. W., & Montoya, J. P. (2002). Trophic relationships and the nitrogen isotopic composition of amino acids in plankton. *Ecology*, 83(8), 2173-2180.
- McCutchan, J. H., Lewis, W. M., Kendall, C., & McGrath, C. C. (2003). Variation in trophic shift for stable isotope ratios of carbon, nitrogen, and sulfur. *Oikos*, 102(2), 378-390.
- McNichol, A. P., & Aluwihare, L. I. (2007). The power of radiocarbon in biogeochemical studies of the marine carbon cycle: Insights from studies of dissolved and particulate organic carbon (DOC and POC). *Chemical reviews*. 107(2), 443-466.

- McQueen, D. J. (1970). Grazing rates and food selection in *Diaptomus oregonensis* (Copepoda) from Marion Lake, British Columbia. *Journal of the Fisheries Board of Canada*, 27(1), 13-20.
- Meyers, P. A. (1997). Organic geochemical proxies of paleoceanographic, paleolimnologic, and paleoclimatic processes. *Organic geochemistry*, 27(5-6), 213-250.
- Meyers, P. A. and S. Ishiwitari (1995). Organic matter accumulation records in lake sediments. *Physics and Chemistry in Lakes*. A. Lerman, D. M. Imboden and J. R. Gat. Berlin, Germany, Springer-Verlag: 279-3282.
- Meyers, P. A., & Eadie, B. J. (1993). Sources, degradation and recycling of organic matter associated with sinking particles in Lake Michigan. *Organic Geochemistry*, 20(1), 47-56.
- Meyers, P. A., Leenheer, M. J., Eadie, B. J., & Maule, S. J. (1984). Organic geochemistry of suspended and settling particulate matter in Lake Michigan. *Geochimica et Cosmochimica Acta*, 48(3), 443-452.
- Meyers, P.A. and J.L. Teranes. (2002). Sediment organic matter. In: *Tracking environmental changes using lake sediments: Volume 2*. Editors: Last, W.M., and J.P. Smol. p 239-269.
- Minagawa, M. and E. Wada. (1986). Nitrogen isotope ratios of red tide organisms in the East China Sea: A characterization of biological nitrogen fixation. *Marine chemistry*. 19(3): 245-259.
- Moran, P., Kornfield, I., & Reinthal, P. N. (1994). Molecular systematics and radiation of the haplochromine cichlids (Teleostei: Perciformes) of Lake Malawi. *Copeia*, 274-288.
- Mollenhauer, G., Eglinton, T. I., Ohkouchi, N., Schneider, R. R., Müller, P. J., Grootes, P. M., & Rullkötter, J. (2003). Asynchronous alkenone and foraminifera records from the Benguela Upwelling System. *Geochimica et Cosmochimica Acta*, 67(12), 2157-2171.
- Mopper, K., & Furton, K. G. (1991). Extraction and Analysis of Polysaccharides, Chiral Amino Acids, and Sfe-Extractable Lipids from Marine POM. In: *Marine Particles: Analysis and Characterization*, p. 151-161.
- Munawar, M., & Munawar, I. F. (1978). Phytoplankton of Lake Superior 1973. *Journal of Great Lakes Research*, 4(3), 415-442.

- Munawar, M., & Munawar, I. F. (1986). The seasonality of phytoplankton in the North American Great Lakes, a comparative synthesis. In *Seasonality of Freshwater Phytoplankton* (pp. 85-115). Springer Netherlands.
- Munawar, M., Munawar, I. F., Fitzpatrick, M., Niblock, H., & Lorimer, J. (2009). The base of the food web at the top of the Great Lakes: structure and function of the microbial food web of Lake Superior. *State of Lake Superior*, 289-318.
- Naeher, S., Niemann, H., Peterse, F., Smittenberg, R. H., Zigah, P. K., & Schubert, C. J. (2014). Tracing the methane cycle with lipid biomarkers in Lake Rotsee (Switzerland). *Organic Geochemistry*, 66, 174-181.
- Odada, E.O., Olago, D.O., Bugenyi, F., Kulindwa, K., Karimumuryango, J., West, K., Ntiba, M., Wandiga, S., Aloo-Obudho, P. and Achola, P. (2003). Environmental assessment of East African Rift Valley lakes. *Aquat. Sci.* 65, 254-271.
- Ohtsuka et al. (1993). Feeding ecology of copepodid stages of *Eucalanus bungii* in the Chukchi and northern Bering Seas in October (1988). In *Proc. NIPR Symp. Polar Biol* (Vol. 6, pp. 27-37).
- OHTSUKA, S., M. S., TANIMURA, A., & FUKUCHI, M. (1996). Relationships between mouthpart structures and in situ feeding habits of five neritic calanoid copepods in the Chukchi and northern Bering Seas in October 1988. In *Proc. NIPR Symp. Polar Biol* (Vol. 9, pp. 153-168).
- Ohkouchi, N., Eglinton, T. I., Keigwin, L. D., & Hayes, J. M. (2002). Spatial and temporal offsets between proxy records in a sediment drift. *Science*, 298(5596), 1224-1227.
- Opsahl, S. P., & Zepp, R. G. (2001). Photochemically-induced alteration of stable carbon isotope ratios ($\delta^{13}\text{C}$) in terrigenous dissolved organic carbon. *Geophysical research letters*, 28(12), 2417-2420.
- O'REILLY, C. M., Hecky, R. E., Cohen, A. S., & Plisnier, P. D. (2002). Interpreting stable isotopes in food webs: recognizing the role of time averaging at different trophic levels. *Limnology and oceanography*, 47(1), 306-309.
- Orr, A. (2000). 'Green Gold': Burley Tobacco, smallholder agriculture, and poverty alleviation in Malawi. *World Development*, 28(2), 347-363.
- Pakulski, J.D., & R. Benner. (1992). An improved method for the hydrolysis and MBTH analysis of dissolved and particulate carbohydrates in seawater. *Marine Chemistry*, 40(3), 143-160.
- Parrish, C. C., Abrajano, T. A., Budge, S. M., Helleur, R. J., Hudson, E. D., Pulchan, K., & Ramos, C. (2000). Lipid and phenolic biomarkers in marine ecosystems:

- analysis and applications. In *Marine Chemistry* (pp. 193-223). Springer Berlin Heidelberg.
- Pasche, N., Schmid, M., Vazquez, F., Schubert, C. J., Wüest, A., Kessler, J. D. & Bürgmann, H. (2011). Methane sources and sinks in Lake Kivu. *Journal of Geophysical Research: Biogeosciences* (2005–2012), 116(G3).
- Patterson, G., Hecky, R. E., & Fee, E. J. (2000). Effect of hydrological cycles on planktonic primary production in Lake Malawi/Niassa. *Advances in Ecological Research*, 31, 421-430.
- Pearson, A., A.P. McNichol, B.C. Benitez-Nelson, J.M. Hayes, and T.I. Eglinton. (2001). Origins of lipid biomarkers in Santa Monica Basin surface sediment: A case study using compound-specific $\Delta^{14}\text{C}$ analysis. *Geochimica et Cosmochimica Acta*. 65(18): 3123-3137.
- Pearson, A., and T.I. Eglinton. (2000). The origin of n-alkanes in Santa Monica Basin surface sediment: A model based on compound specific $\Delta^{14}\text{C}$ and $\delta^{13}\text{C}$ data. *Organic Geochemistry*. 31(11): 1103-1116.
- Peterson, B. J., & Fry, B. (1987). Stable isotopes in ecosystem studies. *Annual review of ecology and systematics*, 293-320.
- Peterson, B. J., and R.W. Howarth. (1987). Sulfur, carbon, and nitrogen isotopes used to trace organic matter flow in the salt-marsh estuaries of Sapelo Island, Georgia. *Limnology and oceanography*. 32(6): 1195-1213.
- Post, D. M. (2002). Using stable isotopes to estimate trophic position: models, methods, and assumptions. *Ecology*, 83(3), 703-718.
- Post, D.M., M.L. Pace, and N.G. Hairston Jr. (2000). Ecosystem size determines food-chain length in lakes. *Nature*. 405: 1047-1049.
- Rau, G. (1978). Carbon-13 depletion in a subalpine lake: carbon flow implications. *Science*, 201(4359), 901-902.
- Rau, G. H. (1980). Carbon-13/carbon-12 variation in subalpine lake aquatic insects: food source implications. *Canadian journal of fisheries and aquatic sciences*, 37(4), 742-746.
- Ricketts, R.D. and T.C. Johnson. (1996). Early Holocene changes in lake level and productivity in Lake Malawi as Interpreted from oxygen and carbon isotopic measurements of authigenic carbonates. P475-493. In: Johnson, T.C. and E.O. Odada. 1996. The limnology, climatology and paleoclimatology of the East African Great Lakes. Gordon and Breach Publishers. The Netherlands.

- Robbins, E.I. (1983). Accumulation of fossil fuels and metallic minerals in active and ancient rift lakes. *Tectonophysics*, 94: 633-658.
- Robinson, N., Cranwell, P. A., Finlay, B. J., & Eglinton, G. (1984). Lipids of aquatic organisms as potential contributors to lacustrine sediments. *Organic Geochemistry*, 6, 143-152.
- Roff, J. C., Turner, J. T., Webber, M. K., & Hopcroft, R. R. (1995). Bacterivory by tropical copepod nauplii: extent and possible significance. *Aquatic Microbial Ecology*, 9(2), 165-175.
- Roland, L. A., McCarthy, M. D., & Guilderson, T. (2008). Sources of molecularly uncharacterized organic carbon in sinking particles from three ocean basins: A coupled $\Delta^{14}\text{C}$ and $\delta^{13}\text{C}$ approach. *Marine Chemistry*, 111(3), 199-213.
- Rosendahl, B. R. (1987). Architecture of continental rifts with special reference to East Africa. *Annual Review of Earth and Planetary Sciences*, 15, 445.
- Schelske, C. L. (1985). Biogeochemical silica mass balances in Lake Michigan and Lake Superior. *Biogeochemistry*, 1(3), 197-218.
- Schock, S. and L.R. LeBlanc. (1990). CHIRP sonar; new technology for sub-bottom profiling. *Sea Technology*, 31: 35-43.
- Scholz, C.A. (2002). Applications of seismic sequence stratigraphy in lacustrine basins. In: *Tracking environmental changes using lake sediments: Volume 1*. Editors: Last, W.M., and J.P. Smol.
- Schouten, S., Klein Breteler, W., Blokker, P., Schogt, N., Rijpstra, W. I. C., Grice, K. & Sinninghe Damsté, J. S. (1998). Biosynthetic effects on the stable carbon isotopic compositions of algal lipids: Implications for deciphering the carbon isotopic biomarker record. *Geochimica et Cosmochimica Acta*, 62(8), 1397-1406.
- Selgeby, J. H. (1975). Life histories and abundance of crustacean zooplankton in the outlet of Lake Superior, 1971-72. *Journal of the Fisheries Board of Canada*, 32(4), 461-470.
- Selgeby, J. H. (1988). Comparative biology of the sculpins of Lake Superior. *Journal of Great Lakes Research*, 14(1), 44-51.
- Shah, S. R., Mollenhauer, G., Ohkouchi, N., Eglinton, T. I., & Pearson, A. (2008). Origins of archaeal tetraether lipids in sediments: Insights from radiocarbon analysis. *Geochimica et Cosmochimica Acta*, 72(18), 4577-4594.

- Shuter, B. J., Jones, M. L., Korver, R. M., & Lester, N. P. (1998). A general, life history based model for regional management of fish stocks: the inland lake trout (*Salvelinus namaycush*) fisheries of Ontario. *Canadian journal of fisheries and aquatic sciences*, 55(9), 2161-2177.
- Sierszen, M. E., Peterson, G. S., & Scharold, J. V. (2006). Depth-specific patterns in benthic planktonic food web relationships in Lake Superior. *Canadian Journal of Fisheries and Aquatic Sciences*, 63(7), 1496-1503.
- Smittenberg, R. H., Hopmans, E. C., Schouten, S., & Sinninghe Damsté, J. S. (2002). Rapid isolation of biomarkers for compound specific radiocarbon dating using high-performance liquid chromatography and flow injection analysis–atmospheric pressure chemical ionisation mass spectrometry. *Journal of Chromatography A*, 978(1), 129-140.
- Smyntek, P. M., Teece, M. A., Schulz, K. L., & Thackeray, S. J. (2007). A standard protocol for stable isotope analysis of zooplankton in aquatic food web research using mass balance correction models. *Limnology and Oceanography*, 52(5), 2135-2146.
- Spigel, R.H. and G.W. Coulter. (1996). Comparison of hydrology and physical limnology of the East African Great Lakes: Tanganyika, Malawi, Victoria, Kivu, and Turkana (with reference to some North American Great Lakes). P103-140. In: Johnson, T.C. and E.O. Odada. 1996. The limnology, climatology and paleoclimatology of the East African Great Lakes. Gordon and Breach Publishers. The Netherlands.
- Steffan, S. A., Chikaraishi, Y., Horton, D. R., Ohkouchi, N., Singleton, M. E., Miliczky, E. & Jones, V. P. (2013). Trophic hierarchies illuminated via amino acid isotopic analysis. *PloS one*, 8(9), e76152.
- Sterner, R. W., Anagnostou, E., Brovold, S., Bullerjahn, G. S., Finlay, J. C., Kumar, S. & Sherrell, R. M. (2007). Increasing stoichiometric imbalance in North America's largest lake: Nitrification in Lake Superior. *Geophysical Research Letters*, 34(10).
- Sun, M. Y., & Wakeham, S. G. (1998). A study of oxic/anoxic effects on degradation of sterols at the simulated sediment–water interface of coastal sediments. *Organic Geochemistry*, 28(12), 773-784.
- Sun, M. Y., Wakeham, S. G., & Lee, C. (1997). Rates and mechanisms of fatty acid degradation in oxic and anoxic coastal marine sediments of Long Island Sound, New York, USA. *Geochimica et Cosmochimica Acta*, 61(2), 341-355.

- Talbot, M. R., and T. Lærdal, T. (2000). The Late Pleistocene-Holocene palaeolimnology of Lake Victoria, East Africa, based upon elemental and isotopic analyses of sedimentary organic matter. *Journal of Paleolimnology*. 23(2): 141-164.
- Tegelaar, E. W., de Leeuw, J. W., Derenne, S., & Largeau, C. (1991). 7.11) Early diagenesis of biochemical constituents in sediments from offshore Peru. *Organic Geochemistry: Advances and Applications in the Natural Environment*, 15, 431.
- Tenzer, G. E., P.A. Meyers, and P. Knoop. (1997). Sources and distribution of organic and carbonate carbon in surface sediments of Pyramid Lake, Nevada. *Journal of Sedimentary Research*. 67(5): 884-890.
- Teranes, J. L. and S. M. Bernasconi. (2000). The record of nitrate utilization and productivity limitation provided by $\delta^{15}\text{N}$ values in lake organic matter—a study of sediment trap and core sediments from Baldeggersee, Switzerland. *Limnol. Oceanogr.* 45(4): 801-813.
- Thomas, R. L. (1969). A note on the relationship of grain size, clay content, quartz and organic carbon in some Lake Erie and Lake Ontario sediments. *Journal of Sedimentary Research*, 39(2), 803-809.
- Thompson, S. and G Eglinton. (1978). The fractionation of a recent sediment for organic geochemical analysis. *Geochimica et Cosmochimica Acta*. 42(2): 199-207.
- Tieszen, L. L., Boutton, T. W., Tesdahl, K. G., & Slade, N. A. (1983). Fractionation and turnover of stable carbon isotopes in animal tissues: implications for $\delta^{13}\text{C}$ analysis of diet. *Oecologia*, 57(1-2), 32-37.
- Tolosa, I., LeBlond, N., Copin-Montégut, C., Marty, J. C., de Mora, S., & Prieur, L. (2003). Distribution of sterol and fatty alcohol biomarkers in particulate matter from the frontal structure of the Alboran Sea (SW Mediterranean Sea). *Marine chemistry*, 82(3), 161-183.
- Trebitz, A. S., Morrice, J. A., & Cotter, A. M. (2002). Relative role of lake and tributary in hydrology of Lake Superior coastal wetlands. *Journal of Great Lakes Research*, 28(2), 212-227.
- Treignier, C., Derenne, S., & Saliot, A. (2006). Terrestrial and marine C_{27} - C_{30} -alcohol inputs and degradation processes relating to a sudden turbidity current in the Zaire canyon. *Organic Geochemistry*, 37(9), 1170-1184.
- Turner, J. T. (2004). The importance of small planktonic copepods and their roles in pelagic marine food webs. *Zool. Stud*, 43(2), 255-266.

- Turner, J. T., & Tester, P. A. (1992). Zooplankton feeding ecology: bacterivory by metazoan microzooplankton. *Journal of Experimental Marine Biology and Ecology*, 160(2), 149-167.
- Turner, J. T., Levinsen, H., Nielsen, T. G., & Hansen, B. W. (2001). Zooplankton feeding ecology: grazing on phytoplankton and predation on protozoans by copepod and barnacle nauplii in Disko Bay, West Greenland. *Marine Ecology Progress Series*, 221, 209-219.
- Urban, N.R., M.T. Auer, S.A. Green, X. Lu, D.S. Apul, K.D. Powell, and L. Bub. (2005). Carbon cycling in Lake Superior. *Journal of Geophysical Research*. 110: C06S90, doi:10.1029/2003JC002230
- Vander Zanden, M. J., & Vadeboncoeur, Y. (2002). Fishes as integrators of benthic and pelagic food webs in lakes. *Ecology*, 83(8), 2152-2161.
- Vanderploeg, H. A., J. F. Cavaletto, J. R. Liebig, and W.S. Gardner. (1998). *Limnocalanus macrurus* (Copepoda: Calanoida) retains a marine arctic lipid and life cycle strategy in Lake Michigan. *Journal of plankton research*. 20(8): 1581-1597.
- Volkman, J. K., Barrett, S. M., Blackburn, S. I., Mansour, M. P., Sikes, E. L., & Gelin, F. (1998). Microalgal biomarkers: a review of recent research developments. *Organic Geochemistry*, 29(5), 1163-1179.
- Volkman, J.K. (2006). Lipid markers for marine organic matter. In: *The handbook of environmental chemistry*. Vol 2, Part N, p 27-70.
- Vollmer, M.K., R.F. Weiss, and H.A. Bootsma. (2000). Ventilation of Lake Malawi/Nyassa. In: *The East African great lakes: limnology, paleolimnology, biodiversity*. Editors: Odada, E.O., and D.O. Olago. *Advances in Global Change Research*. Kluwer Publishers, Dordrecht. p 209-233.
- Wang, X. C., & Druffel, E. R. (2001). Radiocarbon and stable carbon isotope compositions of organic compound classes in sediments from the NE Pacific and Southern Oceans. *Marine chemistry*, 73(1), 65-81.
- Wang, X. C., Druffel, E. R., & Lee, C. (1996). Radiocarbon in organic compound classes in particulate organic matter and sediment in the deep northeast Pacific Ocean. *Geophysical research letters*, 23(24), 3583-3586.
- Warren, G. J. (1983). Predation by *Limnocalanus* as a Potentially Major Source of Winter Naupliar Mortality in Lake Michigan. *Journal of Great Lakes Research*, 9(3), 389-395.

- Warren, G. J. (1985). Predaceous feeding habits of *Limnocalanus macrurus*. *Journal of plankton research*, 7(4), 537-552.
- Weidel, B. C., Carpenter, S. R., Kitchell, J. F., & Vander Zanden, M. J. (2011). Rates and components of carbon turnover in fish muscle: insights from bioenergetics models and a whole-lake ^{13}C addition. *Canadian Journal of Fisheries and Aquatic Sciences*, 68(3), 387-399.
- Weiler, R. R. (1978). Chemistry of Lake Superior. *Journal of Great Lakes Research*, 4(3), 370-385.
- White, D. C., Davis, W. M., Nickels, J. S., King, J. D., & Bobbie, R. J. (1979). Determination of the sedimentary microbial biomass by extractible lipid phosphate. *Oecologia*, 40(1), 51-62.
- Winder, M., and D.E. Schindler. (2004). Climate change uncouples trophic interactions in an aquatic ecosystem. *Ecology*. 85(8): 2100-2106.
- Wuest, A., G. Piepke, and J.D. Halfman. (1996). Combined effects of dissolved solids and temperature on the density stratification of Lake Malawi. P183-202. In: Johnson, T.C. and E.O. Odada. 1996. The limnology, climatology and paleoclimatology of the East African Great Lakes. Gordon and Breach Publishers. The Netherlands.
- Zigah, P.K., E.C. Minor, J.P. Werne, and L. McCallister. 2011. Radiocarbon and stable carbon isotopic insights into provenance and cycling of carbon in Lake Superior. *Limnol. Oceanogr.* 56(3): 867-886.
- Zigah, P. K., Minor, E. C., & Werne, J. P. (2012a). Radiocarbon and stable-isotope geochemistry of organic and inorganic carbon in Lake Superior. *Global Biogeochemical Cycles*, 26(1).
- Zigah, P. K., Minor, E. C., Werne, J. P., & McCallister, S. L. (2012b). An isotopic ($\Delta 14\text{C}$, $\delta 13\text{C}$, and $\delta 15\text{N}$) investigation of the composition of particulate organic matter and zooplankton food sources in Lake Superior and across a size-gradient of aquatic systems. *Biogeosciences*, 9(9).
- Zigah, P. K., Minor, E. C., Abdulla, H. A., Werne, J. P., & Hatcher, P. G. (2014). An investigation of size-fractionated organic matter from Lake Superior and a tributary stream using radiocarbon, stable isotopes and NMR. *Geochimica et Cosmochimica Acta*, 127, 264-284.

